7-28-2011 12:00 AM

Mitochondrial metabolic suppression and reactive oxygen species production during hypometabolism in mammals

Jason CL Brown, *University of Western Ontario*

Supervisor: James Staples, *The University of Western Ontario*

A thesis submitted in partial fulfillment of the requirements for the Doctor of Philosophy degree in Biology

MITOCHONDRIAL METABOLIC SUPPRESSION AND REACTIVE OXYGEN SPECIES PRODUCTION DURING HYPOMETABOLISM IN MAMMALS

(Spine title: Mitochondrial Metabolism & ROS Production in Hypometabolism)

(Thesis format: Integrated Article)

by

Jason Charles Leslie Brown

Graduate Program in Biology

A thesis submitted in partial fulfillment
of the requirements for the degree of
Doctor of Philosophy

The School of Graduate and Postdoctoral Studies
The University of Western Ontario
London, Ontario, Canada

THE UNIVERSITY OF WESTERN ONTARIO
School of Graduate and Postdoctoral Studies

CERTIFICATE OF EXAMINATION

Supervisor

_____
Dr. James Staples

Supervisory Committee

_____
Dr. Louise Milligan

_____
Dr. Denis Maxwell

Examiners

_____
Dr. Denis Maxwell

_____
Dr. Charles Trick

_____
Dr. Stanley Dunn

_____
Dr. Jason Treberg

The thesis by

Jason Charles Leslie Brown

entitled:

Mitochondrial metabolic suppression and reactive oxygen species production during hypometabolism in mammals

is accepted in partial fulfilment of the
requirements for the degree of
Doctor of Philosophy

Date: July 28, 2011-08-11

_____
Chair of the Thesis Examination Board

ABSTRACT

During hibernation, daily torpor, and fasting, mammals reduce metabolic rate (MR) up to 99%, 95%, and 30%, respectively, compared to resting levels. Mitochondrial metabolic suppression likely contributes to this MR reduction, and the first objective of this study was to determine the relative contributions of active, regulated inhibition and passive thermal effects as body temperature (T_b) falls, to mitochondrial metabolic suppression, and to examine the mechanisms involved using top-down elasticity analysis and novel statistical approach. The second objective of this study was to determine how mitochondrial metabolic suppression affects mitochondrial reactive oxygen species (ROS) production, a topic which has been largely ignored previously. To accomplish these objectives, I measured in vitro respiration and ROS production rates of mitochondria from liver, skeletal muscle, and/or heart during hibernation in thirteen-lined ground squirrels (*Ictidomys tridecemlineatus*), spontaneous daily torpor and fasting in dwarf Siberian hamsters *(Phodopus sungorus*), and fasting-induced daily torpor and fasting in laboratory mice (*Mus musculus*) over a range of physiologically-relevant temperatures. In liver, state 3 respiration measured at 37°C was 70%, 35%, and 31% lower during hibernation, daily torpor, and fasting, respectively, resulting largely from substrate oxidation inhibition at complex I and/or II. In skeletal muscle, state 3 respiration measured at 37°C was reduced up to 32% during hibernation. By contrast, in heart, state 3 respiration measured at 37°C was 2-fold higher during daily torpor in hamsters. Therefore, active, regulated mitochondrial metabolic suppression in several tissues characterizes mammalian hypometabolism, accounting

for up to 16% of the MR reduction observed. In all tissues, mitochondrial respiration declined with in vitro assay temperature, and differences among metabolic states were not observed at low temperatures (10-15°C), suggesting that passive thermal effects also play an important role, particularly during steady-state torpor when body temperature is low. In liver and heart (but not skeletal muscle), basal ROS production and/or free radical leak (FRL; proportion of electron flux leading to ROS production) was generally higher during hypometabolism when measured at 37°C, particularly at complex III. However, in all tissues, ROS production and FRL typically declined with temperature, suggesting that, while mitochondrial metabolic suppression may increase the potential for mitochondrial ROS production, perhaps leading to oxidative stress during fasting, low T_b during torpor may, in fact, alleviate the accumulation of oxidative damage.

Key Words: hibernation, daily torpor, heterothermy, fasting, starvation, oxidative phosphorylation, reactive oxygen species (ROS)

CO-AUTHORSHIP

Work for this thesis was completed under the supervision and financial support of Dr. James Staples.

Parts of this thesis have been published:

Brown JCL, Staples JF (2010) Mitochondrial metabolism during fasting-induced daily torpor in mice. Biochim Biophys Acta 1797: 476-486.

Brown JCL, Staples JF (2011) Mitochondrial metabolic suppression in daily torpor: consequences for reactive oxygen species production. Physiol Biochem Zool. (In Press)

Parts of thesis have been submitted for publication:

Brown JCL, Chung DJ, Belgrave KR, Staples JF (In Revision) Mitochondrial metabolic suppression and reactive oxygen species production in liver and skeletal muscle of hibernating thirteen-lined ground squirrels. Am J Physiol Regul Integr Comp Physiol.

Contributions of co-authors:

J.F. Staples – Provided advice on study design; edited manuscripts prior to submission for publication.

D. J. Chung – Maintained ground squirrel colony; assisted with liver and skeletal muscle isolation in grounds squirrels.

K.R. Belgrave – Assisted with skeletal muscle isolation in ground squirrels.

EPIGRAPH

“I appeal to the scientists…, and ask you always to keep before your eyes, in your striving for scientific knowledge, the ultimate aim of your work and of your whole life.”

-John Paul II

DEDICATION

This thesis is dedicated to my children, Emmitt, Caley, and Selena, all of whom were born while this work was in progress. Their smiles and laughter bring richness to life that far surpasses the tribulations of research. May my dedication towards this work serve as an inspiration for their own pursuits in life, whatever they may be.

ACKNOWLEDGEMENTS

I must first acknowledge Dr. Arthur Szabo, the former Dean of Science at Wilfrid Laurier University, who suggested that I apply for an NSERC USRA, and forwarded my name to several biology faculty members—which he did not have to do! As a result, I worked in the laboratory of Dr. M.A. Fieldes for two summers, and she became my honours thesis supervisor. My experiences in her lab were wonderful—and life-changing!—and I am ever-greatful to Dr. Fieldes for the opportunity she provided, as well as her friendship, both then and now.

I also offer my sincere appreciation to my PhD supervisor, Dr. Jim Staples. He has given me the freedom to chase my ideas—including a side project in botany!—but has always been prepared to offer feedback, criticism, and guidance when necessary. He has provided me with the opportunity to showcase my research at the national level, to attend an international conference, and to see a world-class speaker discuss his ideas. He has also generously bestowed his friendship, advice, patience, and hospitality on so many occasions. I am very much aware of how fortunate I have been to have worked under his leadership, and he has provided me with an outstanding model on which to base my own laboratory leadership in the future…if I ever I leave his lab!

My two advisory committee members, Dr. Louise Milligan and Dr. Denis Maxwell, must also be ackwolegded with my gratitude. I always came away from advisory committee meetings feeling proud of my accomplishments and deeply motivated to continue my work, and I came away from both my proposal assessment and comprehensive exams feeling challenged to further expand my knowledge. I

especially thank Dr. Milligan for writing many reference letters on my behalf over the past few years…and thank her, too, for the reference letters she has yet to write!

I wish also to acknowledge all of the friends that I have made over the past six years as a graduate student, both those who are still here with me, and those who have escaped and give me hope that there is a life outside this university. I am thoroughly convinced that the quality of a graduate student experience is largely based on the people that surround you. I wish to particularly acknowledge Lee Stach and Jordan Klaiman for their continued friendship, as well as Chris Armstrong, Dillon Chung, and Katie Belgrave for being such good fellow “Staplers”.

I am also extremely grateful to the Natural Sciences and Engineering Research Council of Canada (NSERC), the Ontario Government, and the University of Western Ontario, all of whom provided me with three years of scholarship funding during my tenure as a PhD student. I have been fortunate to have been so financially well-supported while attending graduate school.

Finally, I want to acknowledge my family, particularly my wife, Casey, who continues to persevere through the uncertainty that a career in science brings; my sister-in-law Sylvia and my parents, Shirley and Harold, who graciously looked after my kids on more than a few occasions so that I could finish this thesis; and my father-in-law, Wayne, who will likely be the only person that voluntarily reads this thesis.

TABLE OF CONTENTS

LIST OF TABLES

LIST OF FIGURES

LIST OF EQUATIONS

LIST OF APPENDICIES

LIST OF ABBREVIATIONS AND SYMBOLS

ΔP	proton motive force
$\Delta\Psi_m$	mitochondrial membrane potential
ΔpH	proton gradient across the inner mitochondrial membrane
αKG	α-ketoglutarate
αKGDH	α-ketoglutarate dehydrogenase
AAT	aspartate aminotransferase
ADF	alternate day fasting
ANT	adenine nucleotide translocator
BMR	basal metabolic rate
BSA	bovine serum albumin
CCCP	carbonyl cyanide chlorophenylhydrazone
CR	calorie restriction
Cyt	cytochrome
DT	dicarboxyalte transpoter
ETC	electron transport chain
FAD	flavin adenine nucleotide
Fe-S	iron-sulfur cluster
FMN	flavin mononucleotide
FMR	field metabolic rate
FRL	free radical leak
GAA	glutamate/asparatate antiporter
GDH	glutamate dehydrogenase
GHS	glutamate/H^+ symporter
HSI	hepatosomatic index
IBE	interbout euthermia/euthermic
IMM	inner mitochondrial membrane
IMS	intermembrane space
IR	ischemia-reperfusion
ISP	Rieske iron sulfur protein
LHB	liver homogenization buffer
MDH	malate dehydrogenase
MHB	skeletal muscle homogenization buffer
MM	mitochondrial matrix
MMR	maximum metabolic rate
MR	metabolic rate
$O_2^{-}\cdot$	superoxide
OAA	oxaloacetate
$OH^{-}\cdot$	hydroxyl radical
OMM	outer mitochondrial membrane
OxPhos	oxidative phosphorylation
PDH	pyruvate dehydrogease
PUFA	polyunsaturated fatty acid
Q	ubiquinone
RCR	respiratory control ratio

RMR	resting metabolic rate
ROS	reactive oxygen species
SA	summer active
SDH	succinate dehydrogenase
SEM	standard error of the mean
SMR	standard metabolic rate
SuMR	sustained metabolic rate
T	torpid
T_a	ambient temperature
T_b	core body temperature
T_{set}	hypothalamic thermoregulatory set-point temperature
TPP^+	tetraphenylphosphonium ion
UCP	uncoupling protein
VDAC	voltage-dependent anion channel

CHAPTER 1

General Introduction

1.1 Mammalian hypometabolism

1.1.1 The metabolic rate of mammals. All animals transform chemical potential energy from foodstuffs into work or heat (Randall et al. 2002; Hill et al. 2008). The rate at which this conversion takes place is called metabolic rate (MR) and can be deconstructed into two basic components: obligatory and facultative. The obligatory component is called basal metabolic rate (BMR) in endotherms (i.e., mammals and birds) and standard metabolic rate (SMR) in ectotherms, and represents the minimal rate of metabolism necessary to sustain life (Hulbert and Else 2004). BMR is measured in resting, post-absorptive adults at thermoneutral temperatures (Kleiber 1961). The facultative component is the additional rate of metabolism used to fuel all other activities (e.g., reproduction, locomotion, feeding, thermogenesis, growth) and increases metabolism above BMR, up to some maximum metabolic rate (MMR) in the shorter term (i.e., minutes/hours), or sustained metabolic rate (SuMR; Hammond and Diamond 1997) in the longer term (i.e., days/months). While animals may operate at BMR or MMR/SuMR at certain times, they typically function at some intermediate rate of metabolism, reflected by measurements of field metabolic rate (FMR), which is a measure of the energy expenditure by animals in their natural environment over an extended period of time (Nagy 1987).

Compared with most vertebrates, mammals have quite high rates of metabolism. BMR of mammals is about 10-fold higher than SMR of similarly-sized fish, amphibians, and reptiles, even when standardized to the same body temperature (T_b; White et al. 2006), and FMR of mammals is 11-fold higher than that of similarly-sized reptiles (Nagy et al. 1999). The selective pressure that drove the evolution of such high rates of metabolism in mammals is a contentious issue. One hypothesis (the "aerobic capacity" hypothesis) is that mammals were selected for high MMR/SuMR, which allowed for better prey capture and/or predator evasion (Bennett and Ruben 1979; Taigen 1983). High MMR/SuMR is thought to have necessitated the co-evolution of an increased size of visceral organs, which are larger in mammals than comparatively-sized reptiles (Else and Hulbert 1981; Franz et al. 2009), to support high rates of metabolism during periods of activity. The maintenance of these larger visceral organs during periods of inactivity is thought to elevate BMR and FMR in mammals. Support for this hypothesis is equivocal, with some (Bozinovic 1992; Hayes and Garland 1995; Boily 2002; Sadowska et al. 2005) but not all authors (Koteja 1987) showing that BMR and MMR/SuMR are correlated both phenotypically and genetically. An alternative hypothesis (the "thermoregulatory" hypothesis) purports that mammals were selected for a high and relatively constant T_b (i.e., endothermy) by increasing their BMR and simultaneously improving their thermal insulation. The proposed benefits of endothermy are the ability to be active in colder environments (higher latitudes/altitudes, night) than ectotherms (Crompton et al. 1978), high activity rates of enzymes adapted to work within a narrow temperature range (Heinrich 1977), and the prevention of fungal infections (Bergman and Casadevall 2010). Despite these potential

benefits of endothermy, there is little empirical evidence to support the thermoregulatory hypothesis (see Cowles 1958; Bennett et al. 2000). A third, more recent hypothesis proposes that mammals were selected for improved parental care (Koteja 2000; Farmer 2000). A high SuMR would permit high rates of foraging for provision of food to young, and concomitantly increased thermoregulatory capabilities would permit mammals to incubate their young at high temperatures, which accelerates development time and reduces developmental abnormalities (Deeming and Ferguson 1991).

Regardless of which hypothesis represents the true course of mammalian evolution, the high metabolism of mammals undoubtedly yields some benefit; however, the high MR of mammals is also costly. The most noteworthy cost is the requirement for large amounts of food. Mammals consume 10-fold more food each day than comparatively-sized reptiles (Karasov et al. 1986; Nagy 1987) and maintain a greater digestive surface to facilitate faster and more efficient digestion (Karasov and Diamond 1985). Both food quality and abundance vary spatially and temporarily, and have considerable effects on the capacity to maintain high BMR (McNab 1986). Moreover, high rates of food consumption necessitate spending considerable time foraging, which itself consumes energy reserves and, perhaps more importantly, increases predation risk (Brown et al. 1994). Another important cost is that endotherms exhibit a distinct aging phenotype, which is thought to be related to high MR (de Magalhaes and Toussaint 2002). These costs of a high metabolism act to offset the benefits, and the evolution of mammals likely involved balancing these benefits and costs. In some mammals, this balance has been achieved by deriving some of the benefits of a high metabolism via

other, less costly mechanisms. For example, improved predator avoidance is realized via armoured plates and life underground in armadillos and naked mole rats, respectively, and these species have lower BMR throughout their lives than other comparably-sized mammals (Buffenstein and Yahav 1991; Boily 2002). These are uncommon examples, however, and many mammals balance the benefits and costs of high MR by suppressing metabolism for periods of time, ranging from hours to days. The most notable hypometabolic states in mammals are hibernation and daily torpor, and mammals that undergo these phenomena are termed heterothermic because their T_b fluctuates over the course their life rather than remaining relatively constant as in homeothermic endotherms. Mammals also become hypometabolic during periods of euthermic fasting, although the degree of MR suppression is much less than that observed during hibernation or daily torpor. A description of important aspects of each of these hypometabolic states is given in the next three sections.

1.1.2 Hypometabolism in mammals: hibernation. Hibernation occurs in a wide variety of mammals, including monotremes, marsupials, and placentals (Carey et al. 2003; Geiser 2004), but has been particularly well-studied in ground squirrels (Rodentia: Sciuridae). As a result, in the present thesis, thirteen-lined ground squirrels (*Ictidomys tridecemlineatus*) were used as the experimental model of hibernation. This species is found in south-central Canada and much of the Midwestern United States (Streubel and Fitzgerald 1978).

Immediately following emergence from hibernation in spring, hibernators undergo a brief period of reproduction (Kenagy 1980), after which they turn their attention to building up energy stores for the impending hibernation season. Some

hibernators hoard food during summer for consumption during the hibernation season (e.g., eastern chipmunks; Humphries et al. 2001), but most hibernators, including ground squirrels, do not eat during the hibernation season and, instead, consume large amounts of food during the summer in order to build up endogenous fat stores. The extent of pre-hibernation fattening may be particularly important for juveniles, for which pre-hibernation body mass correlates with overwintering survival (Murie and Boag 1984), and diet composition during this fattening periods has significant effects on MR and T_b during hibernation, with potential consequences for survival and spring reproduction (Ruf and Arnold 2008).

During the hibernation season, which can last up to 9 months in some species, animals alternate between periods of torpor and periods of interbout euthermia (Figure 1-1A shows data from this study for thirteen-lined ground squirrels). During torpor, MR is suppressed as low as 5% of BMR or 1% of winter resting metabolic (RMR; Figure 1-1B; Geiser 2004), and T_b falls to as low as -3°C in Arctic ground squirrels (Barnes 1989), but typically only as low as 5°C in most other ground squirrel species (Figure 1-1B; Geiser 2004), just a few degrees above ambient temperature (T_a). T_b falls not because animals cease to thermoregulate but rather because the hypothalamic thermoregulatory set-point temperature (T_{set}) is quite reduced, and hibernating animals will increase their metabolism when T_b falls below this new, lower T_{set} (Heller and Colliver 1974; Florant and Heller 1977). Uninterrupted torpor bouts typically last between 5-15 days (Geiser and Ruf 1995), and an individual torpor bout ends with an arousal, which is either spontaneous or provoked by some external stimulus. During arousal, animals rewarm themselves to approximately 37°C within a few hours using

primarily endogenous sources of heat (i.e., shivering and non-shivering thermogenesis; Lyman and Chatfield 1950; Smalley and Dryer 1963), although passive rewarming (via solar insolation) may be used when available. Following arousal, animals enter the interbout euthermic phase, where T_b remains at approximately 37°C and MR remains at typical resting levels for approximately 6 hours (in thirteen-lined ground squirrels). As much as 80% of the energy consumption during the hibernation season occurs during arousal and interbout euthermia, and several hypotheses have been proposed to explain why hibernators arouse during the hibernation season, including the accumulation of sleep debt (Daan et al. 1991) and the inability to detect infections (Prendergrast et al. 2001) during torpor. Following interbout euthermia, MR and T_b decline during entrance into torpor. This pattern of the hibernation season is seen both in laboratory and field animals (Wang 1973).

1.1.3 Hypometabolism in mammals: daily torpor. Bouts of daily torpor last, by definition, no longer than 24 hours, though the typical length of a torpor bout is 5-12 hours. T_b falls as low 12°C, though typical torpid T_b is 18°C, and MR drops by as much as 70% of BMR and 90% of RMR (Geiser 2004). There are two kinds of daily torpor—spontaneous and fasting-induced—and each is represented by the two experimental models used in the present study. Dwarf Siberian hamsters (*Phodopus sungorus*; Figure 1-2 shows data from this study), native to the steppes of Siberia and Kazakhstan (Ross 1998), undergo daily torpor spontaneously (i.e., without any immediately evident stimulus) when acclimated to short photoperiod (8 hours of light) for 3-5 months, even when kept at thermoneutral T_a and fed ad libitum (Heldmaier and Steinlechner 1981).

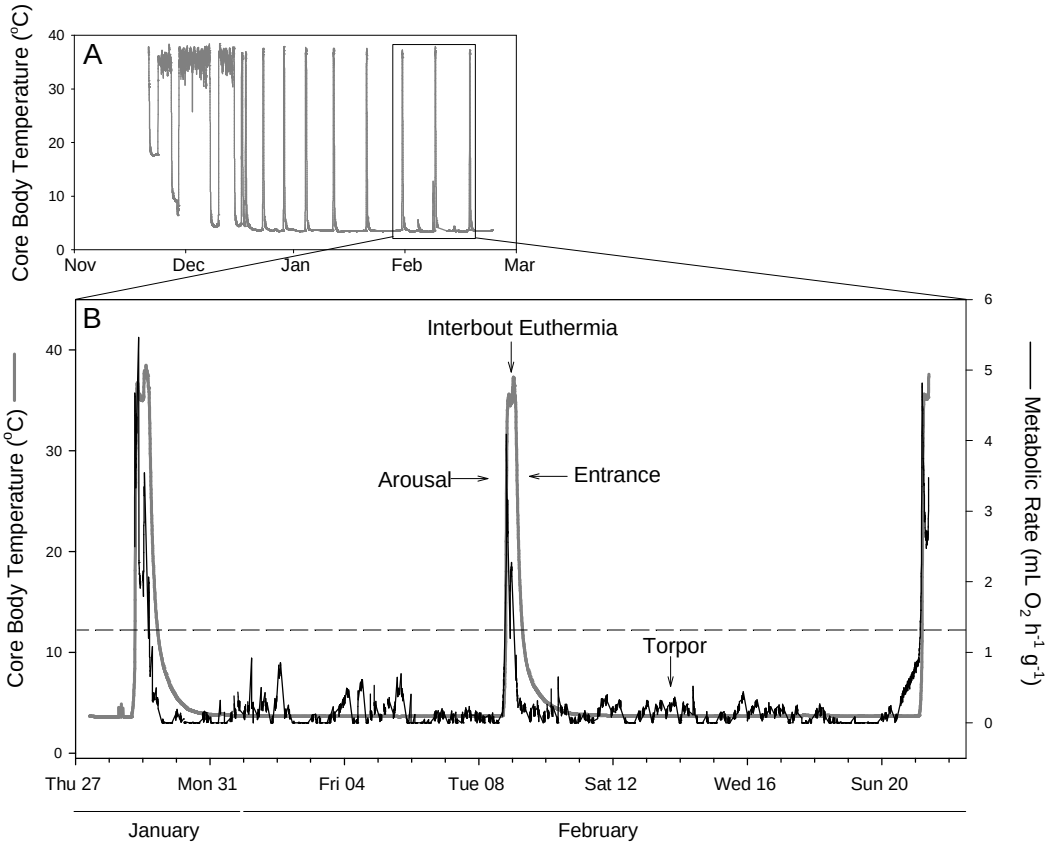

Figure 1-1. **Hibernation in thirteen-lined ground squirrels.** *A.* Body temperature of an individual animal from this study throughout part of the hibernation season shows several hibernation bouts. *B.* Body temperature and metabolic rate of the same individual over a one month period of the hibernation season highlights the phases of a hibernation bout. The dashed line indicates the mean metabolic rate of summer active animals for comparison.

By contrast, laboratory strains of house mice (*Mus musculus*; Figure 1-3 shows data from this study) undergo daily torpor within a day in response to fasting (Hudson and Scott 1979). There is some degree of interaction between these two different forms of daily torpor. For example, the frequency and duration of spontaneous daily torpor increases when animals are food-restricted (Ruf et al. 1993). Moreover, reduced leptin levels, although insufficient to induce spontaneous torpor, are needed before torpor can occur in dwarf Siberian hamsters (Freeman et al. 2003) and are part of the mechanism that invokes fasting-induced torpor in mice (Gavrilova et al. 1999). Nevertheless, fasting alone cannot induce torpor in dwarf Siberian hamsters, except perhaps once considerable body mass has been lost (Ruby and Zucker 1992), whereas photoperiod alone cannot induce torpor in house mice. Therefore, spontaneous and fasting-induced daily torpor are distinct phenomena. Daily torpor occurs predominantly during the inactive phase of circadian cycles, which permits animals to remain active each day following arousal from torpor in order to forage and maintain social interactions.

1.1.4. Hypometabolism in mammals: euthermic fasting. Many mammals may experience periods of fasting brought about by acute food shortages and/or environmental conditions that preclude foraging. In the absence of food, survival is limited by endogenous energy supplies, and small mammals may die within a few days—even faster in cold environments—if food cannot be found (Lindstedt and Boyce 1985). In fact, the ability to find enough of the right kind of food is considered by some as the most important determinant of survival (White 1978), and the capacity to survive acute periods of fasting has important fitness consequences (Wang et al. 2006). It is not surprising, therefore, that much research has focused on how acute fasting shaped

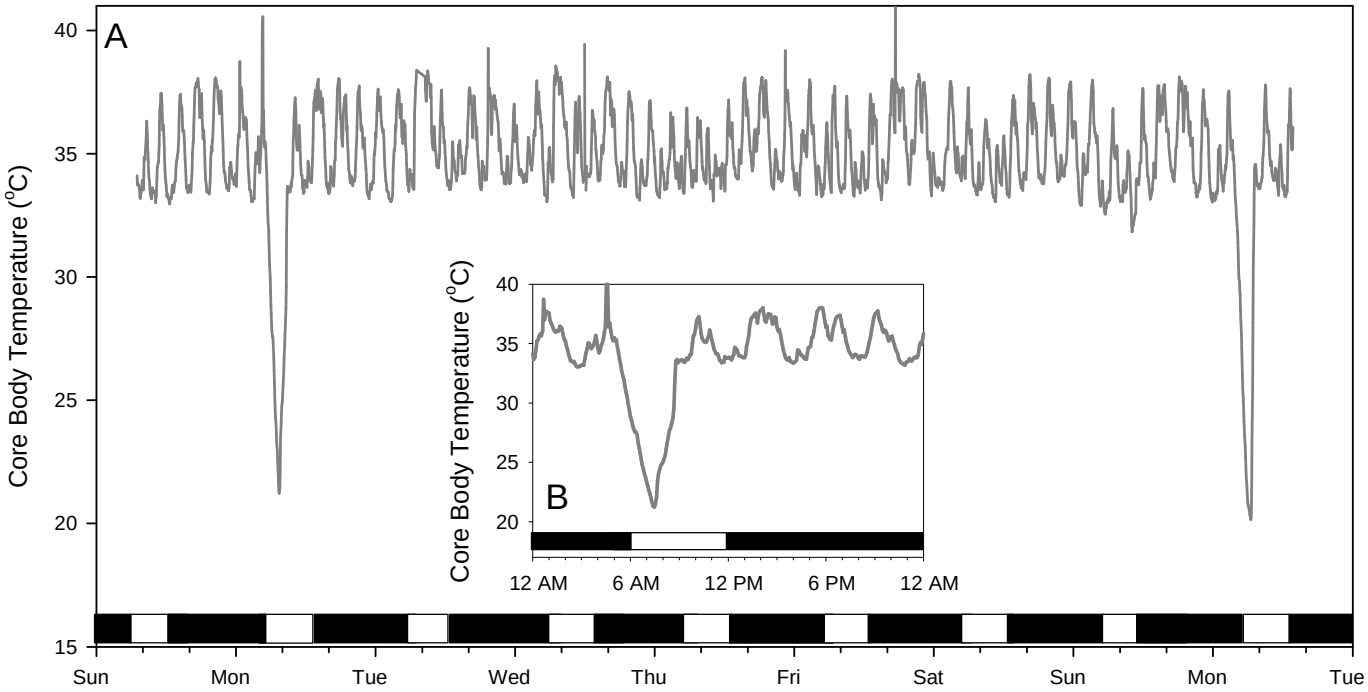

Figure 1-2. **Spontaneous daily torpor in dwarf Siberian hamsters.** Hamsters were acclimated to short photoperiod (8 hours light). *A.* Body temperature of an individual from this study shows two torpor bouts over a 10-day period. *B.* Body temperature of the same individual over a twenty-four hour period during which daily torpor occurred. Black and white bars indicate the scotophase and photophase, respectively.

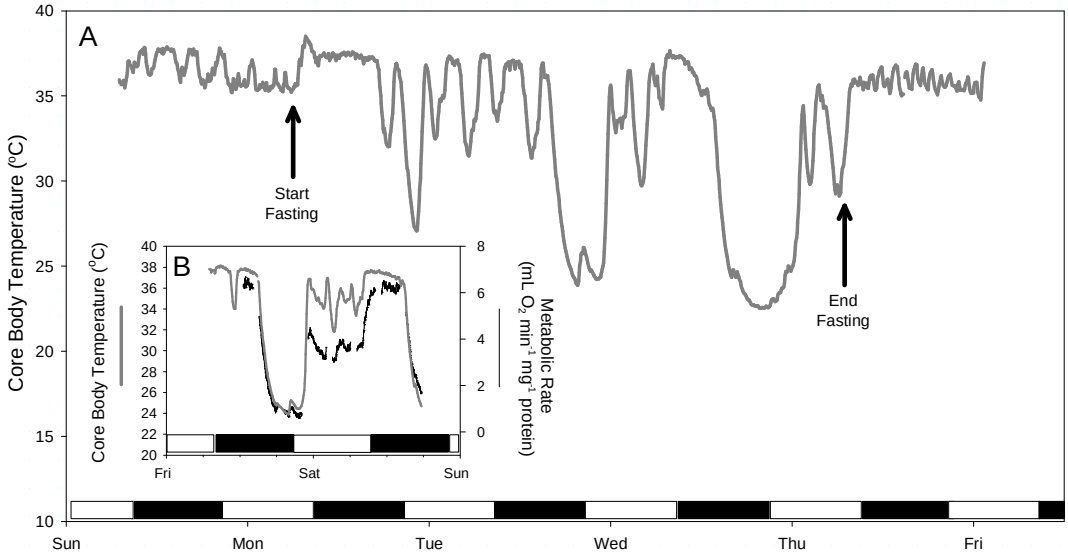

Figure 1-3. **Fasting-induced daily torpor in mice.** *A.* Core body temperature of an individual from this study was monitored for one week during which food was withheld for 72 hours as indicated. *B.* Body temperature and metabolic rate of another fasted mouse sampled during torpor in this study. Black and white bars indicate scotophase and photophase, respectively.

mammalian evolution (Lindstedt and Boye 1985; Millar and Hickling 1990). One of the most important physiological responses to fasting is a significant but modest suppression of metabolism (up to 30% of resting levels; Rixon and Stevenson 1957; Munch et al. 1993; Fuglei and Oritsland 1999) that occurs without core T_b falling more than a few degrees (Markussen and Oritsland 1986; Sakurada et al. 2000). This MR reduction during fasting has even been observed during periods of exercise (Mosin 1984), so it does not simply reflect reduced activity. By moderately suppressing MR, animals reduce the rate at which they consume endogenous energy reserves, which can increase their likelihood of survival until food resources return and/or environmental conditions improve (Wang et al. 2006), but also permit them to remain fully active, unlike hibernation or daily torpor

1.2 Overview of mitochondrial oxidative phosphorylation and reactive oxygen species production

There has been considerable interest in elucidating the mechanisms by which MR is reduced during hypometabolism in mammals. In the next section of this thesis (section 1.3), I propose that mitochondrial oxidative phosphorylation (OxPhos) may play an important role in MR suppression because OxPhos is responsible for ~90% of whole-animal oxygen consumption and has considerable control over cellular energy-demanding processes (Rolfe and Brown 1997). In addition, I propose that mitochondrial metabolic suppression may have consequences for mitochondrial reactive oxygen species (ROS) production and oxidative stress. However, before I elaborate on these

hypotheses, it is necessary to provide an overview of mitochondrial OxPhos and ROS production.

1.2.1 General principles of mitochondrial oxidative phosphorylation. Mitochondria play a number of important roles in the cell (Zorov et al. 1997). The most well-appreciated mitochondrial function, however, is the synthesis of ATP, which is used an energy source by many cellular processes (Buttgereit and Brand 1995). Mitochondrial OxPhos employs the energy released by the oxidative transfer of electrons from chemically-reduced substrates to oxygen as a means to generate a transmembrane electrochemical gradient—the mitochondrial proton motive force (ΔP)—which is subsequently used to power the phosphorylation of ADP via ATP synthase (Hatefi 1985). A complete description of the complexity of OxPhos is beyond the scope of this thesis, and some detailed reviews of OxPhos have been published in the last decade or so (Saraste 1999; Lesnefsky and Hoppel 2006). Therefore, I will limit my description of OxPhos here to those aspects germane to the experimental design and interpretation of results of this thesis. In particular, I will focus on the pathways necessary for transport and oxidation of two substrates commonly used to assess respiration and ROS production rates of isolated mitochondria—glutamate and succinate—as these were used in the present study.

1.2.2 Mitochondrial OxPhos: generation of ΔP. Mitochondria are bounded by two membranes. The inner mitochondrial membrane (IMM) bounds the mitochondrial matrix (MM), and the outer mitochondrial membrane (OMM) bounds the entire organelle. The space between the two membranes is called the intermembrane space (IMS). The two membranes differ considerably in their permeability. The OMM is quite

permeable to most small (less than 1.5kDa) substances, a property attributed to voltage-dependent anion-selective channels (VDAC; Colombini 1979), but its permeability can be regulated (Liu and Colombini 1992; Vander Heiden et al. 2000). The IMM is impermeable to the free passage of most substances but contains a large number of transporters that function to selectively translocate certain substances into and out of the MM (Palmieri 2004). Glutamate can be transported across the IMM via two different transporters: the glutamate/H^+ symporter (GHS) and the glutamate/aspartate antiporter (GAA; Bradford and McGivan 1973; LaNoue and Schoolwerth 1979). Succinate is transported across the IMM via the dicarboxylate transporter (DT), which exchanges succinate for inorganic phosphate (Chappel 1968). Malate, which is often added to mitochondria during respiration with glutamate (as in the present study; see below) is also transported into the MM via DT (Chappel 1968).

Once transported into the MM, glutamate can be oxidized in two ways (Figure 1-4): i) deamination via glutamate dehydrogenase (GDH), which leads to the formation of α-ketoglutarate (αKG) and NADH; or ii) by transamination via aspartate aminotransferase (AAT), in which an amine group is transferred from glutamate to oxaloacetate (OAA) to produce αKG. This latter pathway can only occur when malate is simultaneously supplied to the mitochondria, as was the case in this thesis. Malate is needed to generate OAA via the citric acid cycle enzyme, malate dehydrogenase (MDH), a reaction which itself produces NADH. In either case, αKG is further oxidized via another citric acid cycle enzyme, α-KG dehydrogenase (αKGDH), yielding additional NADH. Which of these pathways (deamination vs. transamination) predominates may be tissue-specific and reflect differences in GDH activity among

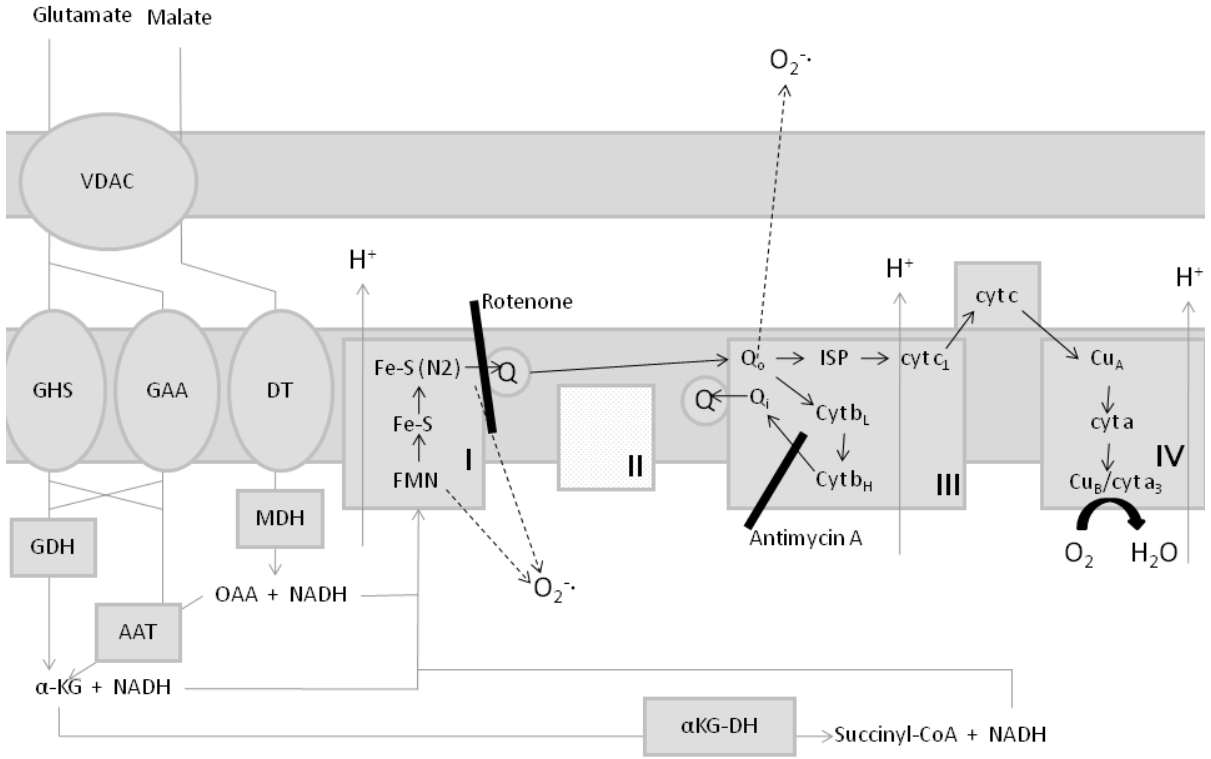

Figure 1-4. Oxidative pathways and reactive oxygen species production with glutamate as oxidative substrate. See List of Abbreviations and Symbols for abbreviations used. Arrows indicate substrate/electron flow pathways. Non-competitive inhibitors are indicated by solid lines at their site of action. Organization of electron transport chain (ETC) simplified for presentation. See Boekema and Bruan (2007) for details of ETC molecular arrangement. For simplicity, components involved in ATP synthesis are not shown.

tissues (Borst 1962). Nevertheless, mitochondrial respiration fueled by glutamate and malate leads to the production of NADH within the MM.

NADH is oxidized via the mitochondrial electron transport chain (ETC) complex I (Zickerman et al. 2009). The first step in NADH oxidation by complex I is the transfer of two electrons from NADH to the flavin mononucleotide (FMN) within the complex. Subsequently, these two electrons are passed from FMN to ubiquinone (Q) through a series of eight iron-sulfur (Fe-S) clusters also within the complex. The final Fe-S cluster in the pathway (known as N2) is responsible for the electron transfer to ubiquinone, which reversibly binds to complex I. In this way, ubiquinone is reduced to ubiquinol. The transfer of electrons from N2 to ubiquinone can be blocked by the inhibitor rotenone (Friedrich et al. 1994). In addition to transferring electrons from NADH to ubiquinone, complex I also translocates protons from the MM into the IMS, thereby contributing the generation of ΔP, though the mechanism involved in this proton translocation remains unknown (Sherwood and Hirst 2006).

Following its transport into the MM, succinate is oxidized by succinate dehydrogenase (SDH; complex II of the mitochondrial ETC; Rutter et al. 2010; Figure 1-5). The initial step in this oxidation process involves a two-electron transfer to a flavin adenine dinucleotide (FAD) within complex II. This step can be competitively inhibited by malonate (Thorn 1953). Reduced FAD transfers its two electrons, via three Fe-S clusters, to a molecule of ubiquinone, leading to the production of ubiquinol. The transfer of electrons from succinate to ubiquinol does not release sufficient free energy for proton translocation, and so, unlike complex I, complex II does not pump protons across the IMM and, therefore, does not contribute the generation of ΔP.

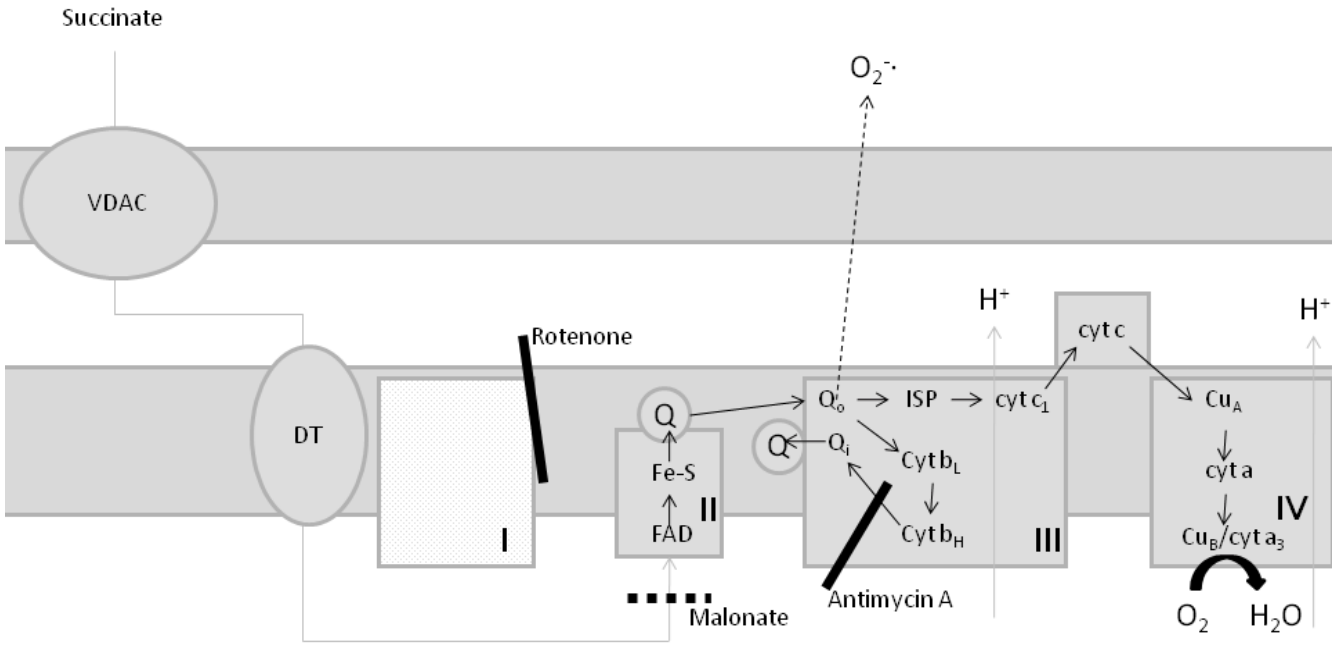

Figure 1-5. Oxidative pathways and reactive oxygen species production with succinate as oxidative substrate. See List of Abbreviations and Symbols for abbreviations used. Arrows indicate substrate and/or electron flow pathways. Competitive and non-competitive inhibitors indicated by dashed and solid lines, respectively, in the electron flow pathway at their site of action. Organization of electron transport chain (ETC) simplified for presentation. See Boekema and Bruan (2007) for details of ETC molecular arrangement. For simplicity, components involved in ATP synthesis are not shown.

Ubiqunol produced by complex II can be oxidized by complex I at the expense of Δp. This “reverse” electron flow is often considered “unphysiological” (e.g., Lambert and Brand 2004) and can be inhibited by addition of rotenone to succinate-fueled mitochondria, as was done in this thesis. Under physiological conditions, ubiquinol produced by both complex I and II is oxidized by complex III of the mitochondrial ETC (Figure 1-4; 1-5). Ubiquinol binds to a site on complex III near the IMS (called Q_o). At this point, one electron from ubiquinol is transferred via the Rieske iron-sulfur protein (ISP) to cytochrome c_1 (found within complex III) and one electron is transferred to cytochrome b_L (also found within complex III). It is unclear whether these electron transfers occur simultaneously (Zhu et al. 2007) or sequentially, with electron transfer to cytochrome c_1 taking place first, briefly leaving a ubisemiquinone bound at the Q_o site (Crofts et al. 2008). The electron passed to cytochrome c_1 is subsequently transferred to cytochrome c, a mobile electron carrier located within the IMS, loosely bound to the IMM (Garrido et al. 2006). Cytochrome c is subsequently oxidized via complex IV of the electron transport chain. Within complex IV, electrons from cytochrome c are transferred to a cytochrome a_3/Cu_B centre—the site of oxygen reduction—via two other redox centres, Cu_A and cytochrome a. The transfer of electrons from cytochrome to the cytochrome a_3/Cu_B centre initiates the translocation of protons by complex IV across the IMM (Belevich et al. 2008), contributing to the generation of ΔP.

The ubisemiquinone bound at the Q_o site transfers another electron to cytochrome b_L and subsequently cytochrome b_H, both of which are found within complex III. From cytochrome b_H, the electron is transferred to a molecule of

ubiquinone which is bound to another site on complex III near the MM (called the Q_i site). This electron transfer leads to the production of a bound ubisemiquinone at the Q_i site. The oxidation of a second ubiquinol molecule, following its binding to the Q_o site, leads to the production of another reduced cytochrome c (which is oxidized by complex IV) as well as the transfer of an electron to the bound ubisemiquinone at the Q_i site, which leads to the production and release of ubiquinol. This is known as the Q-cycle mechanism of complex III (Trumpower 1990). The electron transfer from cytochrome b_H to the Q_i site can be inhibited by antimycin A (Gao et al. 2003), and this ultimately prevents the oxidation of ubisemiquinone molecules bound at the Q_o site by complex III.

1.2.3 Mitochondrial OxPhos: dissipation of ΔP. In the presence of saturating ADP and inorganic phosphate, ΔP is dissipated considerably as protons flow through ATP synthase, leading to ATP production (Boyer 1997). This dissipation of ΔP stimulates the activity of the mitochondrial ETC, leading to high rates of mitochondrial oxygen consumption. Mitochondrial oxygen consumption rate measured under these conditions (i.e., in the presence of ADP, inorganic phosphate, and respiratory substrate) is referred to as state 3 respiration. ADP is transported into the MM via the adenine nucleotide translocator (ANT) in exchange for ATP (Pfaff and Klingenberg 1968), and inorganic phosphate is transported into the MM by the phosphate transporter via H^+ symport, and thus depends on ΔP (Tyler 1969).

In the absence of ADP, or when ATP synthase activity is inhibited by oligomycin (Chappel and Crofts 1965), both of which prevent proton flow into the MM via ATP synthase, ΔP is still dissipated, although to a much lesser extent, as protons

flow back into the MM via other pathways. The exact nature of these pathways, with exception of the uncoupling proteins (UCPs; Stuart et al. 1999), is poorly understood, but membrane-protein interfaces may be an important site of much proton leak (Jastroch et al. 2010). Because ΔP dissipation is limited in the absence of ADP, the activity of the ETC and mitochondrial oxygen consumption are low. Mitochondrial respiration rate measured under these conditions (i.e., in the presence of a respiratory substrate but following exhaustion of exogenous ADP) is referred to as state 4 respiration, and is commonly measured by adding oligomycin (which inhibits ATP synthase) to ADP-phosphorylating mitochondria.

1.2.4 Top-down elasticity analysis of oxidative phosphorylation. OxPhos is a complex process comprised of a large number of reactions, and trying to determine which of these many individual reactions change in activity between metabolic states can be a quite difficult task requiring several dozen enzyme assays. One approach which has greatly simplified this task is top-down elasticity analysis (Brand 1998). This analysis uses a simplified view of mitochondrial metabolism in which OxPhos is considered as a system consisting of only three components (Figure 1-6): (i) substrate oxidation, which includes any reactions that contribute to the generation of ΔP, such as substrate transporters, Krebs cycle, and the mitochondrial ETC; (ii) ADP phosphorylation, which includes any reactions that contribute to the dissipation of ΔP in the process of generating ATP, such as ATP synthase, ANT, and the phosphate transporter; and (iii) proton leak, which includes any reactions that dissipate ΔP without generating ATP, including both UCPs and constitutive pathways. The three components of OxPhos are all connected to ΔP, with substrate oxidation producing it as a product,

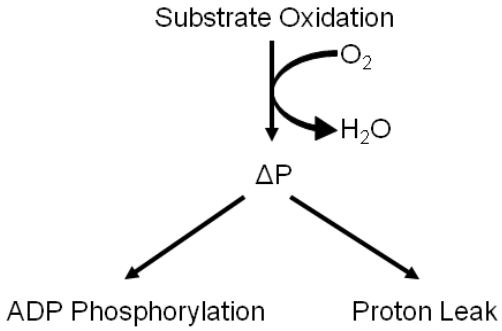

Figure 1-6. A simplified view of mitochondrial oxidative phosphorylation. Substrate oxidation generates the proton motive force (ΔP) while simultaneously reducing oxygen to water. During state 3 respiration, ΔP is consumed largely by ADP phosphorylation, whereas during state 4 respiration, ΔP is consumed exclusively by proton leak.

and ADP phosphorylation and proton leak consuming it as a substrate. The kinetics of each component of OxPhos can be empirically determined by simultaneously measuring mitochondrial respiration rate and ΔP (using $\Delta\Psi_m$ as an approximation). Thus, top-down elasticity analysis simplifies our approach to determining how OxPhos is modified between two states by requiring that we measure the activity of only these three components, rather than dozens of individual enzymes.

To illustrate how the kinetics of a particular component of OxPhos can be measured experimentally, let us consider state 4 respiration (Figure 1-7). The oxygen consumption rate and $\Delta\Psi_m$ measured under state 4 conditions represents a point on the kinetic curves for both substrate oxidation and proton leak. In fact, state 4 can be considered as the point at which substrate oxidation and proton leak activity are in equilibrium, such that the quantity of protons leaking into the MM across the IMM is balanced by the protons being pumped out by the ETC. In order to measure the kinetics of proton leak, the activity of substrate oxidation must be inhibited in a step-wise manner. Following each inhibition of substrate oxidation, new steady-state values of respiration rate and $\Delta\Psi_m$ will be reached. Each inhibition of substrate oxidation will cause mitochondrial respiration rate and ΔP to decline (since both parameters result from substrate oxidation), and a new equilibrium will be reached. These new steady-state values of mitochondrial respiration rate and $\Delta\Psi_m$ represent another point on the curve that describes the kinetics of proton leak. Continued step-wise inhibition of substrate oxidation will allow for the kinetic curve of proton leak to be determined. Kinetic curves for substrate oxidation and ADP phosphorylation can be determined similarly. If the kinetics of all three components is measured, a quantitative analysis can

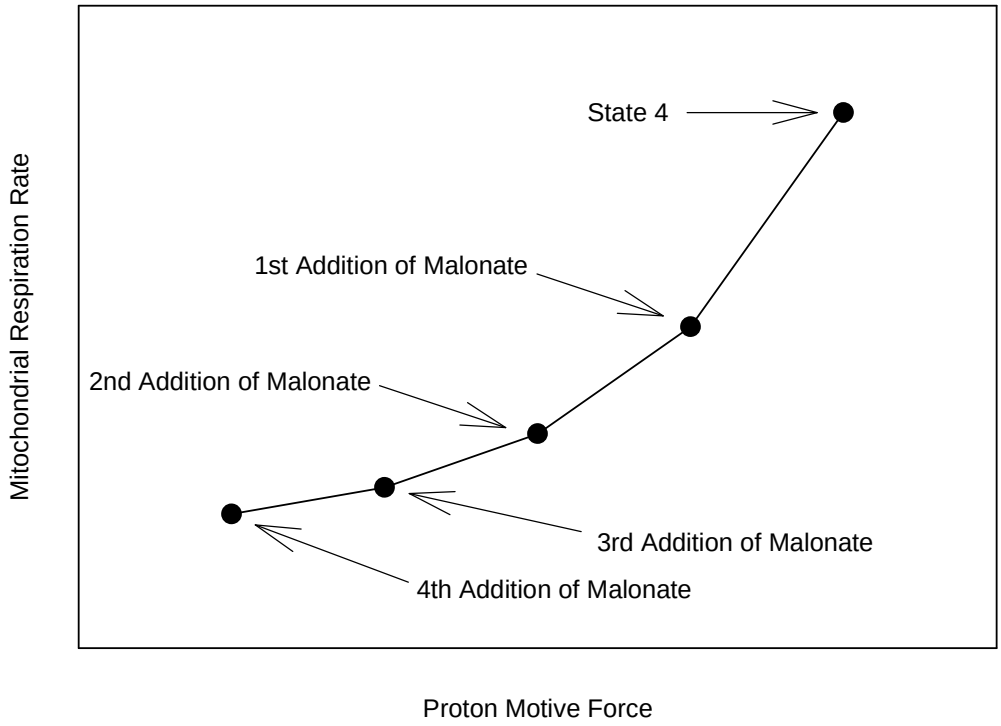

Figure 1-7. Experimental determination of the kinetics of the components of oxidative phosphorylation. The kinetics of proton leak are shown as an example of how the kinetics of oxidative phosphorylation can be assessed. State 4 values of mitochondrial respiration and proton motive force are determined in the presence of saturating substrate concentrations and oligomycin. The kinetics of proton leak are then experimentally determined by step-wise additions of malonate (a competitive inhibitor substrate oxidation). Each addition generates new steady-state values for mitochondrial respiration rate and ΔP, all of which lie upon the kinetic curve for proton leak. A kinetic curve for substrate oxidation could be similarly generated starting from state 4 conditions by step-wise additions of carbonyl cyanide chlorophenylhydrazone (CCCP), which stimulates proton leak.

be performed to determine the extent to which each component contributes to changes in mitochondrial respiration rate between states (see Appendix A).

1.2.5 Mitochondrial reactive oxygen species production. As described above, during OxPhos, electrons removed from substrates ultimately reduce oxygen to water by a four-electron process at complex IV. The oxygen molecule bound to complex IV is not released until all four electrons are transferred. However, oxygen can interact with other redox centres in the mitochondrial ETC, and, in these cases, oxygen usually receives only a single electron, leading to the production of superoxide ($O_2^{-}\cdot$). Superoxide is subsequently converted to hydrogen peroxide (H_2O_2) either spontaneously or via superoxide dismutase, and H_2O_2 can convert into hydroxyl radicals ($OH^{-}\cdot$). These derivatives of oxygen ($O_2^{-}\cdot$, H_2O_2, and $OH^{-}\cdot$) are collectively referred to as reactive oxygen species (ROS). ROS are known to react with biomolecules, such as DNA, proteins, and lipids, and cause oxidative damage to these cellular components. In theory, any component of the ETC can produce ROS, but most mitochondrial ROS production is derived from complex I and complex III.

The mechanism by which complex I produces ROS is not well understood. ROS production may occur at or near the site of ubiquinone binding (Raha and Robinson 2000; Genova et al. 2001; Lambert and Brand 2004; Ohnishi et al. 2005), or the FMN site (Liu et al. 2002; Kudin et al. 2004), or at both sites (Brand 2010). Notwithstanding, ROS produced at complex I are released into the MM where they are subjected to matrix antioxidants (St. Pierre et al. 2002; Han et al. 2001). Therefore, much of the ROS produced at complex I is degraded before it can leave the mitochondria. Most assays that detect mitochondrially-derived ROS, such as those used in this thesis, only detect

ROS that are released from the mitochondria into the surrounding medium; therefore, ROS that are produced towards the MM (such as ROS from complex I) are only partially detected by most assays. As a result, these assays are said to measure ROS "release" and will underestimate total ROS production.

ROS production via complex III is better understood compared with complex I. The principle mechanism involves electron transfer from ubisemiquinone, either directly after its formation at the Q_o site (Raha and Robinson 2000) or via cytochrome b_L (Drose and Brandt 2008), though other poorly-characterized sites have also been proposed (Han et al. 2001). Although ubisemiquinone also forms at the Q_i site, it appears to be more stable and far less likely to lead to ROS production (Zhang and Gutterman 2006). Consistent with this notion, ROS produced at complex III is largely released in the IMS (i.e., the side on which the Q_o site is found), where it easily diffuses across the OMM into the cytosol (St. Pierre et al. 2002; Han et al. 2001), and only some complex III ROS production may also be released in the matrix (i.e., the side on which the Q_i site is found; Han et al. 2001). Therefore, most of the ROS produced at complex III is released from the mitochondria and is detected by assays measuring mitochondrially-derived ROS.

Complex II does not produce ROS because of the presence of a cytochrome b within the complex. This cytochrome b is not necessary for electron flux from succinate to ubiquinone (Oyedotun et al. 2007), but its inhibition has been shown to lead to ROS production in a number of studies (e.g., Senoo-Matsuda et al. 2001). Complex II may also produce ROS under certain cellular conditions (e.g., hypoxia) that favour a reverse electron flow through this site, such that the enzyme catalyzes the reduction of fumarate

to succinate (Paddenberg et al. 2003). Complex IV is also not known to produce ROS despite that several reactive oxygen intermediate are generated within the complex as the oxygen molecule receives four electrons sequentially (Hill 1994). Nicholls and Ferguson (2002) outline a mechanism by which this could be achieved.

1.3 Mitochondrial metabolic suppression and reactive oxygen species production during mammalian metabolism: the objectives of my thesis project.

During hypometabolism, MR declines considerably. Facultative metabolism might be reduced by inactivity and/or cessation of feeding (Storey and Storey 2004), as well as the decrease in T_{set} which would decrease thermogenesis. In fact, some authors propose that cessation of thermogenesis and passive thermal effects are sufficient to fully account for MR reduction during hypometabolism (Guppy and Withers 1999). However, many heterotherms undergo torpor, with large drops in MR, even when held at thermoneutral T_a where facultative thermogenesis would be minimal (Heldmaier and Steinlechner 1981). Moreover, large heterothermic species (e.g., black bears) achieve considerable MR suppression (25%) although T_b never drops below 30°C (Töien et al. 2011), and hypometabolism during fasting occurs with T_b falling only a few degrees. Therefore, the obligatory component of metabolism (i.e., BMR) is also likely reduced by some temperature-independent mechanisms.

Rolfe and Brown (1997) provided a comprehensive analysis of the processes that contribute to BMR. The major contributors (~70% of BMR) are ATP-consuming processes such as Na^+/K^+-ATPase, protein and nucleotide synthesis, gluconeogenesis, Ca^{2+}-ATPase, actinomyosin ATPase, and ureagenesis. Therefore, if BMR is actively

reduced during hypometabolism, the activity of many of these ATP-consuming processes must also be inhibited. Indeed, there is considerable evidence that many ATP-consuming processes are suppressed during hypometabolism. Na^+/K^+-ATPase is suppressed in skeletal muscle (MacDonald and Storey 1999) and heart (Charnock et al. 1980) during hibernation in ground squirrels, and in erythrocytes of hibernating bears (Chauhan et al. 2002). Moreover, protein synthesis is suppressed in brain of hibernating ground squirrels (Frerichs et al. 1998) and liver of dwarf Siberian hamsters (Diaz et al. 2004). While active inhibition of each ATP-consuming process individually could be a mechanism to suppress MR, mitochondrial ATP production also has significant control over all of these ATP-consuming processes (Buttgereit and Brand 1995), and so BMR could also be reduced by inhibiting mitochondrial ATP synthesis. In addition, mitochondrial proton leak is responsible for about 20% of BMR, and its reduction during hypometabolism could also contribute to MR reduction. To this end, in this thesis, I examined mitochondrial respiration rates and the activity of OxPhos during hibernation and daily torpor (Chapter 2) and fasting (Chapter 4) in order to assess whether and how mitochondrial metabolism is suppressed during periods of hypometabolism.

In addition to generating ATP, mitochondria are also the principle site of reactive oxygen species (ROS) production in mammalian cells. A small proportion (0.15-2%) of all oxygen consumed by mitochondria is converted into ROS (St. Pierre et al. 2002; Masayasu et al. 2003), which are thought to cause oxidative damage to cellular components like DNA, proteins, and phospholipids, and, in this way, contribute to aging and disease (Raha and Robinson 2000). Suppressing mitochondrial respiration

during hypometabolism may be beneficial in terms of reducing MR, but the consequences of mitochondrial metabolic suppression in terms of ROS production have not been well-studied. Mitochondrial metabolic suppression could either simultaneously reduce the rate at which ROS are produced by decreasing electron flux through the mitochondria, or it could simultaneously increase the rate at which ROS are produced by interfering with efficient electron flow through the mitochondria, thereby increasing the reduction state of ROS-producing sites. To date, little work has been done to understand how changes in oxidative phosphorylation affect mitochondrial ROS production, particularly changes resulting from natural effectors, such as hypometabolism, because most studies examine changes in ROS production without simultaneously evaluating oxidative phosphorylation. In the present thesis, therefore, I examined mitochondrial ROS production rates during hibernation and daily torpor (Chapter 3) and fasting (Chapter 4) in order to assess how mitochondrial ROS production changes during hypometabolism, and I linked changes in ROS production during hypometabolism to changes in mitochondrial oxidative phosphorylation.

1.4 References

Barnes BM (1989) Freeze avoidance in a mammal: body temperature below 0°C in an Arctic hibernator. Science 244: 1593-1595.

Belevich I, Verkhovsky MI (2008) Molecular mechanism of proton translocation by cytochrome c oxidase. Antiox Redox Signal 10: 1-30.

Bennett AF, Ruben JA (1979) Endothermy and activity in vertebrates. Science 206: 649-654.

Bennett AF, Hicks JW, Cullum AJ (2000) An experimental test of the thermoregulatory hypothesis for the evolution of endothermy. Evol 54: 1768-1773.

Bergman A, Casadevall A (2010) Mammalian endothermy optimally restricts fungi and metabolic costs. mBio 1: doi10.1128/mBio.00212-10.

Boekema EJ, Braun H-P (2007) Supramolecular structure of the mitochondrial oxidative phosphorylation system. J Biol Chem 282: 1-4.

Boily P (2002) Individual variation in metabolic traits of wild nine-banded armadillos (*Dasypus novemcinctus*), and the aerobic capacity model for the evolution of endothermy. J Exp Biol 205: 3207-3214.

Borst P (1962) The pathway of glutamate oxidation by mitochondria isolated from different tisssues. Biochim Biophys Acta 57: 256-269.

Boyer PD (1997) The ATP synthase – a splendid molecular machine. Ann Rev Biochem 66: 717-749.

Bozinovic F (1992) Scaling of basal and maximum metabolic rate in rodents and the aerobic capacity model for the evolution of endothermy. Phys Zool 65: 921-931.

Bradford NM, McGivan JD (1973) Quantitative characteristics of glutamate transport in rat liver mitochondria. Biochem J 134: 1023-1029.

Brand MD (1998) Top-down elasticity analysis and its application to energy metabolism in isolated mitochondria and intact cells. Mol Cell Biochem 184: 13-20.

Brand MD (2010) The sites and topology of mitochondrial superoxide production. Exp Gerontol 45: 466-472.

Brown JS, Kotler BP, Valone TJ (1994) Foraging under predation: a comparison of energetic and predation costs in rodent communities of the Negev and Sonoran deserts. Aust J Zool 42: 435-448.

Buffenstein R, Yahav S (1991) Is the naked mole-rat *Hereocephalus glaber* an endothermic yet poikilothermic mammal? J Therm Biol 16: 227-232.

Buttgereit F, Brand MD (1995) A hierarchy of ATP-consuming processes in mammalin cells. Biochem J 312: 163-167.

Carey HV, Andrews MT, Martin SL (2003) Mammalian hibernation: cellular and molecular responses to depressed metabolism and low temperatures. Physiol Rev 83: 1153-1181.

Chappell JB (1968) Systems used for the transport of substrates into the mitochondria. Br Med Bull 24: 150-157.

Chappel JB, Crofts AR (1965) The effect of atracylate and oligomycin on the behavior of mitochondria towards adenine nucleotides. Biochem J 95: 707-716.

Charnock JS, Simonson LP, Dryden WF (1980) Seasonal variation in myocardial (Na^+ + K^+)-ATPase activity and [^{3}H]oubain binding in a hibernating mammals: positive correlation with the pharmacological effects of oubain. Comp Biochem Physiol B 65: 681-686.

Chauhan VPS, Tsiouris JA, Chauhan A, Sheikh AM, Brown WT, Vaughan M (2002) Increased oxidative stress and decreased activities of Ca^{2+}/Mg^{2+}-ATPase and Na^+/K^+-ATPase in the red blood cells of the hibernating black bear. Life Sci 71: 153-161.

Colombini M (1979) A candidate for the permeability pathway of the outer mitochondrial membrane. Nature 279: 643-645.

Cowles RB (1958) Possible origin of dermal temperature regulation. Evol 12: 347-357.

Crofts AR, Holland JT, Victoria D, Kolling DRJ, Dikanov SA, Gilbreth R, Lhee S, Kuras R, Kuras MG (2008) The Q-cycle reviewed: how well does a monomeric mechanism of the bc_1 complex account for the function of a dimeric complex? Biochim Biophys Acta 1777: 1001-1019.

Crompton AW, Tayloer CR, Jagger JA (1978) Evolution of homeothermy in mammals. Nature 272: 333-336.

Daan S, Barnes BM, Strijkstra AM (1991) Warming up for sleep? – Ground squirrels sleep during arousals from hibernation. Neurosci Lett 128: 265-268.

de Magalhaes JP, Toussaint O (2002) The evolution of mammalian aging. Exp Gerontol 37: 769-775.

Deeming DC, Ferguson MWJ (1991) Physiological effects of incubation temperature on embryonic development in reptiles and birds. In: Egg incubation: its effects on embryonic development in birds and reptiles. Deeming DC, Ferguson MWJ (eds). Cambridge University Press, Cambridge.

Diaz MB, Lange M, Heldmaier G, Klingenspor M (2004) Depression of transcription and translation during daily torpor in the Djungarian hamster (*Phodopus sungorus*). J Comp Physiol B 174: 495-502.

Drose S, Brandt U (2008) The mechanism of mitochondrial superoxide production by the cytochrome bc_1 complex. J Biol Chem 283: 21649-21654.

Else PL, Hulbert AJ (1981) Comparision of the “mammal machine” and the “reptile machine”: energy production. Am J Physiol Regul Integr Comp Physiol 240: R3-R9.

Farmer CG (2000) Parental care: the key to understanding endothermy and other convergent features in birds and mammals. Am Nat 155: 326-334.

Florant GL, Heller HC (1977) CNS regulation of body temperature in euthermic and hibernating marmots (*Marmota flaviventris*). Am J Physiol 232: R203-R208.

Franz R, Hummel J, Kienzle E, Kolle P, Gunga H-C, Clauss M (2009) Allometry of visceral organs in living amniotes and its implications for sauropod dinosaurs. Proc Royal Soc B 276: 1731-1736.

Freeman DA, Lewis DA, Kauffman AS, Blum RM, Dark J (2003) Reduced leptin concentrations are permissive for display of daily torpor in Siberian hamsters. Am J Physiol Regul Integr Comp Physiol 287: R97-R103.

Frerichs KU, Smith CB, Brenner M, DeGracia DJ, Krause GS, Marrone L, Dever TE, Hallenbeck JM (1998) Suppression of protein synthesis in brain during hibernation involves inhibition of protein initiation and elongation. PNAS 95: 14511-14516.

Friedrich T, Van Heek P, Leif H, Ohnishi T, Forche E, Kunze B, Jansen R, Trowitzch-Kienast W, Holfe G, Reichenbach H, Weiss H (1994) Two binding sites of inhibitors in NADH:ubiquinone oxidoreductae (complex I). Eur J Biochem 219: 691-698.

Fuglei E, Ortisland NA (1999) Seasonal trends in body mass, food intake and resting metabolic rate, and induction of metabolic depression in arctic foxes (*Alopex lagopus*) at Svalbard. J Comp Physiol 169: 361-369.

Gao X, Wen X, Esser L, Quinn B, Yu L, Yu C-A, Xia D (2003) Structural basis for the quinone reduction in the bc_1 complex: a comparative analysis of crystal structures of mitochondrial cytochrome bc_1 with bound substrate and inhibitors at the Q_i site. Biochem 42: 9067-9080.

Garrido C, Galluzzi L, Brunet M, Puig PE, Didelot C, Kroemer G (2006) Mechanisms of cytochrome c release by mitochondria. Cell Death Diff 13: 1423-1433.

Gavrilova O, Leon LR, Marcus-Samuels B, Mason MM, Castle AL, Refetoff S, Vinson C, Reitman ML (1999) Torpor in mice is induced by both lepin-dependent and -independent mechanisms. PNAS 96: 14623-14628.

Geiser F (2004) Metabolic rate and body temperature reduction during hibernation and daily torpor. Ann Rev Physiol 66: 239-274.

Geiser F, Ruf T (1995) Hibernation versus daily torpor in mammals and birds: physiological variables and classification of torpor patterns. Phys Zool 68: 935-945.

Genova ML, Ventura B, Giuliano G, Bovina C, Formiggini G, Parenti CG, Lenaz G (2001) The site of production of superoxide radical in mitochondrial complex I is not a bound ubisemiquinone but presumably iron-sulfur cluster N2. FEBS Lett 505: 364-368.

Guppy M, Withers P (1999) Metabolic depression in animals: physiological perspectives and biochemical generalizations. Biol Rev 74: 1-40.

Hammond KA, Diamond J (1997) Maximal sustained energy budgets in humans and mammals. Nature 386: 457-462.

Han D, Williams E, Cadenas E (2001) Mitochondrial respiratory chain-dependent generation of superoxide anion and its release into the intermembrane space. Biochem J 353: 411-416.

Hatefi Y (1985) The mitochondrial electron transport and oxidative phosphorylation system. Ann Rev Biochem 54: 1015-1069.

Hayes JP, Garland T (1995) The evolution of endothermy: testing the aerobic capacity model. Evol 49: 836-846.

Heinrich B (1977) Why have some animals evolved to regulate a high body temperature? Am Nat 111: 623-640.

Heldmaier G, Steinlechner S (1981) Seasonal pattern and energetics of short daily torpor in the Djungarian hamster, *Phodopus sungorus*. Oecologia 48: 265-270.

Heller HC, Colliver GW (1974) CNS regulation of body temperature during hibernation. Am J Physiol 227: 583-593.

Hill BC (1994) Modeling the sequence of electron transfer reactions in the single turnover of reduced, mammalian cytochrome c oxidase with oxygen. J Biol Chem 269: 2419-2425.

Hill RW, Wyse GA, Anderson M (2008) Animal Physiology. 2nd ed. Sinauer Associates: Sunderland MA.

Hudson JW, Scott IM (1979) Daily torpor in the laboratory mouse, Mus musculus var. albino. Phys Zool 52: 205-215.

Hulbert AJ, Else PL (2004) Basal metabolic rate: history, composition, regulation, and usefulness. Physiol Biochem Zool 77: 869-876.

Humphries MM, Thomas DW, Kramer DL (2001) Torpor and digestion in food-storing hibernators. Physiol Biochem Zool 74: 283-292.

Jastroch M, Divakaruni AS, Mookerjee S, Treberg JR, Brand MD (2010) Mitochondrial proton and electron leaks. Essays Biochem 47: 53-67.

Karasov WH, Diamond JM (1985) Digestive adaptations for fueling the cost of endothermy. Science 228: 202-204.

Karasov WH, Petrossian E, Rosenberg L, Diamond JM (1986) How do food passage rate and assimilation differ between herbivorous lizards and nonruminant mammals? J Comp Physiol B 156: 599-609.

Kenagy GJ (1980) Interrelation of endogenous annual rhythms of reproduction and hibernation in the golden-mantled ground squirrel. J Comp Physiol 135: 333-339.

Kleiber M (1961) The fire of life – an introduction to animal energetics. Wiley and Sons: New York, London.

Koteja P (1987) On the relation between basal and maximum metabolic rate in mammals. Comp Biochem Physiol A 87: 205-208.

Kojeta P (2000) Energy assimilation, parental care and the evolution of endothermy. Proc Roy Soc B 267: 479-484.

Kudin AP, Bimpong-Buta NY-B, Vielhaber S, Elger CE, Kunz WS (2004) Characterization of superoxide-producing sites in isolated brain mitochondria. J Biol Chem 279: 4127-4135.

Lambert AJ, Brand MD (2004) Inhibitors of the quinone-binding site allow rapid superoxide production from mitochondrial NADH:ubiquinone oxidoreductase (complex I). J Biol Chem 279: 39414-39420.

LaNoue KF, Schoolwerth AC (1979) Metabolite transport in mitochondria. Ann Rev Biochem 48: 871-922.

Lesnefsky EJ, Hoppel CL (2006) Oxidative phosphorylation and aging. Ageing Res Rev 5: 402-433.

Lindstedt SL, Boyce MS (1985) Seasonality, fasting endurance, and body size in mammals. Am Nat 125: 873-878.

Liu G, Fiskum G, Schubert D (2002) Generation of reactive oxygen species by the mitochondrial electron transport chain. J Neurochem 80: 780-787.

Liu MY, Colombini M (1992) Regulation of mitochondrial respiration by controlling the permeability of the outer mitochondrial membrane through the mitochondrial channel, VDAC. Biochim Biophys Acta 1098: 255-260.

Lyman CP, Chatfield PO (1950) Mechanisms of arousal in the hibernating hamster. J Exp Zool 114: 491-515.

MacDonald JA, Storey KB (1999) Regulation of ground squirrel Na^+K^+ATPase activity by reversible phosphorylation during hibernation. Biochem Biophys Res Comm 254: 424-429.

Markussen NH, Oritsland NA (1986) Metabolic depression and heat balance in starving Wistar rats. Comp Biochem 84: 771-776.

Masayasu I, Eisuke S, Manabu N, Ah-Mee P, Yukimi K, Isuke I, Kozo U (2003) Mitochondrial generation of reactive oxygen species and its role in aerobic life. Curr Med Chem 10: 2495-2505.

McNab BK (1986) The influence of food habits on the energetics of eutherian mammals. Ecol Monographs 56: 1-19.

Millar JS, Hickling GJ (1990) Fasting endurance and the evolution of mammalian body size. Func Ecol 4: 5-12.

Mosin AF (1984) On the energy fuel in voles during their starvation. Comp Biochem Physiol 77: 563-565.

Munch IC, Markussen NH, Ortisland NA (1993) Resting oxygen consumption in rats during food restriction, starvation and refeeding. Acta Phys Scand 148: 335-340.

Murie JO, Boag DA (1984) The relationship of body weight to overwinter survival in Columbian ground squirrels. J Mamm 65: 688-690.

Nagy KA, (1987) Field metabolic rate and food requirement scaling in mammals and birds. Ecol Monographs 57: 111-128.

Nagy KA, Girard IA, Brown TK (1999) Energetics of free-ranging mammals, reptiles, and birds. Ann Rev Nutr 19: 247-77.

Nicholls DG, Ferguson SJ (2002) Bioenergetics 3. Academic Press: San Diego.

Ohnishi ST, Ohnishi T, Muranaka S, Fujita H, Kimura H, Uemura K, Yoshida K, Utsumi K (2005) A possible site of superoxide generation in the complex I segment of rat heart mitochondria. J Bioenerg Biomembr 37: 1-10.

Oyedotun KS, Sit CS, Lemire BD (2007) The *Saccharomyces cerevisiae* succinate dehydrogenase does not require heme for ubiquinone reduction. Biochim Biophys Acta 1767: 1436-1445.

Paddenberg R, Ishaq B, Goldenberg A, Faulhammer P, Rose F, Weissmann N, Braun-Dullaeus RC, Kummer W (2003) Essential role of complex II of the respiratory chain in hypoxia-induced ROS generation in the pulmonary vasculature. Am J Physiol Lung Cell Mol Physiol 284: L710-L719.

Palmieri F (2004) The mitochondrial transporter family (SLC25): physiological and pathological implications. Pflugers Arch Eur J Biochem 447: 689-709.

Pfaff E, Klingenberg M (1968) Adenine nucleotide translocation of mitochondria – specificity and control. Eur J Biochem 6: 66-79.

Prendergast BJ, Freeman DA, Zucker I, Nelson RJ (2001) Periodic arousal from hibernation is necessary for initiation of immune responses in ground squirrels. Am J Physiol Regul Integr Comp Physiol 282: R1054-R1062.

Raha S, Robinson BH (2000) Mitochondria, oxygen free radicals, disease and aging. Trends Biochem Sci 25: 502-508.

Randall D, Burggren W, French K (2008) Animal physiology: mechanisms and adaptations. WH Freeman and Company: New York.

Rixon RH, Stevenson JAF (1957) Factors influencing survival of rats in fasting: metabolic rate and body weight loss. Am J Physiol 188: 332-336.

Rolfe DFS, Brown GC (1997) Cellular energy utilization and molecular origin of standard metabolic rate in mammals. Physiol Rev 77: 731-759.

Ross PD (1998) Phodopus sungorus. Mammalian Species 595: 1-9.

Ruby NF, Zucker I (1992) Daily torpor in the absence of the suprachiamastic nucleus in Siberian hamsters. Am J Physiol Regul Integr Comp Physiol 263: R353-R362.

Ruf T, Arnold W (2008) Effects of polyunsaturated fatty acids on hibernation and torpor: a review and hypothesis. Am J Physiol Regul Integr Comp Physiol 294: R1044-R1052.

Ruf T, Stieglitz S, Steinlechner S, Blank JL, Heldmaier G (1993) Cold exposure and food restriction facilitate physiological responses to short photoperiod in Djungarian hamsters (*Phodopus sungorus*). Comp Physiol Biochem 267: 104-112.

Rutter J, Winge DR, Schiffman JD (2010) Succinate dehydrogenase – assembly, regulation, and role in human disease. Mitochondrion 10: 393-401.

Sadowska ET, Labocha MK, Baliga K, Stanisz A, Wroblewska AK, Jagusiak W, Koteja P (2005) Genetic correlations between basal and maximum metabolic rates in a wild rodent: consequences for evolution of endothermy. Evol 59: 672-681.

Sakurada S, Shido O, Sugimoto N, Hiratsuka Y, Yoda T, Kanouse K (2000) Autonomic and behavioural thermoregulation in starved rats. J Physiol 526: 417-424.

Saraste M (1999) Oxidative phosphorylation at the fin de siècle. Science 283: 1488-1493.

Senoo-Matsuda N, Yasuda K, Tsuda M, Ohkubo T, Yoshimura S, Nakazawa H, Hartman PS, Ishii N (2001) A defect in the cytochrome b large subunit in complex II causes both superoxide anion overproduction and abnormal energy metabolism in *Caenorhabditis elegans*. J Biol Chem 276: 41553-41558.

Sherwood S, Hirst J (2006) Investigation of the mechanism of proton translocation by NADH:ubiquinone oxidoreductase (complex I) from bovine heart mitochondria: does the enzyme operate by a Q-cycle mechanism. Biochem J 400: 541-550.

Smalley R, Dryer R (1963) Brown fat: thermogenic effect during arousal from hibernation in the bat. Science 140: 1333-1336.

St. Pierre J, Buckingham JA, Roebuck SJ, Brand MD (2002) Topology of superoxide from different sites in the mitochondrial electron transport chain. J Biol Chem 277: 44784-44790.

Storey KB, Storey JM (2004) Metabolic rate depression in animals: transcriptional and translational controls. Biol Rev 79: 207-233.

Streubel DP, Fitzgerald JP (1978) Spermophilus tridecemLineatus. Mammalian Species 103: 1-5.

Stuart JA, Brindle KM, Harper JA, Brand MD (1999) Mitochondrial proton leak and the uncoupling proteins. J Bioenerg Biomembr 31: 517-525.

Taigen TL (1983) Activity metabolism in anuran amphibians: implications for the origin of endothermy. Am Nat 121: 94-109.

Thorn MB (1953) Inhibition by malonate of succinate dehydrogenase in heart-muscle preparations. Biochem J 54: 540-547.

Toien O, Blake J, Edgar DM, Grahn DA, Heller HC, Barnes BM (2011) Hibernation in black bears: independence of metabolic suppression from body temperature. Science 331: 906-909.

Trumpower BL (1990) The protonmotive Q cycle: energy transduction by coupling of proton translocation to electron transfer by the cytochrome bc_1 complex. J Biol Chem 265: 11409-11412.

Tyler DD (1969) Evidence of a phosphate-transporter system in the inner membrane of isolated mitochondria. Biochem J 111: 665-678.

Vander Heiden MG, Chandel NS, Li XX, Schumacker PT, Colombini M, Thompson CB (2000) Outer mitochondrial membrane permeability can regulate coupled respiration and cell survival. PNAS 97: 4666-4671.

Wang LCH (1973) Radiotelemetric study of hibernation under natural and laboratory conditions. Am J Physiol 224: 673-677.

Wang T, Hung CCY, Randall DJ (2006) The comparative physiology of food deprivation: from feast to famine. Ann Rev Physiol 68: 223-251.

White TCR (1978) The importance of a relative food shortage in animal ecology. Oecologia 33: 71-86.

White CR, Phillips NF, Seymour RS (2006) The scaling and temperature dependence of vertebrate metabolism. Biol Lett 2: 125-127.

Zhang DX, Gutterman DD (2006) Mitochondial reactive oxygen species-mediated signaling in endothelial cells. Am J Physiol Heart Circ Physiol 292: H2023-H2031.

Zhu J, Egawa T, Yeh S-R, Yu L, Yu C-A (2007) Simultaneous reduction of iron-sulfur protein and cytochrome b_L during ubiquinol oxidation in cytochrome bc_1 complex. PNAS 104: 4864-4869.

Zickerman V, Kerscher S, Zwicker K, Tocilescu MA, Radermacher M, Brandt U (2009) Architecture of complex I and its implications for electron transfer and proton pumping. Biochim Biophys Acta – Bioenerg 1787: 574-583.

Zorov DB, Krasnikov BF, Kuzminova AE, Ysokikh MY, Zorova LD (1997) Mitochondria revisited: alternative functions of mitochondria. Biosci Rep 17: 507-520.

CHAPTER 2

Suppression of oxidative phosphorylation during hibernation and daily torpor

2.1 Introduction

On average, whole-animal oxygen consumption is suppressed during torpor by 70% and 90% compared to BMR in daily heterotherms and hibernators, respectively (Geiser 2004). Because torpor is usually expressed at T_a below thermoneutrality, the extent of suppression is even greater, up to 90% and 99%, respectively, when compared to RMR (Geiser 2004). Given that mitochondrial oxidative phosphorylation is responsible for ~90% of whole-animal oxygen consumption and has considerable control over cellular energy demands (Rolfe and Brown 1997), it is reasonable to predict that mitochondrial respiration rates from at least some tissues are significantly reduced during torpor. Considerable data support this hypothesis (Pehowich and Wang 1984; Fedotcheva et al. 1985; Gehnrich and Aprille 1988; Brustovetsky et al. 1989; Martin et al. 1999; Barger et al. 2003; Muleme et al. 2006; Gerson et al. 2008; Armstrong and Staples 2010; Chung et al. 2011). What remains unresolved, however, is the mechanism(s) by which this reduction of mitochondrial respiration is achieved. Because T_b typically declines during hibernation and daily torpor to 5°C and 15°C, respectively (Geiser 2004), mitochondrial respiration can be reduced during torpor in two ways: i) via active, regulated inhibition of mitochondrial OxPhos; or ii) via passive thermal effects as T_b falls. Whether, and to what extent, these two mechanisms

contribute to the reduction of mitochondrial respiration during torpor remains poorly understood; therefore, it is the focus of this chapter of my thesis.

Whether active, regulated inhibition of mitochondrial respiration occurs during torpor can be established by isolating mitochondria from animals during periods of euthermia and torpor, and measuring respiration rates of these mitochondria at a common temperature (37°C). Any differences in respiration rates measured at 37°C between torpid and euthermic mitochondria cannot be attributed to passive, temperature effects and must result from active, regulated inhibition of OxPhos. Such inhibition of OxPhos in mitochondria from torpid animals does not preclude the possibility that passive thermal effects also contribute to mitochondrial metabolic suppression during torpor. The contribution of passive thermal effects can be assessed by measuring respiration rates of mitochondria from torpid animals at temperatures below 37°C, preferably temperatures reflecting the range of T_b experienced during torpor. By also examining passive thermal effects in euthermic animals, it can be determined whether mitochondria from torpid animals are more temperature-sensitive than those from euthermic animals—which would augment the impact of any passive thermal effects—and whether active, regulated suppression plays a role in reducing mitochondrial respiration at all temperatures.

A number of previous studies have shown that mitochondrial respiration rate is actively suppressed during torpor in liver mitochondria, although this suppression may depend on dietary fatty acid composition (Gerson et al. 2008). When fed standard rodent diets, liver mitochondrial state 3 respiration rate measured at 37°C was suppressed by 38-83% during torpor in several species of ground squirrels, including

thirteen-lined ground squirrels (Gehnrich and Aprille 1988; Muleme et al. 2006; Gerson et al. 2008; Armstrong and Staples 2010; Chung et al. 2011) and Arctic ground squirrels (Barger et al. 2003), compared to euthermic animals (whether summer active, interbout euthermic, or cold-acclimated non-hibernating animals). State 3 liver mitochondrial respiration rate was also up to 70% lower when measured at 37°C during bouts of spontaneous daily torpor in dwarf Siberian hamsters compared to short-day acclimated euthermic controls (Brown et al. 2007). State 4 liver mitochondrial respiration rate may also be suppressed by 18-75% in torpid compared to euthermic hibernators when measured at 37°C (Pehowich and Wang 1984; Barger et al. 2003; Armstrong and Staples 2010), though no such suppression is seen in some studies of hibernators (Gerson et al. 2008) and daily heterotherms (Brown et al. 2007).

Few studies have considered the effect of temperature on liver mitochondrial respiration rate in torpid animals, or, for that matter, in mammals in general (Dufour et al. 1996). Martin et al. (1999), Fedotcheva et al. (1985), and Brustovetsky et al. (1989) measured state 3 respiration at 25°C, 26°C, and 27°C, respectively, in isolated liver mitochondria from ground squirrels. All three studies showed significant suppression of respiration rates (by 42-75%) during torpor, suggesting that active, regulated mitochondrial metabolic suppression can also be observed at temperatures between 25° and 37°C. Muleme et al. (2006) found active suppression of torpid mitochondrial respiration measured in vitro at 37°C but not at 25°C or 5°C. Similarly, in dwarf Siberian hamsters, Brown et al. (2007) showed no active suppression of liver mitochondria at 15°C, though it had been observed at 37°C. Taken together, these studies suggest that active, regulated inhibition is most important at high temperatures

(e.g., during entrance into torpor) and passive thermal effects are most important at low temperatures (e.g., during steady-state torpor).

The first objective of this thesis, therefore, was two-fold. First, to my knowledge, only a single study of mitochondrial respiration in daily heterotherms has ever been conducted. Therefore, I wanted to determine whether liver mitochondrial state 3 and 4 respiration rates are actively suppressed during fasting-induced daily torpor in several laboratory strains of mice, *Mus musculus*, at physiologically-relevant temperatures. Mice provide a useful comparative model because they undergo daily torpor in response to fasting (Hudson and Scott 1979), whereas the previously-studied daily heterotherm, dwarf Siberian hamsters (*Phodopus sungorus*), undergoes torpor spontaneously when acclimated to short photoperiods, even when fed ad libitum (Heldmaier and Steinlechner 1981; Brown et al. 2007). Second, although Muleme et al. (2006) conducted a thorough examination of temperature effects on mitochondrial respiration in ground squirrels, they used summer active animals as their euthermic control and, therefore, did not control for seasonal effects. In the present thesis, I measured state 3 and 4 respiration rates at physiologically-relevant temperatures for liver mitochondria from torpid and interbout euthermic ground squirrels, eliminating any such seasonal effects.

Most previous work on changes in mitochondrial respiration during torpor has used mitochondria isolated from the liver because, although it accounts for only 6% of body mass in small mammals (Else and Hulbert 1981; Konarzewski and Diamond 1995), the liver is responsible for up to 12% of whole-animal oxygen consumption, making it one of the largest contributors to BMR (Martin and Fuhrman 1955). The liver

may also contribute to non-shivering thermogenesis (Stoner 1973), and so may be a quite significant contributor to RMR as well. However, observations made in liver mitochondria are often extrapolated to all other tissues even though there is no compelling evidence that mitochondria from other tissues are suppressed. No studies have examined mitochondrial respiration in tissues other than liver in any daily heterotherm, but a few studies have examined mitochondrial respiration in skeletal muscle (Barger et al. 2003; Muleme et al. 2006) and heart (South 1960) of hibernators. These studies showed no active suppression of mitochondrial respiration during torpor, and, in fact, an increased oxidative capacity of torpid heart mitochondria; however, they all used non-hibernating animals (summer active or cold-acclimated non-hibernators) as controls and, therefore, did not control for the confounding influences of seasonal and/or metabolic effects. Therefore, the second objective of the present study was to measure respiration rates at physiologically-relevant temperatures in skeletal muscle mitochondria of hibernating ground squirrels during torpor and interbout euthermia, and heart of short photoperiod-acclimated dwarf Siberian during torpor and euthermia.

On their own, measurements of mitochondrial respiration rate provide only limited information about the mechanisms by which either active suppression or passive thermal effects might reduce oxidative capacity during torpor. To elucidate mechanisms, one of two different approaches can be taken. The first, so-called “bottom-up”, approach compares rates of individual enzyme-catalyzed steps of mitochondrial OxPhos between euthermic and torpid animals. This approach has been used previously to show that pyruvate dehydrogenase (PDH) is considerably suppressed during torpor in hibernators (Storey 1997) and daily heterotherms (Heldmaier et al. 1999), for example.

While useful, there are several limitations to the "bottom-up" approach. First, enzyme activities are measured under optimal rather than physiological conditions, so extrapolation to in vivo conditions can be speculative. Second, the rates of individual reactions are measured in homogenized tissue preparations, which disrupts the IMM and other cellular structures. Therefore, there is no $\Delta\Psi_m$, which can stimulate or depress reactions that contribute to its production and consumption, respectively, and enzymes are separated from their phospholipid membrane environment, the composition of which is known to influence the activity of some membrane-bound proteins (Wu et al. 2001; 2004). Finally, changes in the rate of physiological processes among metabolic states may be regulated by changes in subcellular distribution of particular enzymes rather than any inherent change in their activity (e.g., Suozzi et al. 2009), and this would not be detected using the "bottom-up" approach unless cellular fractionation techniques were simultaneously employed.

In the present study, I chose to utilize a different approach—a so-called "top-down" approach—which groups the individual reactions of OxPhos into three components—substrate oxidation, ADP phosphorylation, and proton leakiness—which are all interrelated via ΔP (see Chapter 1 for a complete review of the "top-down" approach). Subsequently, the kinetics of each of these components can be measured and compared among metabolic states and assay temperatures. Aside from circumventing the disadvantages of the "bottom-up" approach, the "top-down" approach also permits the determination of how mitochondrial respiration is controlled and the extent to which each component contributes to any change in mitochondrial respiration among states. This provides another advantage over the "bottom-up" approach because demonstrating

suppression of a particular enzyme reaction during torpor does not simultaneously demonstrate whether that suppression actually contributes to lower rates of mitochondrial respiration observed.

The “top-down” approach has been used extensively to determine sites of inhibition of mitochondrial metabolism by several effectors (e.g., ethanol, Marcinkeviciute et al. 2000; calcium, Kavanaugh et al. 2000; thyroid hormone, Lombardi et al. 1998) for more than a decade, but few studies have used this approach to determine the sites of inhibition of mitochondrial metabolism during torpor in hibernation (Barger et al, 2003; Gerson et al., 2008) or daily torpor (Brown et al., 2007). At the same time, to my knowledge, few studies have used top-down elasticity analysis to examine temperature effects on OxPhos (Dufour et al. 1996; Chamberlain 2004; Brown et al. 2007), and only one of these studies examined a heterothermic mammal (Brown et al. 2007). Moreover, although Brown et al. (2007) examined all three components of OxPhos in their study of daily torpor in hamsters, neither study conducted using hibernators examined all three components. Therefore, the third objective of this thesis was to use the “top-down” approach to comprehensively determine the pattern of control of OxPhos in heterothermic mammals, the mechanisms responsible for active mitochondrial metabolic suppression during torpor in thirteen-lined ground squirrels and mice, as well as the effects on temperature on OxPhos in these same species, and whether temperature effects on OxPhos differ between torpid and euthermic animals. This objective was undertaken for both ground squirrels and mice using liver mitochondria, where patterns of metabolic suppression are well-established.

2.2 Experimental Procedures

2.2.1 Animals. This project was approved by the local Animal Use Subcommittee (Appendix B) and conformed to the guidelines of the Canadian Council on Animal Care. Thirteen-lined ground squirrels (*Ictidomys tridecemlineatus*) were either live-trapped in Carman, Manitoba, Canada (49°30´N, 98°01´W) or bred in captivity according to established protocols (Vaughan et al. 2006). Both males and females were used. Animals were housed individually in plastic cages (26.7 x 48.3 x 20.3 cm) and provided with corn-cob bedding, paper towel (for nest building), and a transparent red polycarbonate tube (for enrichment; 8 x 15cm; BioServ, Frenchtown NJ). Summer active animals were housed from April to October at 22°C ± 3°C with photoperiod adjusted weekly to match that of Carman, Manitoba. Food (Lab Diet 5P00) and tap water were provided ad libitum, and sunflower seeds (~10) were provided three times per week. In June, all animals underwent surgical procedures for radiotelemeter implants (see section 2.2.2). Summer active animals were acclimated to the conditions described above for at least 12 weeks prior to being sampled in August. Body mass was measured weekly throughout the summer, as well as at the time of sampling. In October, animals began to hibernate, even under these “summer” conditions, and were moved to an environmental chamber and maintained at 4°C ± 2 on a 2 h light/22 h dark photoperiod (lights on at 8h00 EST). I provided water ad libitum, but food was removed after one week of uninterrupted torpor. Torpid and interbout euthermic animals were sampled throughout January and February. Torpid animals were sampled when T_b had been at or below 5°C for at least 72 hours, and interbout euthermic animals were sampled when T_b had been 37°C ± 1 for at least 3 hours. Body mass was not measured

throughout the hibernation season but only at the time of sampling. All summer, interbout euthermic, and torpid animals were sampled at the same time of day (8h00-10h00 EST).

Three strains (Balb/c, CD1, and C57) of female house mice (*Mus musculus*) were examined in this study. Animals from all strains were obtained from Charles River Laboratories (Saint-Constant, Quebec, Canada). Animals were 2-3 months old upon arrival, and were housed individually in plastic cages (30 x 12 x 12 cm) filled with Beta Chips (for bedding) and two, 2-inch nesting squares, which they readily converted to nests. Animals were housed at 20 ± 1°C, 12 h light/12 h dark and were provided with food and tap water ad libitum. Balb/c and CD1 mice were split into two diet groups: one group was fed standard rodent chow (Prolab RMH 3000 5P00), and the other group was fed a high-linoleic acid diet (5.5 mg g^{-1} diet, TestDiets; Gerson et al. 2008) to assess diet effects on mitochondrial metabolism during torpor. Diet had no significant effect on any parameter examined in this study, and data from the two diet groups were combined. C57 mice were only fed standard rodent chow. Following recovery from surgical procedures to implant radiotelemeters (see section 2.2.2), euthermic and torpid animals were sampled randomly over a three month period. Two hours prior to the onset of darkness, animals were transferred from their cages to a Plexiglas chamber for simultaneous measurement of MR and T_b (see section 2.2.2). Water was provided ad libitum, but there was no food in the chamber because torpor in mice is induced via fasting (Hudson and Scott 1979). In our study, we considered animals torpid when T_b had been less than 31°C for at least 30 consecutive minutes, based on previous criteria (Dark et al. 1994; Brown et al. 2007), and T_b was not increasing, to ensure that animals

arousing from torpor were not sampled in this study. Animals were considered euthermic when T_b had been greater than 31°C for at least 30 consecutive minutes, and T_b was not declining. Daily torpor usually occurred for the first time about 12 hours after food was removed, and then occurred again 24 and 48 hours after the first bout. Fasting was never permitted to exceed 72 hours before animals were refed. Torpid animals used in this study were sampled during a torpor bout on the second day of fasting, allowing sufficient time for them to adjust to the respirometry chamber. Euthermic controls were sampled following spontaneous arousal from this second torpor bout, without being refed.

Male hamsters (*Phodopus sungorus*), 1 month old, were obtained from Dr. Katherine Wynne-Edwards (Queen's University, Kingston, Ontario, Canada). Animals inhabited plastic cages (30cm x 18 x 13) filled with bedding and nesting material, and were maintained at 15 ± 1°C initially on a 14-hour photoperiod, which was gradually (15 min day^{-1}) reduced to 8 hours to induce spontaneous daily torpor. All hamsters responded to the short-photoperiod acclimation, as evidenced by a change in pelage colour, characteristic in this species (Hoffmann 1973). Hamsters consumed a modified rodent chow containing 5.5 mg linoleic acid g^{-1} diet (Gerson et al. 2008), as diets high in polyunsaturated fatty acids are preferred when animals are held at this ambient temperature (Hiebert et al. 2000; 2003). Hamsters were supplied with food and tap water ad libitum throughout the experiment, and torpor occurred spontaneously over a five month period. Torpor and euthermia were determined according to the definitions above. Torpid and euthermic animals were sampled at the same time of day (9h00-11h00 EST).

2.2.2 Measurements of whole-animal oxygen consumption and body temperature. Flow-through respirometry was used to measure whole-animal oxygen consumption in ground squirrels and mice. Oxygen consumption was not measured in hamsters. Animals were placed in airtight 6L Plexiglas containers with bedding, nesting material, tap water and food (where applicable). Air scrubbed of water vapor was pumped through the container at approximately 1.8L min^{-1} (summer active squirrels), 400mL min^{-1} (hibernating squirrels), and 200 mL min^{-1} (mice). Precise flow rates were measured by a mass flow meter (model 245, Qubit Systems, Kingston, Ontario, Canada). Expired gas was subsampled at 150mL min^{-1}, scrubbed of water vapor, and the oxygen content was determined by a galvanic cell oxygen meter (model S102, Qubit Systems).

Body temperature was measured using radiotelemetry. Radiotelemeters (model TA-F20, Data Sciences International, Arden Hills, MN) were implanted intraperitoneally under isofluorane anesthesia. Postoperative analgesia (subcutaneous buprenorphrine, 0.03mg mL^{-1}, 0.1mL $100g^{-1}$) was administered twice daily for 3 days. T_b was recorded every 4-5 min using telemetry receivers (models RA1010 and RPC-1, Data Sciences International) with data acquisition software and hardware (Dataquest ART, Data Sciences International).

2.2.3 Mitochondrial isolation. For all species, torpid animals were killed by cervical dislocation to prevent arousal, whereas euthermic animals were killed by anaesthetic overdose (Euthanyl, 270 mg mL^{-1}, 0.2 mL 100 g^{-1}, intraperitoneal), as required by animal care protocols. Euthanyl has been shown to have no effects on mitochondrial metabolism (Takaki et al. 1997).

Liver mitochondria were isolated from mice using a procedure that yields a crude mitochondrial pellet. A pure mitochondrial pellet could not be obtained because mitochondrial yield is low in mice because of their small liver size (~1g). The liver was rinsed with ice-cold liver homogenization buffer (LHB: 250mM sucrose, 10mM HEPES, 1mM EGTA, pH 7.4 at 4°C) containing 1% fatty acid-free bovine serum albumin (BSA) and then cut into small pieces on ice in LHB and homogenized using three passes of a loose-fitting Teflon pestle at 100rpm in a 30mL glass mortar. The homogenate was filtered through one layer of cheesecloth and centrifuged at 1000g for 10 min at 4°C in polycarbonate centrifuge tubes. Floating lipid was aspirated from the supernatant, which was then filtered through four layers of cheesecloth and centrifuged again at 1000g for 10 min at 4°C. Once again, floating lipid was aspirated from the supernatant and filtered through four layers of cheesecloth; then, the supernatant was centrifuged at 8700g for 10 min at 4°C. The supernatant, adhering lipid, and the light pellet fraction were removed as much as possible. The dark pellet was resuspended in 30mL LHB and centrifuged at 8700g for 10 min at 4°C. The supernatant and adhering lipid were removed again, and the final pellet was resuspended in 500μL of ice-cold LHB and kept on ice until assayed.

For ground squirrels, a crude mitochondrial pellet was obtained first using the same procedure described above. This crude mitochondrial suspension was then layered on top of a Percoll gradient containing 10mL each of 10, 18, 30, and 70% Percoll (made in LHB) and centrifuged at 13,500*g* for 35 min at 4°C. Mitochondria accumulated at the boundary between the 30% and 70% layers, were removed and resuspended in LHB without BSA, and centrifuged at 8700 *g* for 10 min at 4°C to remove residual Percoll.

The mitochondrial pellet was resuspended again in LHB without BSA and centrifuged again in the same way. This purification procedure removes 85-96% of contamination from endoplasmic reticulum, peroxisomes, plasma membrane, and lysosomes, as determined through marker enzyme activity, from the mitochondrial pellet (Armstrong et al. 2010).

Skeletal muscle mitochondria from ground squirrels were isolated using a protocol that yields a crude mitochondrial pellet (Bhattacharya et al. 1991) followed by purification of this pellet (Yoshida et al. 2007). Following euthanasia, muscle tissue from both hind-limbs was excised and washed in ice-cold skeletal muscle homogenization buffer (MHB; 100mM sucrose, 10mM EDTA, 100mM Tris-HCl, 46mM KCl, pH 7.4 at 37°C). Fat, connective tissue, nerves and hair were removed. The remaining muscle tissue was decanted and suspended in 9 volumes of MHB with protease (from *Bacillus licheniformis*, Sigma, 5 mg g^{-1} wet muscle mass) while continuing to mince with fine scissors. Following 5 minutes of incubation and mincing, muscle tissue was homogenized with a loose-fitting Teflon pestle in a glass mortar (three double passes). The muscle tissue suspension was incubated on ice for 5 minutes, followed by further homogenization with a tight-fitting Teflon pestle and glass mortar (three double passes). This suspension was filtered through cheesecloth and centrifuged at 2000g for 10 min at 4°C. The supernatant was again filtered through cheesecloth and centrifuged at 10,000g for 10 min at 4°C. The remaining pellet was suspended in 5mL MHB with BSA (0.5%) and centrifuged again at 10,000*g* for 10 min at 4°C. This pellet was then suspended in MHB yielding a raw muscle mitochondrial suspension, which was purified via Percoll density gradient centrifugation. The raw mitochondrial

suspension was layered on top of a 60% Percoll solution (made in MHB) and centrifuged at 21,000*g* for 1 h at 4°C. Purified muscle mitochondria accumulated at the boundary between the MHB and 60% Percoll solution and were removed and suspended in MHB. In order to remove residual Percoll, this solution was centrifuged at 21,000*g* for 10 min at 4°C.

Heart mitochondria were isolated from hamsters using the same protocol described above for liver mitochondria from mice, with the following two modifications. First, heart homogenization buffer (HHB: 220mM mannitol, 70mM sucrose, 1mM EDTA, 10mM Tris-Cl, pH 7.4 at 4°C) was used instead of LHB. Second, following homogenization with the loose-fitting pestle, 10μg of protease (from *Bacillus licheniformis*) was added, and the homogenate was incubated on ice for 5 min. Subsequently, the homogenate was re-homogenized using three passes of a tight-fitting pestle before the first centrifugation, which was the same as described for liver mitochondria isolation for mice.

2.2.4 Mitochondrial respiration rate, membrane potential, and kinetics of oxidative phosphorylation in mice and hamsters. In mice and hamsters, mitochondrial respiration rates were measured using temperature-controlled polarographic O_2 meters (Dual Digital Model 20, Rank Brothers, Bottisham, UK) in 2mL (glutamate oxidation) or 3mL (proton leak and ADP phosphorylation kinetics) of assay buffer (225mM sucrose, 20mM HEPES, 10mM KH_2PO_4, 1% BSA, pH 7.4 at 37°C). O_2 electrodes were calibrated to air-saturated buffer using O_2 contents previously reported (Reynafarje et al. 1985), corrected for local atmospheric pressure. Unless otherwise stated, all compounds used were dissolved in assay buffer. In all cases, the

concentrations provided are the final concentrations of the compounds in the chamber of the oxygen electrodes during measurements of respiration rate.

For measurements of glutamate oxidation, mitochondria were added to the chamber of the O_2 meter, and glutamate (5mM) and malate (1mM) were added thereafter, followed by ADP (0.1mM). The addition of ADP brought about state 3 respiration rate. Oligomycin (10μg mL^{-1}, dissolved in ethanol) was added to inhibit ATP synthase, approximating state 4 respiration.

In mice and hamsters, both proton leak and ADP phosphorylation kinetics were measured using succinate to fuel respiration. State 3 and 4 respiration rates for succinate oxidation were taken from these curves rather than measured separately. Proton leak and ADP phosphorylation kinetics require simultaneous measurements of oxygen consumption and ΔP, which is the sum of $\Delta\Psi_m$ and ΔpH. I measured $\Delta\Psi_m$ as an approximation of ΔP. In some other studies (e.g, Barger et al. 2003), nigericin has been added to collapse ΔpH so that ΔP is fully expressed as $\Delta\Psi_m$; however, in the current study, nigericin was not used. This is appropriate if changes in the mitochondrial pH gradient (ΔpH) are negligible, which has been demonstrated for mammalian mitochondria in other studies (Dufour et al. 1996; Marcinkeviciute et al. 2000).

To measure proton leak kinetics, rotenone (2μg mL^{-1}, dissolved in ethanol) was added to inhibit complex I, and oligomycin (10μg mL^{-1}, dissolved in ethanol) was added to inhibit ATP synthase (i.e., to inhibit the phosphorylation component of OxPhos). To measure $\Delta\Psi_m$, we used tetraphenylphosphonium (TPP^+), a lipophilic cation, whose uptake by mitochondria is $\Delta\Psi_m$-dependent (Kamo et al. 1979). A TPP^+-selective electrode (World Precision Instruments, Sarasota FL) was inserted into the O_2 electrode

chamber to measure external [TPP^+]. The TPP^+ electrode was calibrated by making five additions of TPP^+: each addition increased external [TPP^+] by 1μM, and the final total [TPP^+] was 5μM. Once calibrated, mitochondria (~1.0mg protein at 37°C; ~1.3mg protein at 15°C) were added to the chamber. Subsequently, succinate (6mM) was added to stimulate state 4 respiration. The kinetics of proton leak were determined by inhibiting substrate oxidation stepwise by adding malonate (5 additions, each of which increased the concentration of malonate by 0.5mM in the assay buffer) and measuring the effect on $\Delta\Psi_m$ (see section 1.2.4 for theoretical details). After the final malonate addition, carbonyl cyanide chlorophenylhydrazone (CCCP; 0.1μM, dissolved in ethanol) was added to completely uncouple the mitochondria and allow for correction of electrode drift.

$\Delta\Psi_m$ was calculated from the external [TPP^+] using a modified Nernst equation (Equation 2-1) , as in Barger et al. (2003):

$$\Delta\Psi_m = a \log \left(\frac{([TPP^+]_{added} - [TPP^+]_{external})(b)}{(v)(\text{mg protein})([TPP^+]_{external})} \right) \quad \text{(Equation 2-1).}$$

In Equation 2-1, *a* is a temperature-dependent coefficient ($a = 2.3RT/F$, where R is the universal gas constant, T is absolute temperature, and F is the Faraday constant), *b* is a binding constant used to correct for non-specific binding of TPP^+, and *v* is the mitochondrial matrix volume. The value of *b* was 0.16 (Lombardi et al. 1998) and the value of *v* was 0.001mL mg^{-1} protein (Halestrap 1989), both of which were determined for rat liver mitochondria. Although I did not determine whether mitochondrial volume

changes with metabolic state and/or temperature, the effect of changes in mitochondrial volume is negligible when TPP^+ is used (Rottenberg 1984). It is also assumed that non-specific binding of TPP^+ does not change with temperature.

For determination of the kinetics of ADP phosphorylation, oxygen consumption and $\Delta\Psi_m$ were again measured simultaneously. Rotenone (2μg mL^{-1}, dissolved in ethanol) was added to inhibit complex I. $\Delta\Psi_m$ was measured as described for proton leak kinetics, above. Once the TPP^+ electrode was calibrated, mitochondria were added to a final concentration of ~0.7mg protein mL^{-1} for 37°C and ~1.0mg protein mL^{-1} for 15°C. Succinate (6mM) and ADP (1mM) were added to stimulate state 3 respiration; this concentration of ADP was sufficient to support state 3 respiration for the period of time required to complete the required measurements. The kinetics of ADP phosphorylation were determined by inhibiting substrate oxidation stepwise by adding malonate (5 additions to 0.33mM each in assay). After the final malonate addition, CCCP (0.1μM) was added to allow for correction of electrode drift.

Both proton leakiness and ADP phosphorylation kinetics data were fitted to a 3-parameter exponential curve using SigmaPlot 2001. Because some small amount of proton leak contributes to state 3 respiration, oxygen consumption values for the ADP phosphorylation curves were corrected by calculating proton leak-dependent oxygen consumption at all $\Delta\Psi_m$ values. The kinetics of the substrate oxidation component were not measured directly. Instead, they were represented by the straight line that connects the uninhibited state 3 (from the phosphorylation kinetics) and uninhibited state 4 (from the proton leak kinetics) measurements, as in Barger et al. (2003).

2.2.5 Mitochondrial respiration rate, membrane potential, and kinetics of oxidative phosphorylation in ground squirrels. In ground squirrels, mitochondrial respiration rates and membrane potentials were measured using a high-resolution respirometer equipped with a TPP^+-selective electrode and a MI-401 micro-reference electrode (O2k-MiPNetAnalyzer, Oroboros, Innsbruck, Austria). Oxygen electrodes were calibrated to air-saturated buffer and oxygen-depleted buffer (obtained by addition of yeast suspension) using published oxygen solubilities (Forstner and Gnaiger 1983), corrected for local atmospheric pressure.

Unless otherwise noted, all compounds were dissolved in MiR05 buffer (110mM sucrose, 0.5mM EGTA, 3mM $MgCl_2$, 60mM K-lactobionate, 20mM taurine, 10mM KH_2PO_4, 20mM HEPES, pH 7.1 at 30°C, 1% BSA), and the concentrations provided are the final concentrations of the compounds in the chamber of the oxygen electrode during respiration rate measurements. For glutamate-fueled respiration, mitochondria were added to 2mL of MiR05 buffer equilibrated to 37°C, 25°C, or 10°C. Glutamate (10mM) and malate (2mM) were subsequently added, followed by ADP (0.2mM) to stimulate state 3 respiration. State 4 respiration was subsequently estimated by adding oligomycin (10μg mL^{-1}, dissolved in ethanol).

State 3 and 4 respiration rates for succinate-fueled respiration were taken from ADP phosphorylation and proton leak kinetic curves, respectively. ADP phosphorylation, proton leak, and substrate oxidation kinetics were measured as described above, except for the following changes. For TPP^+ electrode calibration, the first addition increased TPP^+ concentration in the chamber to 1μM, and each subsequent addition increased TPP^+ concentration by 0.5μM. The final concentration in the

chamber was 3μM. 10mM succinate was used for both ADP phosphorylation and proton leak kinetics, and 2mM ADP was used to stimulate state 3 respiration for determination of ADP phosphorylation kinetics. Effects of compounds used on TPP^+ concentration readings in the absence of mitochondria, as well as dilution effects caused by addition of compounds, were determined, and all measurements of TPP^+ were corrected for these effects. $\Delta\Psi_m$ was calculated from TPP^+ concentration via a modified Nernst equation from Labajova et al. (2006):

$$\Delta\Psi_m = a \log\left(\frac{V_0\,[TPP^+]_{added}/[TPP^+]_{external} - V_t - K_o(\text{mg protein})}{v(\text{mg protein}) + K_i P}\right) \quad \text{(Equation 2-2).}$$

In Equation 2-2, a, $[TPP^+]_{added}$, $[TPP^+]_{external,}$ and v are the same as described in section 2.2.4; V_0 and V_t are the amount of assay buffer in the chamber before and after addition of mitochondria, respectively; and K_o and K_i are partition coefficients that reflect the passive distribution of TPP^+. Proton leakiness and ADP phosphorylation curves were fitted as described in section 2.2.4, and ADP phosphorylation curves were corrected for the contribution of proton leak.

2.2.6 Data analysis. All values presented are means ± SEM. Differences in state 3 and 4 respiration were analyzed separately for each tissue and species using a general linear model (SAS 9.2) that examined the effect of metabolic state (euthermic vs. torpid), assay temperature, and strain (for mice), and their interactions. Non-significant interactions were dropped from all models. Correlations between respiration rate and T_b at sampling (in mice) were also analyzed using a general linear model. Both linear and

quadratic correlations were examined, and a quadratic relationship was fitted when it was significant.

Differences in ADP phosphorylation, proton leak, and substrate oxidation curves between metabolic states and assay temperatures were analyzed using a custom-designed algorithm in Excel 2003 (see Appendix A). Overall control coefficients and integrated elasticity values were calculated from the mean values of mitochondrial respiration rate and $\Delta\Psi_m$ from these kinetic curves according to equations in Hafner et al. (1990) and Ainscow and Brand (1999; see also Appendix A). In this way, these values reflect data from a number of individuals even though no measure of variability was derived.

2.3 Results

2.3.1 Changes in whole-animal parameters during torpor. Thirteen-lined ground squirrels underwent considerable changes in body mass, T_b, and MR over the course of the year. In spring, the body mass of ground squirrels used in this study was 228.7 g ± 5.1 (n=21). Body mass increased over the summer, and by late August, when summer active animals were sampled, body mass had increased by 15% and reached its plateau (264.8g ± 18.4; n=8). Body mass subsequently declined over the late fall and early winter, while animals were hibernating, and by January and February, when torpid and interbout euthermic animals were sampled, body mass had declined by nearly half of the maximal summer value (146.0g ± 6.67; n=13). Summer active animals had a body temperature of 36.0°C ± 1.0 (n=8) and an average MR of 1.4 mL O_2 g^{-1} h^{-1} (n=2). Hibernating animals showed a typical pattern of changes in T_b and MR over the

hibernation season (Figure 1-1B). During torpor, T_b and MR were quite low (3.8°C ± 0.11, n=8; and 0.21 mL O_2 g^{-1} h^{-1} ± 0.03, n=4; respectively), whereas during interbout euthermia, T_b returned to levels not different from summer active animals (37.1°C ± 0.94; n=5), while MR was, on average, 4.43 mL O_2 g^{-1} h^{-1} ± 1.5 (n=4), nearly 5-fold higher than summer active levels.

A preliminary experiment with Balb/c mice, in which T_b but not MR was monitored, was carried out to characterize fasting-induced daily torpor in mice. Over a 72-hour fasting period, mice typically underwent one or two torpor bouts each day (Figure 1-3A) and spent nearly 40% of their time in torpor (T_b < 31°C). Torpor bouts typically began during the late part of the scotophase (active phase for these nocturnal mice) and terminated during the early part of the photophase. Average bout length duration was 5.6 h ± 0.4 (n=16), with no bouts lasting longer than 8 hours. Animals from three different mouse strains (Balb/c, CD1, C57) were sampled for mitochondrial isolation studies. Over the ~40-hour fasting period used to induce torpor bouts, body mass declined by 18% in all strains, predominantly over the first 24 hours. At sampling, in all three strains, T_b was 36.2°C ± 0.51 and 25.5°C ± 0.75, and MR was 3mL O_2 g^{-1} h^{-1} ± 0.39 and 1.15mL O_2 g^{-1} h^{-1} ± 0.22, for euthermic (n=20) and torpid (n=23) animals, respectively (Figure 1-3B).

Hamsters underwent torpor spontaneously (Figure 1-2). Torpor bouts generally started just as the photophase (the resting period for these nocturnal hamsters) began and terminated before the scotophase began. At the time of sampling, T_b was 36.1°C ± 0.09 and 24.4°C ± 0.38 in euthermic (n=3) and torpid (n=3) animals, respectively. In addition, there was a significant difference in body mass at sampling between euthermic

(35.2g ± 1.6) and torpid (26.5g ± 0.48) animals, consistent with previous work in this species (Brown et al. 2007). Whether this reflects a chronic difference in body mass throughout the period of acclimation to short days between animals that underwent torpor and animals that did not, or whether it reflects a decline in body mass that is closely associated with the expression torpor, is unknown since body mass was only measured at sampling.

2.3.2 Liver mitochondrial respiration rate during hibernation and daily torpor. In thirteen-lined ground squirrels, state 3 and 4 mitochondrial respiration rate with glutamate did not differ between torpor and interbout euthermia (Figure 2-1A); by contrast, with succinate, state 3 and 4 respiration rate were 70% and 25% lower, respectively, in torpid animals than interbout euthermic animals (Figure 2-1B). In mice, state 3 respiration with glutamate was lower in torpid animals compared to euthermic animals in CD1 and C57 mice by 34% and 33%, respectively, but not Balb/c mice; however, state 4 respiration did not differ between metabolic states in any strain (Figure 2-2A-C). With succinate, on the other hand, while state 4 respiration did not differ among metabolic states in any strain, state 3 respiration rate was 35% and 22% lower during torpor than interbout euthermia in Balb/c and C57 mice, respectively, but was actually 17% higher in CD1 mice during torpor (Figure 2-2D-F).

Mice were sampled either when euthermic or torpid according to established criteria (see Experimental Procedures, section 2.2.2); notwithstanding, the steady-state T_b of euthermic animals at the time of sampling ranged from 33.9°C to 37.6°C, while that of torpid animals ranged from 21.5°C to 30.5°C. Similar variation in MR, which correlated with T_b (data not shown; euthermic: $r^2 = 0.34$, $P = 0.03$; torpid: $r^2 = 0.30$, $P =$

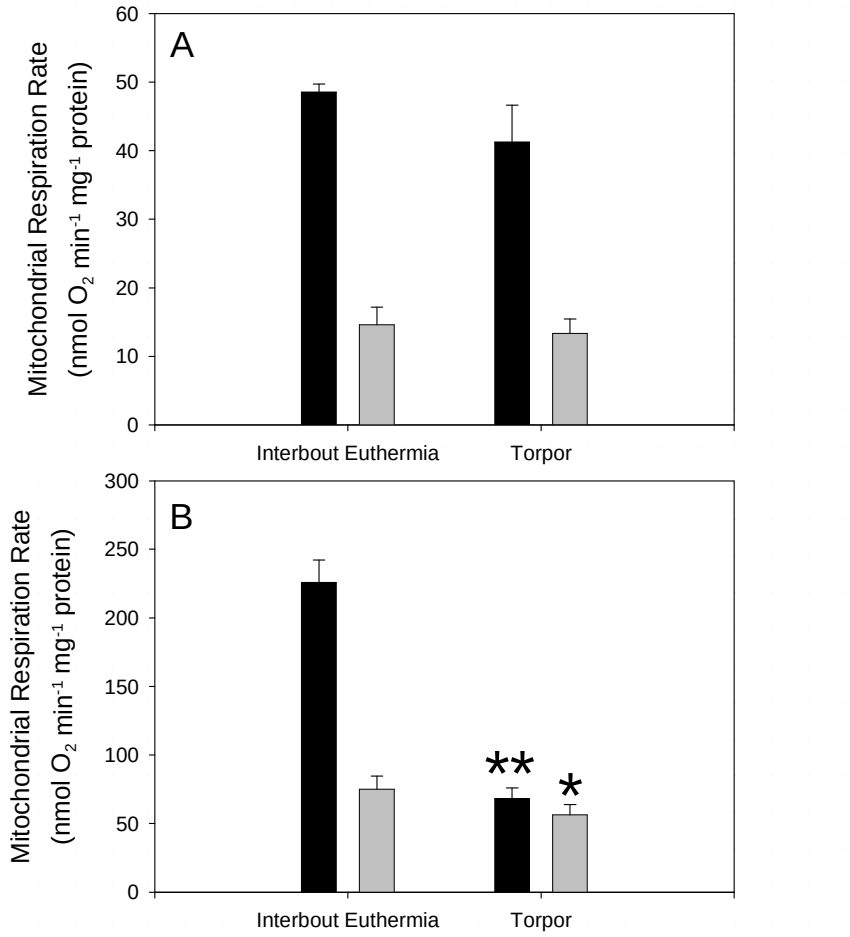

Figure 2-1. Liver mitochondrial respiration rate measured at 37°C during hibernation in thirteen-lined ground squirrels. Respiration fueled by glutamate (A) or succinate (B) was measured during torpor and interbout euthermia. Black and grey bars represent state 3 and 4 respiration rates, respectively. **, $P < 0.01$; *, $P < 0.05$ compared to interbout euthermia. Data shown are mean ± SEM. N=5 for interbout euthermia, N=8 for torpor.

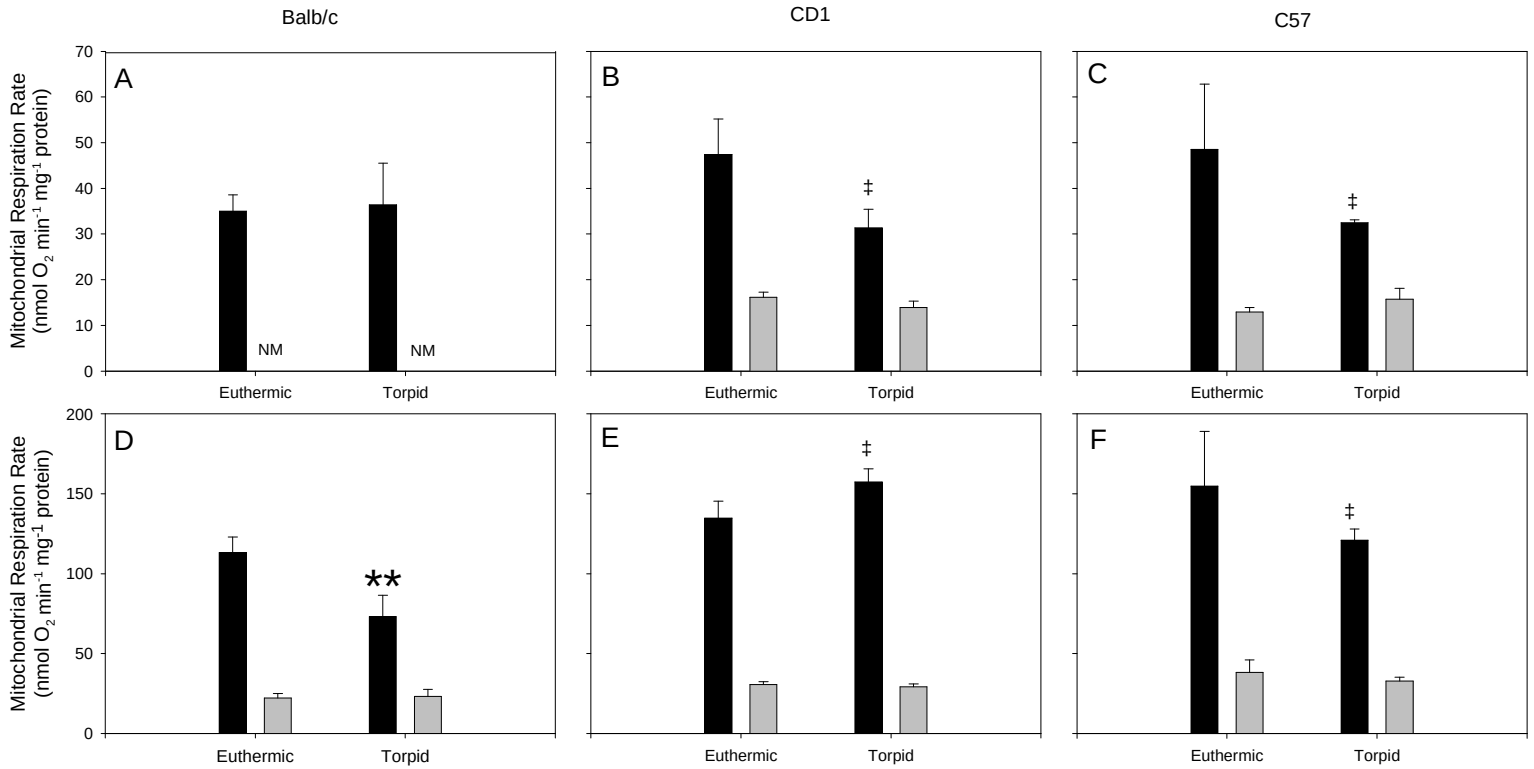

Figure 2-2. Liver mitochondrial respiration rate measured at 37°C in three strains of mice during fasting. Respiration was fueled by glutamate (upper panels) or succinate (lower panels). Black and grey bars represent state 3 and 4 respiration rates, respectively. **, P<0.01; ‡, P < 0.10 compared to euthermic animals. NM, not measured. Data shown are mean ± SEM. For Balb/c and CD1, N=8 for both euthermia and torpor. For C57, N=4 for euthermia, N=7 for torpor.

0.03), was observed. There was no effect of T_b at sampling on state 4 respiration rate regardless of substrate (data not shown), and glutamate-driven state 3 respiration tended to decrease as T_b declined in euthermic animals, but this was not statistically significant (Figure 2-3A). With succinate, however, the correlation between T_b and state 3 respiration rate was positive and linear for euthermic animals, such that mitochondrial respiration declined with T_b (Figure 2-3B). During torpor, glutamate-driven respiration was negatively correlated with T_b, such that respiration rate was lowest in animals sampled when T_b was relatively high (Figure 2-3C). For torpid animals, on the other hand, in the two strains of mice in which succinate oxidation was suppressed (Balb/c and C57), the correlation was quadratic, and mitochondrial respiration rate was lowest in animals with T_b near 25°C at sampling (Figure 2-3D).

2.3.3 Effects of assay temperature on liver mitochondrial respiration rates. In ground squirrels, while state 3 respiration rate with glutamate did not differ among metabolic states at 37°C, it was 57% and 64% lower in torpid animals than interbout euthermic animals at 25°C and 10°C, respectively (Figure 2-4A). On the other hand, state 4 respiration rate did not differ between metabolic states regardless of assay temperature (Figure 2-4B). With succinate, state 3 respiration, which was lower in torpid animals by 70% at 37°C, was also 77% lower in torpid animals at 25°C but did not differ among metabolic states at 10°C (Figure 2-4C). On the other hand, state 4 respiration rate was 20-40% lower in torpid animals regardless of the temperature (Figure 2-4D). In Balb/c mice, with succinate, while state 3 respiration rate was lower in torpid animals than euthermic animals at 37°C, it was not lower in torpid animals at 15°C (Figure 2-5A). By contrast, state 4 respiration rate did not differ among metabolic

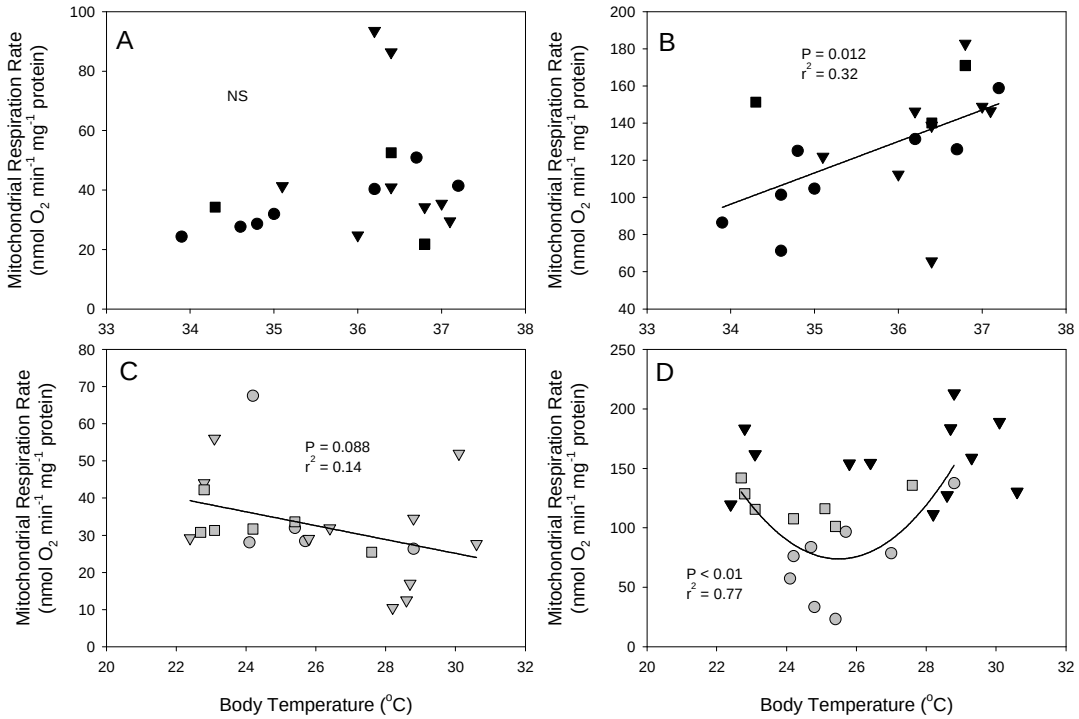

Figure 2-3. Effect of body temperature at time of sampling on liver mitochondrial state 3 respiration rate measured at 37°C in three strains of mice during fasting. In all panels, Balb/c (circles), CD1 (triangles), and C57 (squares) are shown. Data for euthermic and torpid animals are shown as black and grey symbols, respectively, except for CD1 torpid mice with succinate (panel D), which are shown in black because no suppression was observed during torpor in this strain. Respiration in euthermic animals with glutamate (A) or succinate (B), and respiration in torpid animals with glutamate (C) or succinate (D) are shown. Significant linear and quadratic relationships between respiration rate and body temperature are shown.

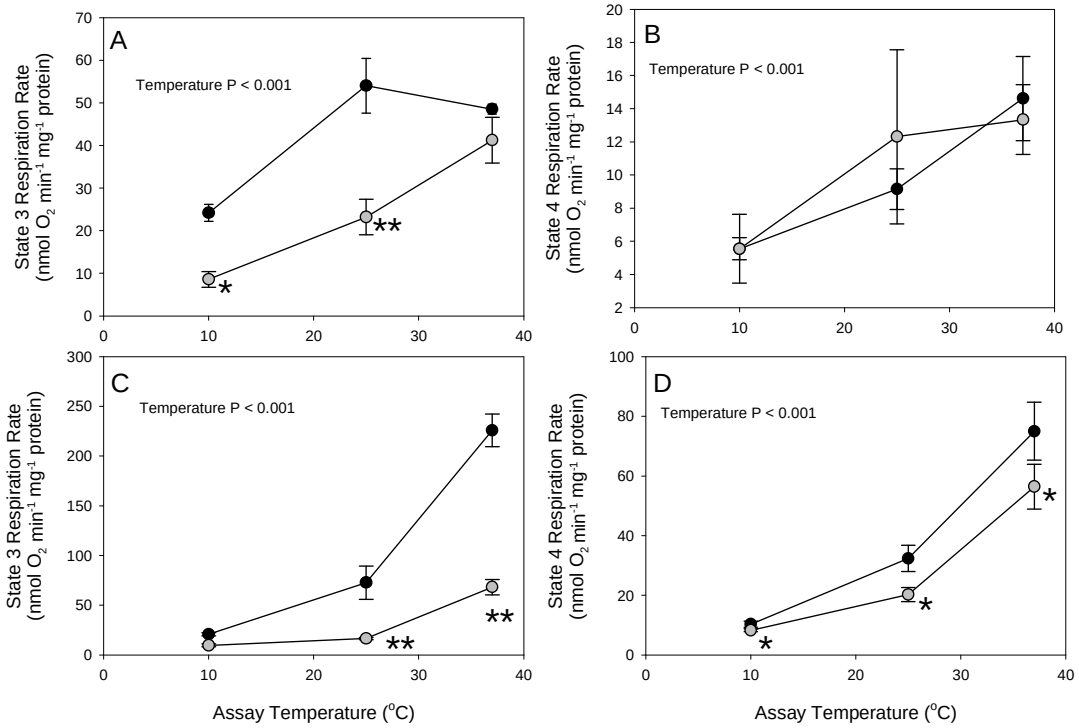

Figure 2-4. Effect of assay temperature on liver mitochondrial respiration in hibernating thirteen-lined ground squirrels. Respiration rates of interbout euthermic (black symbols) and torpid (grey symbols) animals were measured using glutamate (A,B) or succinate (C,D). The data at 37°C is the same as shown in Figure 2-1. The statistical significance of assay temperature effects are indicated by P values in each panel. These temperature effects did not differ between metabolic states in any case. Data shown are mean ± SEM. N=5 for interbout euthermia, N=8 for torpor. At each temperature, differences between interbout euthermic and torpid animals are shown using symbols. **, $P < 0.01$; *, $P < 0.05$ vs. interbout euthermic animals.

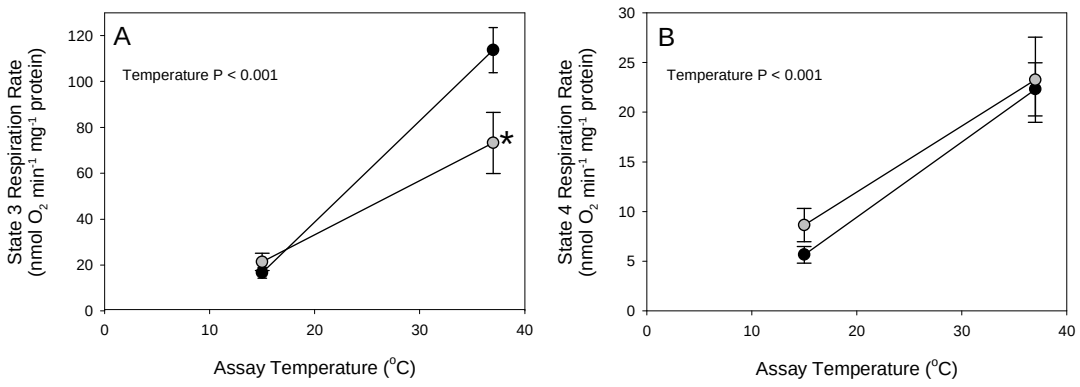

Figure 2-5. Effect of assay temperature on liver mitochondrial respiration in fasted Balb/c mice. Respiration rates of euthermic (black symbols) and torpid (grey symbols) animals were measured using only succinate under state 3 (A) and state 4 (B) conditions. The data at 37°C is the same as shown in Figure 2-2. Data shown are mean ± SEM. N=8 for both euthermia and torpor. The statistical significance of temperature effects are indicated by P values in each panel. Temperature effects did not differ between metabolic states in any case. At each temperature, differences between euthermic and torpid animals are shown using symbols. *, $P < 0.05$ vs. euthermic animals.

states regardless of the assay temperature (Figure 2-5B). I did not measure respiration rate with glutamate at any temperature other than 37°C, and I did not measure respiration rates in either CD1 or C57 mice at 15°C. In both ground squirrels and Balb/c mice, respiration rates declined with temperature. For the most part, the temperature-sensitivity of mitochondrial respiration, as inferred from Q_{10} values, did not differ among metabolic states (data not shown).

2.3.4 Changes in mitochondrial respiration during torpor in skeletal muscle and heart. Skeletal muscle mitochondrial respiration was measured in torpid and interbout euthermic ground squirrels. When measured at 37°C, state 3 respiration rate with glutamate did not differ between metabolic states, but state 4 respiration rate was 60% higher in torpid animals compared to interbout euthermic animals (Figure 2-6A). On the other hand, with succinate, state 4 respiration rate did not differ between metabolic states, but state 3 respiration rate was 32% lower in torpid animals than interbout euthermic controls (Figure 2-6B). For mitochondria from both torpid and interbout euthermic animals, a drop in assay temperature from 37°C to 5°C led to a decline in state 3 and 4 respiration rates up to 92% and 68%, respectively, with both respiratory substrates. With glutamate, state 3 respiration rate did not differ between metabolic states at either 25°C or 10°C, consistent with my observations at 37°C (Figure 2-7A), but state 4 respiration rate remained higher in torpid animals than interbout euthermic animals at both low assay temperatures, being almost 90% higher at 10°C (Figure 2-7B). With succinate, state 3 respiration rate remained 33% lower in torpid animals than interbout euthermic animals at 25°C but not 10°C (Figure 2-7C), and state 4 respiration did not differ between metabolic states regardless of temperature (Figure 2-7D).

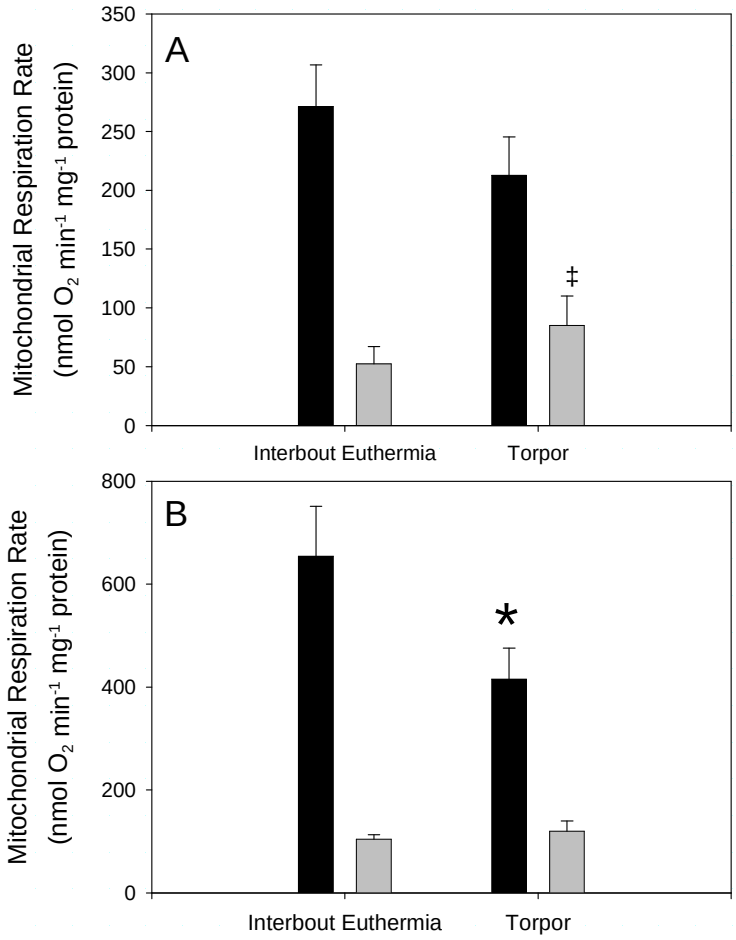

Figure 2-6. Skeletal muscle mitochondrial respiration rate measured at 37°C during hibernation in thirteen-lined ground squirrels. Respiration rate fueled by glutamate (A) or succinate (B) was measured during either torpor or interbout euthermia. Black and grey bars represent state 3 and 4 respiration rates, respectively. Data shown are mean ± SEM. N=5 for interbout euthermia, N=8 for torpor. *, $P < 0.05$; ‡, $P < 0.10$, compared to interbout euthermia.

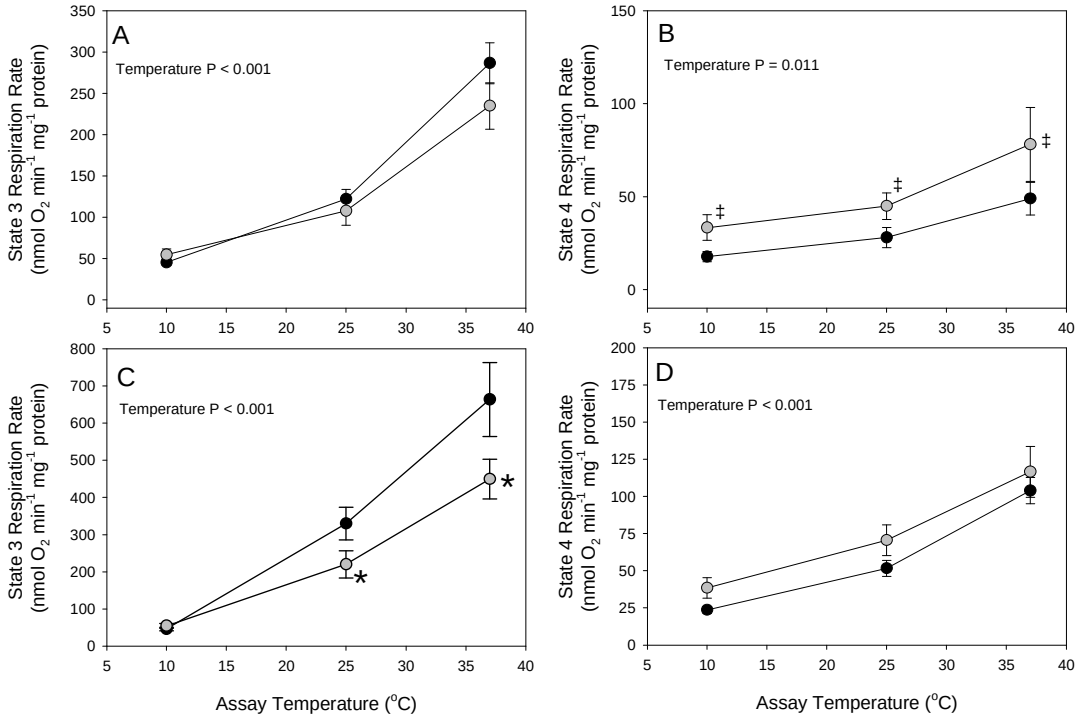

Figure 2-7. Effect of assay temperature on skeletal muscle mitochondrial respiration in hibernating thirteen-lined ground squirrels. Respiration rates of interbout euthermic (black symbols) and torpid (grey symbols) animals were measured using glutamate (A,B) or succinate (C,D). The data at 37°C is the same as shown in Figure 2-6. Data shown are mean ± SEM. N=5 for interbout euthermia, N=8 for torpor. The statistical significance of temperature effects are indicated by P values in each panel. Temperature effects did not differ between metabolic states in any case. At each temperature, differences between interbout euthermic and torpid animals are shown using symbols. ‡, $P < 0.10$; *, $P < 0.05$ vs. interbout euthermic animals.

Heart mitochondrial respiration was measured in short photoperiod-acclimated dwarf Siberian hamsters during torpor and euthermia. At 37°C, both state 3 and 4 respiration rates were more than 2-fold higher in torpid animals compared to euthermic animals when glutamate fueled respiration (Figure 2-8A), but the respiratory control ratio (RCR; state 3/state 4), often used as an indicator of the quality of a mitochondrial preparation, was quite low (1.02 ± 0.14). When succinate fueled respiration, there was no difference in either state 3 or state 4 respiration rate between metabolic states (Figure 2-8B), but the respiratory control ratio was 2.65 ± 0.29, consistent with previous studies of heart mitochondria using succinate in rats (e.g. Chen et al. 2008). I believe that the heart mitochondria isolated for this study were not damaged during isolation but rather that glutamate transport and/or GDH (rather than ADP) limits glutamate oxidation in heart mitochondria (see Discussion). For the most part, respiration rate declined with temperature, except for state 3 respiration with glutamate. Both state 3 (Figure 2-9A) and state 4 (Figure 2-9B) respiration rate fueled by glutamate were higher in torpid animals at both 15°C and 26°C, consistent with observations at 37°C. Interestingly, however, RCR was higher at these lower temperatures such that it was 2.9 ± 0.98 and 2.1 ± 0.27 at 26°C and 15°C, respectively. With succinate, regardless of assay temperature, neither state 3 (Figure 2-9C) nor state 4 (Figure 2-9D) respiration differed between metabolic states, and RCR remained as high at 15°C (2.62 ± 0.19) and 26°C (3.25 ± 0.38) as at 37°C.

2.3.5 Kinetics and control of oxidative phosphorylation in liver mitochondria during hibernation and daily torpor. In ground squirrels, when measured at 37°C, substrate oxidation activity was lower in torpid animals than interbout euthermic

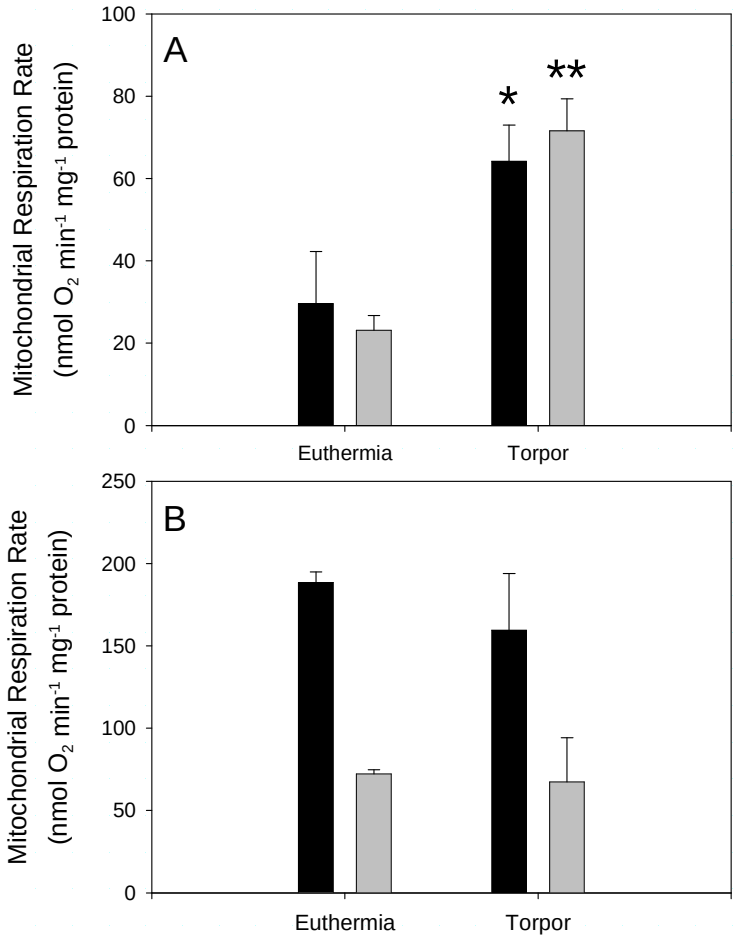

Figure 2-8. Heart mitochondrial respiration rate measured at 37°C in short photoperiod-acclimated dwarf Siberian hamsters. Respiration rate fueled by glutamate (A) or succinate (B) was measured during either torpor or euthermia. Black and grey bars represent state 3 and 4 respiration rates, respectively. Data shown are mean ± SEM. N=3 for both euthermia and torpor. **, $P < 0.01$; *, $P < 0.05$ compared to interbout euthermia.

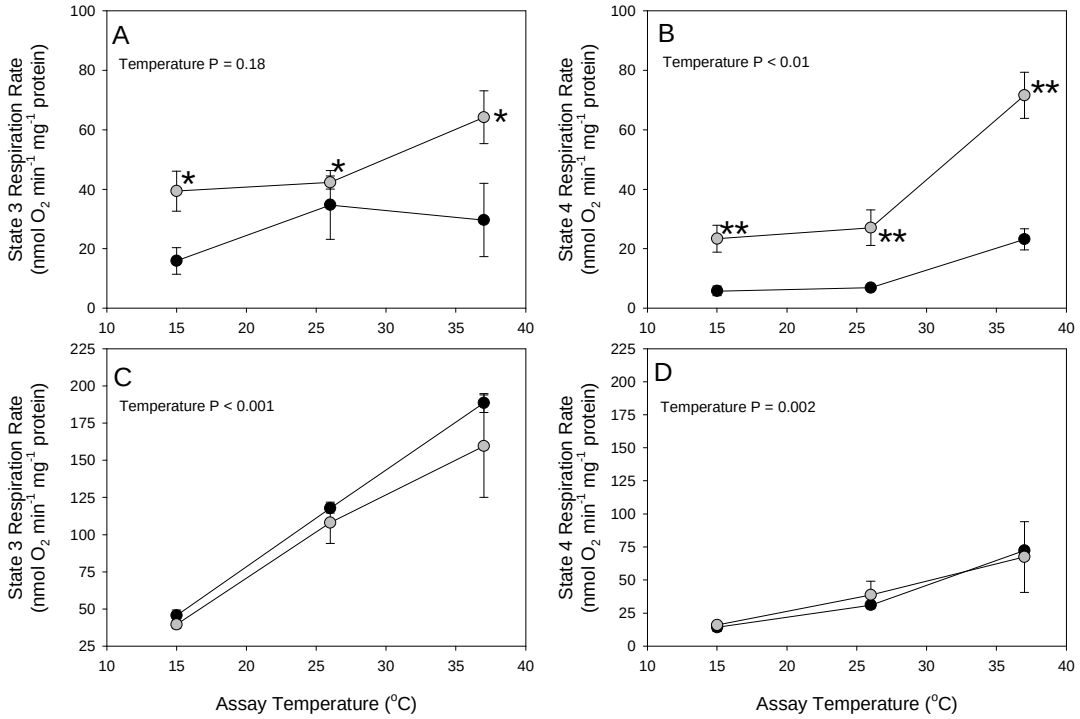

Figure 2-9. Effect of assay temperature on heart mitochondrial respiration in short photoperiod-acclimated dwarf Siberian hamsters. Respiration rates of euthermic (black symbols) and torpid (grey symbols) animals were measured using glutamate (A,B) or succinate (C,D). The data at 37°C is the same as shown in Figure 2-8. Data shown are mean ± SEM. N=3 for both euthermia and torpor. The statistical significance of temperature effects are indicated by P values in each panel. Temperature effects did not differ between metabolic states in any case. At each temperature, differences between interbout euthermic and torpid animals are shown using symbols. **, $P < 0.01$; *, $P < 0.05$ vs. interbout euthermic animals.

animals (Figure 2-10A). Similarly, ADP phosphorylation activity was also lower in torpid animals (Figure 2-10B). By contrast to substrate oxidation and ADP phosphorylation, IMM proton leakiness was actually higher in torpid animals than interbout euthermic animals (Figure 2-10C). In interbout euthermic animals, substrate oxidation had the majority of the control over both state 3 and 4 respiration rate, and this control increased considerably in torpid animals, leaving ADP phosphorylation and IMM proton leakiness with little control over state 3 and state 4 respiration, respectively, in torpid animals (Table 2-1).

In Balb/c mice, at 37°C, substrate oxidation activity was lower in torpid animals than interbout euthermic animals at state 3 $\Delta\Psi_m$ values, but was higher at state 4 $\Delta\Psi_m$ values (Figure 2-11A). By contrast, substrate oxidation activity did not differ in either CD1 (Figure 2-11B) or C57 mice (Figure 2-11C). In both Balb/c (Figure 2-12A) and C57 mice (Figure 2-12C), ADP phosphorylation activity was lower in torpid animals than interbout euthermic animals, particularly at $\Delta\Psi_m$ values above 100mV. By contrast, in CD1 mice (Figure 2-12B), ADP phosphorylation activity was higher in torpid animals. IMM proton leakiness differed between metabolic states only in Balb/c mice, where leakiness was lower in torpid animals than interbout euthermic animals at $\Delta\Psi_m$ values above 145mV (Figure 2-13A). In both CD1 (Figure 2-13B) and C57 mice (Figure 2-13C), there was no difference in leakiness among metabolic states. Control over mitochondrial respiration in mice showed little variation among strains and did not shift drastically during torpor for the most part (Table 2-2). In all three mouse strains, substrate oxidation had the majority of control over state 3 respiration rate in euthermic animals. In Balb/c and CD1 mice, the control exerted by substrate oxidation increased

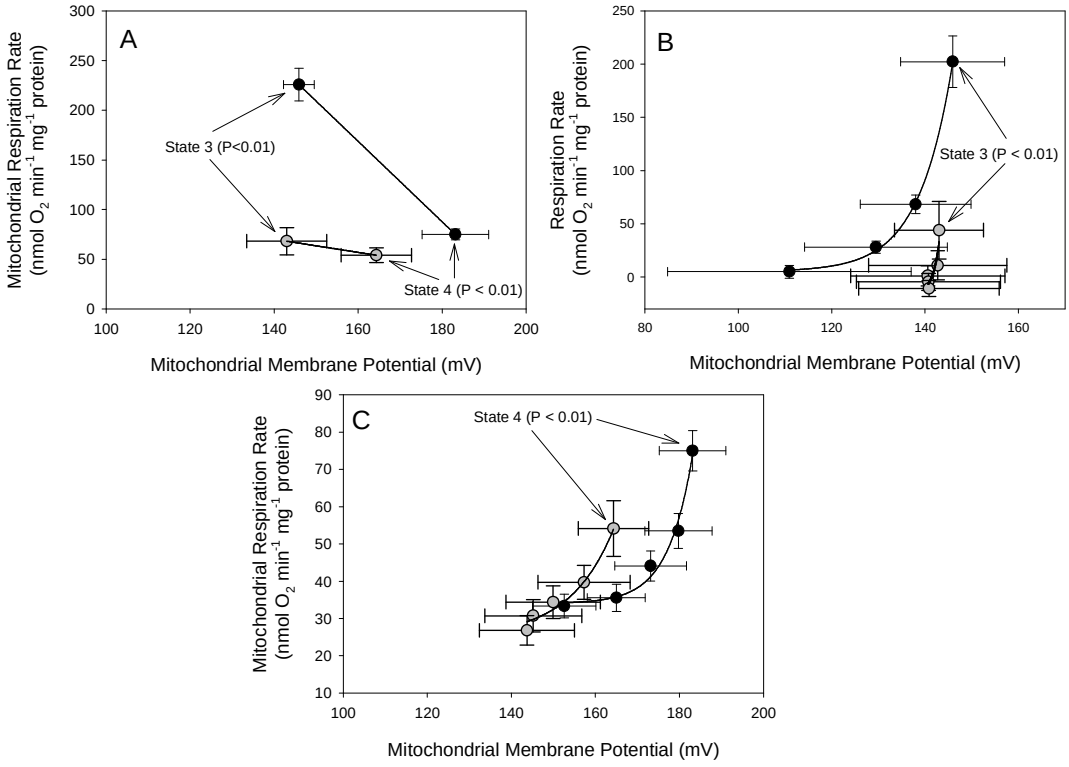

Figure 2-10. Kinetics of oxidative phosphorylation measured at 37°C in liver mitochondria during hibernation in thirteen-lined ground squirrels. The kinetics of substrate oxidation (A), ADP phosphorylation (B), and proton leakiness (C) were measured in torpid (grey symbols) and interbout euthermic (black symbols) animals. Data shown are mean ± SEM. N=5 for interbout euthermia, N=8 for torpor. Kinetic differences between metabolic states were determined by a custom-designed algorithm (see Experimental Procedures), and P-values are presented. P-values indicate whether the two curves differ only at the level of respiration rate indicated, not along the entire length of the curve.

Table 2-1. Distribution of control over liver mitochondrial respiration by the three components of oxidative phosphorylation at three assay temperatures during interbout euthermia (IBE) and torpor in thirteen-lined ground squirrels. Overall control coefficients for state 3 (A) and state 4 (B) were calculated using mean values for membrane potential and respiration rate from kinetic curves measured in Figure 2-10 for 37°C, and kinetic curves measured at 25°C and 10°C (data not shown), as well as the equations described in the Experimental Procedures.

A.	37°C		25°C		10°C	
	IBE	Torpor	IBE	Torpor	IBE	Torpor
Substrate Oxidation	0.87	0.98	0.92	1.77	0.93	1.09
ADP Phosphorylation	0.12	0.01	0.07	-0.18	0.06	-0.05
Proton Leakiness	0.02	0.01	0.01	-0.59	0.01	-0.05

B.	37°C		25°C		10°C	
	IBE	Torpor	IBE	Torpor	IBE	Torpor
Substrate Oxidation	0.63	0.81	0.66	4.44	0.66	1.19
ADP Phosphorylation	0	0	0	0	0	0
Proton Leakiness	0.37	0.19	0.34	-3.43	0.34	-0.19

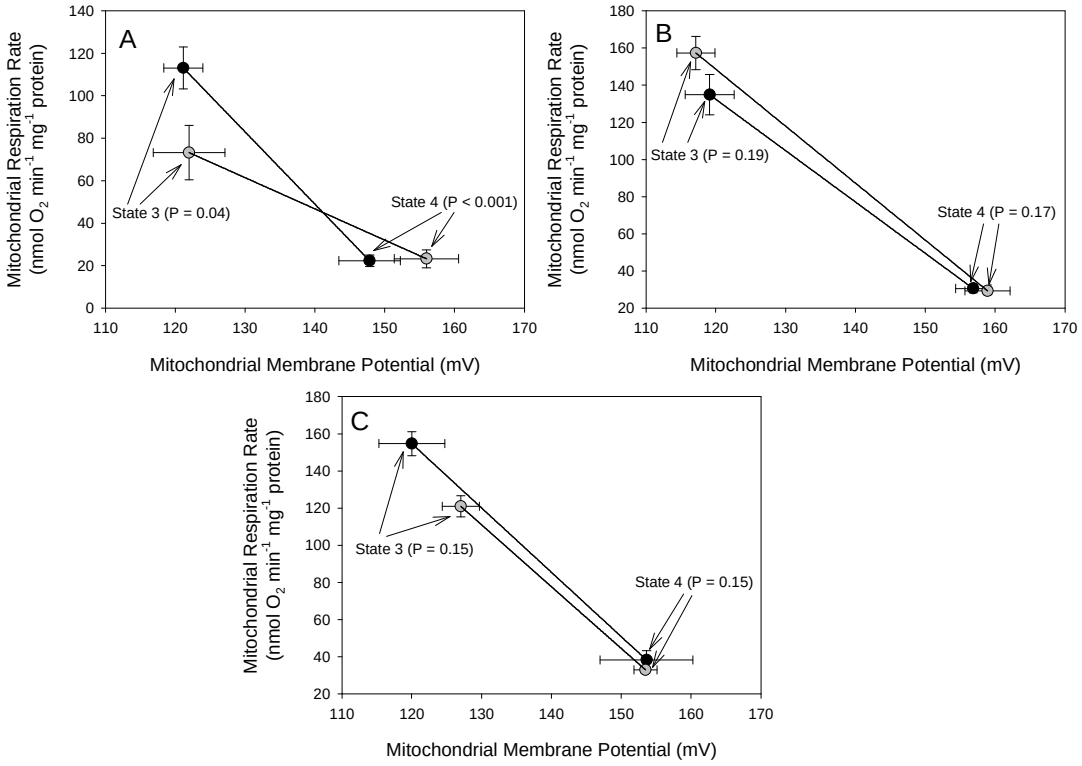

Figure 2-11. Kinetics of substrate oxidation measured at 37°C in liver mitochondria from three strains of mice during fasting. In each panel, substrate oxidation kinetics is shown for mitochondria from euthermic (black symbols) and torpid (grey symbols) animals. Kinetics were measured in Balb/c (A), CD1 (B), and C57 (C). Data shown are mean ± SEM. For Balb/c and CD1, N=8 for both euthermia and torpor. For C57, N=4 for euthermia, N=7 for torpor. Within each strain, kinetic differences between euthermic and torpid animals were determined by a custom-designed algorithm (see Experimental Procedures). P-values indicate whether the two curves differ only at the level of respiration rate indicated, not along the entire length of the curve.

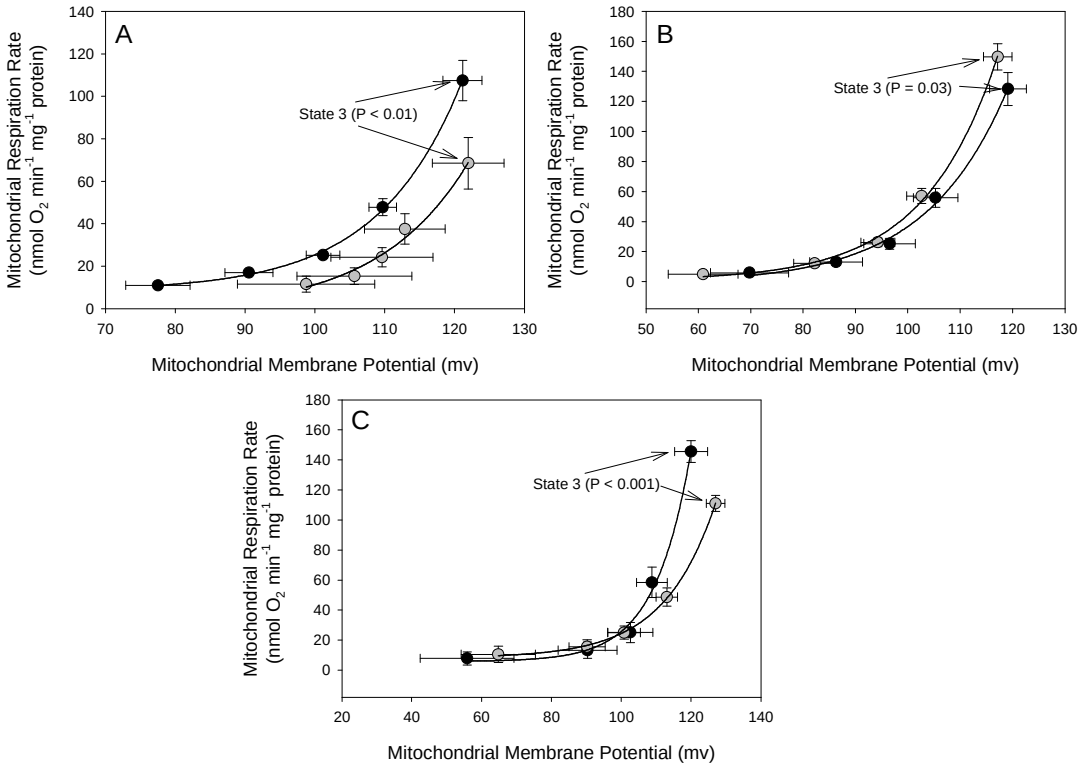

Figure 2-12. Kinetics of ADP phosphorylation measured at 37°C in liver mitochondria in three strains of mice during fasting. In each panel, ADP phosphorylation kinetics is shown for mitochondria from euthermic (black symbols) and torpid (grey symbols) animals. Data shown are mean ± SEM. For Balb/c and CD1, N=8 for both euthermia and torpor. For C57, N=4 for euthermia, N=7 for torpor. Kinetics were measured in Balb/c (A), CD1 (B), and C57 (C). Within each strain, differences between euthermic and torpid animals were determined using a custom-designed algorithm (see Experimental Procedures). P-values indicate whether the two curves differ only at the level of respiration rate indicated, not along the entire length of the curve.

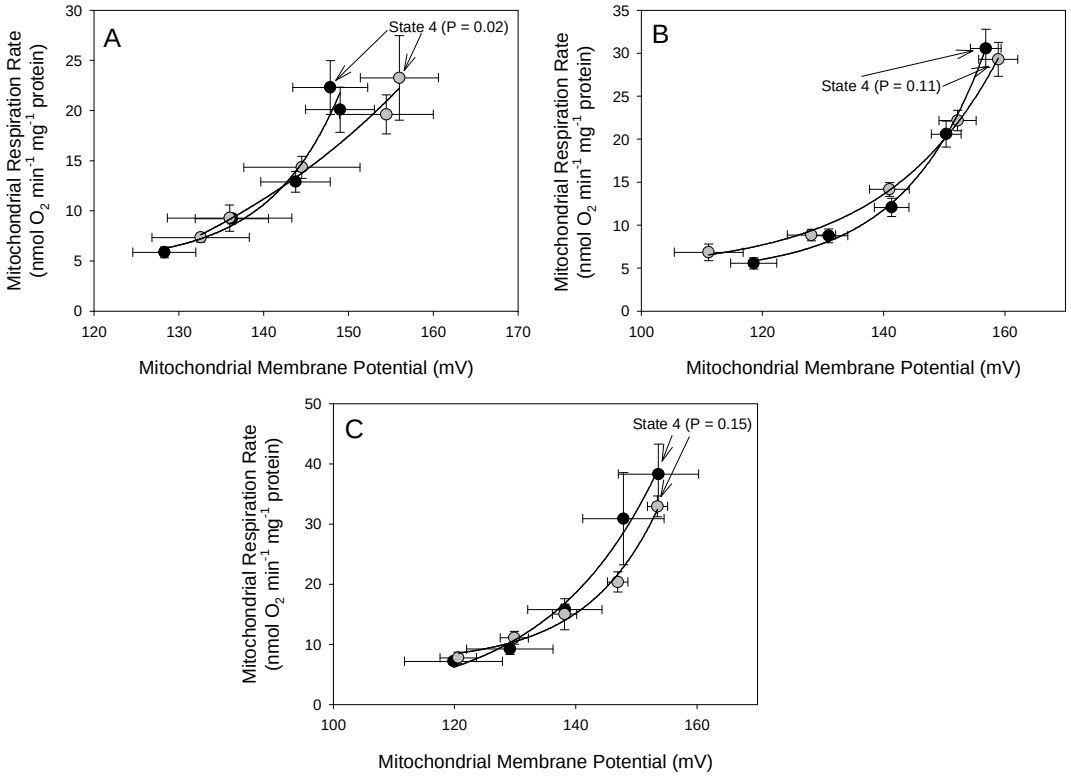

Figure 2-13. Kinetics of proton leakiness measured at 37°C in liver mitochondria in three strains of mice during fasting. In each panel, proton leakiness kinetics is shown for mitochondria from euthermic (black symbols) and torpid (grey symbols) animals. Data shown are mean ± SEM. For Balb/c and CD1, N=8 for both euthermia and torpor. For C57, N=4 for euthermia, N=7 for torpor. Kinetics are shown for Balb/c (A), CD1 (B), and C57 (C) mice. Within each strain, kinetic differences between euthermic and torpid animals were determined using a custom-designed algorithm (see Experimental Procedures). P-values indicate whether the two curves differ only at the level of respiration rate indicated, not along the entire length of the curve.

Table 2-2. Distribution of control over liver mitochondrial respiration by the three components of oxidative phosphorylation in euthermic and torpid mice. Overall control coefficients for state 3 (A) and state 4 (B) were calculated using the mean values for membrane potential and respiration rate from kinetic curves measured in Figures 2-11, 2-12, and 2-13, and kinetic curves measured at 15°C for Balb/c mice (not shown), as well as the equations described in the Experimental Procedures.

A.	Balb/c				CD1		C57	
	Euthermia		Torpor		Euthermia	Torpor	Euthermia	Torpor
	37°C	15°C	37°C	15°C	37°C	37°C	37°C	37°C
Substrate Oxidation	0.71	0.77	0.80	0.60	0.75	0.78	0.80	0.69
ADP Phosphorylation	0.28	0.19	0.19	0.34	0.23	0.21	0.19	0.29
Proton Leakiness	0.01	0.05	0.01	0.05	0.01	0.01	0.01	0.03

B.	Balb/c				CD1		C57	
	Euthermia		Torpor		Euthermia	Torpor	Euthermia	Torpor
	37°C	15°C	37°C	15°C	37°C	37°C	37°C	37°C
Substrate Oxidation	0.34	0.36	0.37	0.53	0.42	0.30	0.38	0.39
ADP Phosphorylation	0	0	0	0	0	0	0	0
Proton Leakiness	0.66	0.64	0.63	0.47	0.58	0.70	0.62	0.61

during torpor, but in C57 mice, substrate oxidation control dropped whereas that of ADP phosphorylation rose. In contrast to the pattern observed in ground squirrels, proton leak had more control over state 4 respiration rate than did substrate oxidation in euthermic mice, and this control over respiration by proton leakiness was retained or increased during torpor.

In order to analyze the effects of T_b at sampling on the kinetics of oxidative phosphorylation in euthermic mice, it was necessary to bin T_b into discrete 1^oC intervals. Compared to animals with T_b near 37°C, ADP phosphorylation was lower in animals with T_b near 36°C, 35°C, and 34°C. Substrate oxidation (at both state 3 and 4 $\Delta\Psi_m$ values) was lower only in animals with T_b near 36°C and 35°C, though it tended to be lower at 34°C as well. Proton leakiness was higher only in animals with T_b near 35°C (Figure 2-14A). For torpid mice, I binned T_b into discrete 2°C intervals and examined only the two strains that had shown active regulated inhibition of succinate oxidation during daily torpor (Balb/c and C57). For torpid Balb/c mice (Figure 2-14B), substrate oxidation at state 3 $\Delta\Psi_m$ activity was lower only once T_b declined to 24°C, but substrate oxidation at state 4 $\Delta\Psi_m$ was higher at all T_b values. ADP phosphorylation, on the other hand, was lower once T_b declined to 26°C, and proton leakiness was lower once T_b was below 28°C (and possible at higher T_b, although no animals were sampled above 28°C). For torpid C57 mice (Figure 2-14C), as in Balb/c mice, substrate oxidation at state 3 $\Delta\Psi_m$ values was lower only once T_b had reached 24°C, and ADP phosphorylation was lower only once T_b had reached 26°C. Substrate oxidation activity at state 4 $\Delta\Psi_m$ was lower when T_b was 28°C and 24°C, but showed a transient reversal to euthermic levels when T_b was 26°C. On the other hand, proton leakiness was only

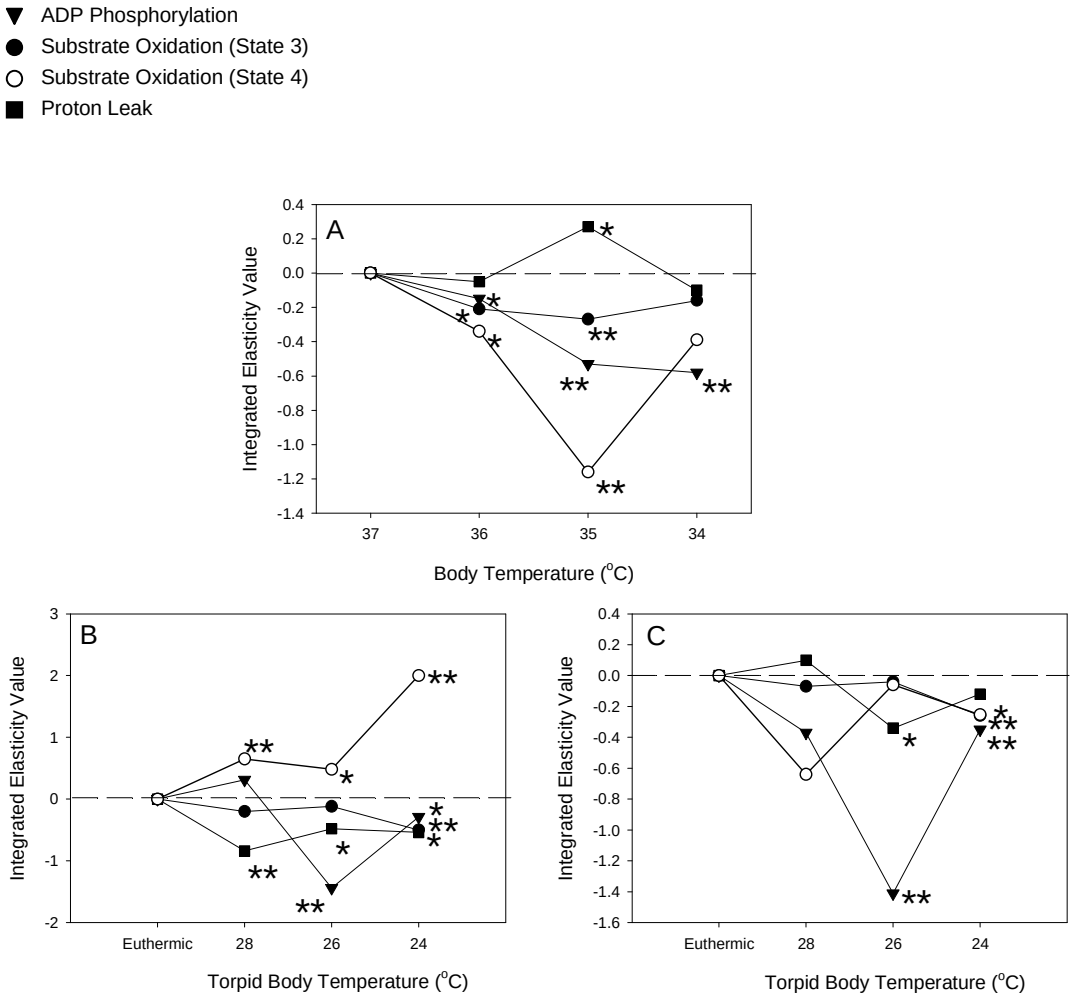

Figure 2-14. Effect of body temperature at sampling on the kinetics of the components of OxPhos measured at 37°C in fasted mice. Animals were binned into 1°C (euthermic animals) or 2°C (torpid animals) T_b intervals. *A.* Euthermic animals from all strains together. *B.* Balb/c torpid animals. *C.* C57 torpid animals. Kinetic differences are expressed as mean integrated elasticity values, which were statistically analyzed using a custom-designed algorithm (see Experimental Procedures). *, $P < 0.10$; **, $P < 0.01$, compared to euthermic animals at 37°C.

transiently lower, when T_b was around 26°C, but returned to euthermic levels as T_b further declined.

2.3.6 Effect of temperature on the kinetics of OxPhos. In ground squirrels (Figure 2-15) and mice (Figure 2-16), responses of oxidative phosphorylation kinetics to changes in assay temperature differed among metabolic states and affected how mitochondrial respiration was controlled (Table 2-1; 2-2). In ground squirrels, substrate oxidation activity (at both state 3 and 4 $\Delta\Psi_m$) declined with temperature, for the most part. IMM proton leakiness also declined with temperature in summer active and torpid animals, but actually increased with temperature in interbout euthermic animals. ADP phosphorylation activity declined with temperature in mitochondria from torpid animals, but moderately increased in activity with temperature in interbout euthermic animals. In summer active animals, ADP phosphorylation activity was higher at 25°C than 37°C, as was observed in interbout euthermic animals, but activity declined drastically when temperature was reduced to 10°C. Substrate oxidation, which had the majority of control over state 3 and 4 respiration at 37°C, regardless of metabolic state, saw its control over state 3 respiration increase as temperature fell in both euthermic and torpid animals, leaving ADP phosphorylation with even less control at low temperatures. By contrast, the control over substrate oxidation over state 4 respiration increased only in torpid animals. In mice, substrate oxidation activity generally declined with temperature regardless of metabolic state at both state 3 and 4 $\Delta\Psi_m$ values, as was observed in ground squirrels. IMM proton leakiness also declined with temperature in euthermic, but not torpid, animals. ADP phosphorylation activity, on the other hand,

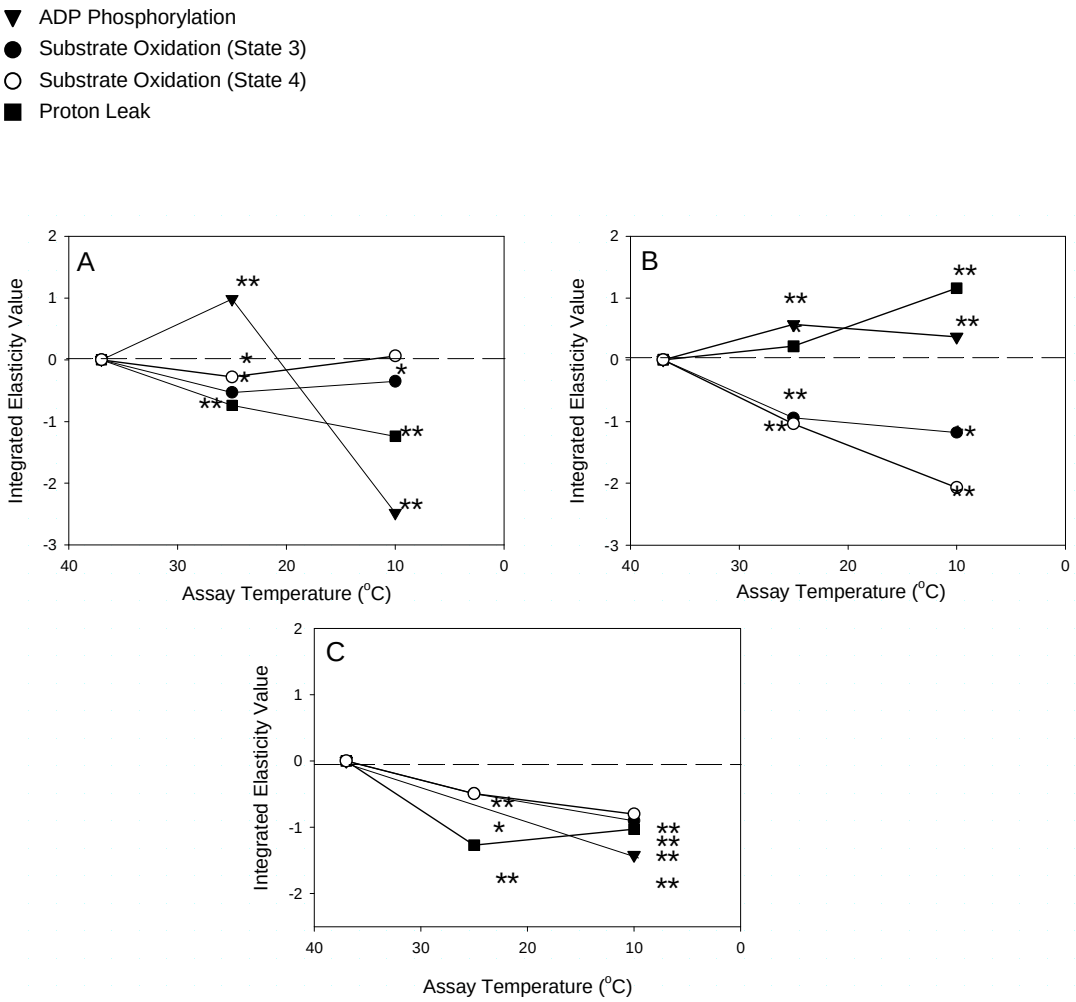

Figure 2-15. Effect of assay temperature on the kinetics of the components of OxPhos in hibernating and summer active thirteen-lined ground squirrels. Animals were either summer active (A), interbout euthermic (B), or torpid (C). Kinetic differences are expressed as mean integrated elasticity values, which were statistically analyzed using a custom-designed algorithm (see Experimental Procedures). *, $P < 0.10$; **, $P < 0.01$, compared to 37°C.

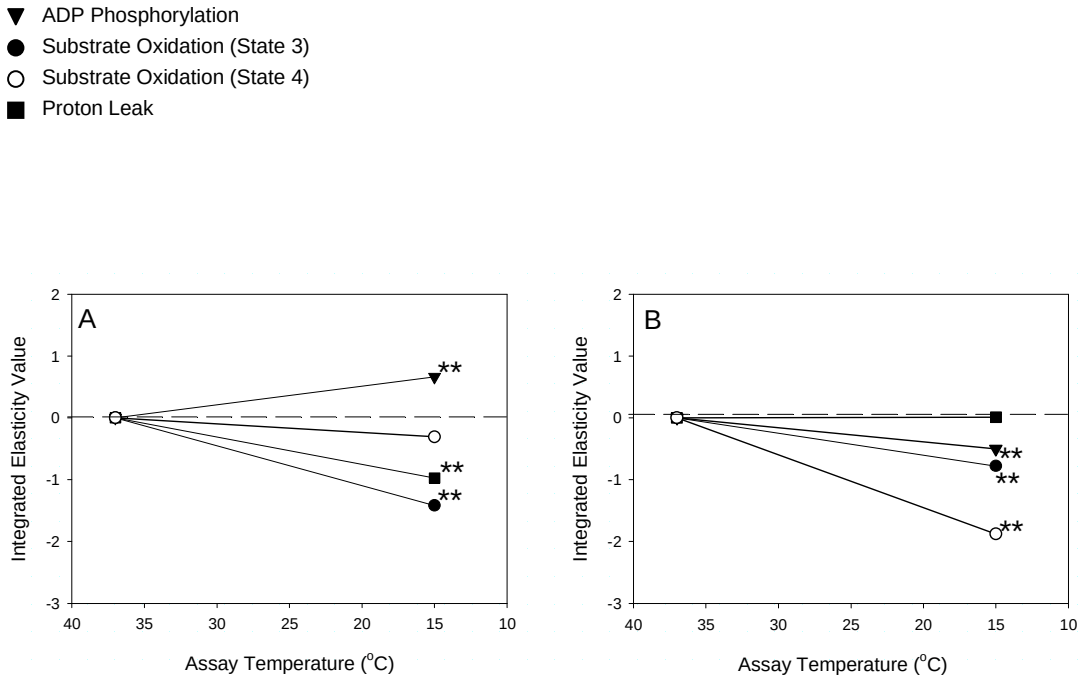

Figure 2-16. Effect of assay temperature on the kinetics of the components of OxPhos in fasted Balb/c mice. Animals were measured when euthermic (A) or torpid (B). Kinetic differences are expressed as mean integrated elasticity values, which were statistically analyzed using a custom-designed algorithm (see Experimental Procedures). **, $P < 0.01$, compared to 37°C.

declined with temperature in torpid mice but actually increased with temperature in euthermic mice.

2.4 Discussion

2.4.1 Active mitochondrial metabolic suppression during torpor is tissue-specific. Active, regulated suppression of liver mitochondrial state 3 respiration characterizes torpor in hibernating ground squirrels (Barger et al. 2003; Muleme et al. 2006; Gerson et al. 2008; Armstrong et al. 2010; Chung et al. 2011; Figure 2-1), and both fasting-induced (Figure 2-2) and spontaneous daily heterotherms (Brown et al. 2007). In hibernators, this suppression is observed regardless of whether summer active or interbout euthermic animals were used as controls. Suppression of state 4 liver mitochondrial respiration rate characterizes torpor in hibernators in most studies (Pehowich and Wang 1984; Barger et al. 2003; Armstrong et al. 2010; Figure 2-1) but not all (Gerson et al. 2008); however, state 4 liver respiration is not suppressed in daily heterotherms (Brown et al. 2007; Figure 2-2).

Which respiratory state (i.e., state 3 vs. state 4) best approximates mitochondrial respiration in vivo, and whether in vivo respiratory state might differ between euthermic and torpid animals, is unclear, but it has been suggested that mitochondria in a resting animal may be in an intermediate respiratory state ("state 3.5") in vivo (Korzeniewski and Mazat 1996). Notwithstanding, the capacity for ATP production is undoubtedly reduced during torpor, which likely contributes to the inhibition of numerous ATP-consuming processes in the cell, given that ATP production has significant control over the rates of these processes (Rolfe and Brown 1997), leading to suppression of cellular

metabolism. Moreover, the extent of suppression of liver mitochondrial respiration during torpor seems greater in hibernators than daily heterotherms (e.g., compare Figures 2-1, 2-2, and Brown et al. 2007), suggesting that there may be some relationship between the extent of active liver mitochondrial metabolic suppression and the extent of whole-animal MR suppression during torpor.

Two previous studies showed no difference in skeletal muscle mitochondrial respiration rate in thirteen-lined ground squirrels (Muleme et al. 2006) and Arctic ground squirrels (Barger et al. 2003) during torpor compared to euthermic animals. These observations led to the conclusion that mitochondrial metabolic suppression during hibernation was tissue-specific. By contrast, in the present study, skeletal muscle mitochondrial respiration was actively suppressed during torpor (Figure 2-6), although the extent of active suppression of skeletal muscle mitochondria was considerably less than that observed in liver (compare Figures 2-1 and 2-6). There are a few possible explanations for the disparity among studies.

First, in both previous studies, non-hibernating animals (either summer active or cold-acclimated), rather than interbout euthermic animals, were used as controls. Skeletal muscle mitochondrial respiration is known to increase in winter in hibernating species (Brustovetsky et al. 1992), which would dampen any differences in respiration rate between torpid and summer active animals. This could explain why Muleme et al. (2006) saw no difference between summer active and torpid animals. It may also be that hibernating animals have a higher capacity for skeletal muscle mitochondrial respiration rates than even cold-acclimated non-hibernating animals because ATP production is routinely needed for shivering thermogenesis during arousals from torpor (Lyman and

Chatfield 1950; Opazo et al. 1999). This could explain why Barger et al. (2003) saw no difference between cold-acclimated non-hibernators and torpid animals.

Second, both previous studies of skeletal muscle mitochondria used only the gastrocnemius as a source of muscle mitochondria. In contrast, in the present study, the whole hindleg was used because thirteen-lined ground squirrels are smaller compared to Arctic ground squirrels used in some previous studies, and the purification protocol required more tissue to compensate for lost yield during purification. The ground squirrel hindlimb is likely similar in composition to that of the rat, which contains about 32 muscles that differ in fiber type composition (Armstrong and Phelps 1984), and it remains possible that the occurrence and/or extent of mitochondrial metabolic suppression differs among different muscles/fibre types. While fast glycolytic fibres comprise 76% of the whole rat hindlimb, these same fibres comprised only 62% of the gastrocnemius.

Third, Barger et al. (2003) showed a similar extent of suppression in skeletal muscle mitochondria in Arctic ground squirrels as the present study but failed to obtain statistical significance for their results. Like the present study, both previous studies that examined skeletal muscle mitochondria during torpor in hibernators (Barger et al. 2003; Muleme et al. 2006) also examined liver mitochondrial respiration and showed greater variability in mitochondrial respiration rate for skeletal muscle than liver mitochondria. This may have impeded statistical significance in the previous studies and been overcome in the present study by a larger sample size and the use of high-resolution respirometry. This higher variability in muscle may also be due to the fact that skeletal muscle mitochondria consist of two distinct mitochondrial subpopulations (Cogswell et

al. 1983). Subsarcolemmal mitochondria are located just beneath the sarcolemma and can be easily isolated using only homogenization, whereas intermyofibrillar mitochondria are located among the muscle fibers and can only be isolated following digestion with protease incubation. A number of studies have shown that state 3 and 4 respiration rates of intermyofibrilar mitochondria are higher than that of subsarcolemmal mitochondria and/or that these mitochondrial subpopulations respond differently to experimental conditions, such as training and immobilization (e.g., Krieger et al. 1980; Bizeau et al. 1998; Servais et al. 2003). Protease was employed in the present study and, therefore, both mitochondrial subpopulations were likely isolated. Future studies should examine changes in each subpopulation independently during torpor to determine whether the presence and/or extent of suppression differ between mitochondrial subpopulations within tissues.

In contrast to my observations in liver and skeletal muscle, there was no suppression of respiration rate in heart mitochondria during torpor in dwarf Siberian hamsters; in fact, glutamate-fueled respiration rate was 2-fold higher in mitochondria from torpid animals. To my knowledge, only one other study has examined heart mitochondria during torpor. South (1960) showed that heart mitochondrial respiration rate was higher during torpor in hibernating golden hamsters using complex I-linked substrates, consistent with my observations in dwarf Siberian hamsters. It seems likely that the increase in glutamate-fueled heart mitochondrial respiration in dwarf Siberian hamsters is caused by increased activity of glutamate transporters, GDH, and/or complex I, as these sites are unique to glutamate oxidation. Given that South (1960) used pyruvate to fuel respiration, this may suggest that complex I activity is the site of

upregulation of heart mitochondrial metabolism, as this is the only site common to both glutamate and pyruvate oxidation (but not succinate oxidation). Heart mitochondrial metabolism may increase during torpor because, unlike liver and skeletal muscle, which are responsible for 12% and 26% of BMR, respectively, heart is responsible for only 0.5% (Martin and Fuhrman 1955). In addition, both liver and skeletal muscle contribute to thermogenic metabolism, whereas heart does not, except indirectly through its effects on circulating warm blood. Given that heart makes little contribution to whole-animal metabolism, there may be little benefit to suppress oxidative phosphorylation in this tissue. In fact, it may be necessary to maintain the metabolic capacity of heart mitochondria in order to maintain contractile function at low temperatures. In most homeothermic mammals, heart function ceases at temperatures below 20°C (Johansson 1994), yet heterothermic animals routinely maintain proper heart function at lower temperatures.

2.4.2 Active suppression and passive thermal effects work together to reduce mitochondrial respiration during torpor. Decreasing assay temperature to 10-15°C reduces oxidative capacity by as much as 83% in daily heterotherms and 93% in hibernators in mitochondria isolated from euthermic animals compared to measured rates at 37°C. Given that whole-animal oxygen consumption rate declines up to 70% and 95% compared to BMR in daily heterotherms and hibernators, respectively (Geiser 2004), it would appear that passive thermal effects alone could be sufficient to account for most, if not all, of the reduction of mitochondrial respiration rates during torpor. This is consistent with the arguments of other authors who have questioned the role of

any active metabolic inhibition in reducing MR during torpor (Guppy and Withers 1999).

While active mitochondrial metabolic suppression has been routinely observed at high assay temperatures (i.e., > 25°C), it has seldom been observed at lower assay temperatures (Muleme et al. 2006; Brown et al. 2007; Figures 2-4; 2-5; 2-7). Therefore, it seems unlikely that active mitochondrial metabolic inhibition during torpor suppresses mitochondrial metabolism to its lowest levels. Over the last decade, it has become well-established that T_b falls during torpor as a consequence of metabolic suppression rather than being itself the mechanism by which metabolic suppression is achieved (Heldmaier et al. 2004). On this basis, active mitochondrial metabolic suppression may be a mechanism to suppress metabolism during the early stages of torpor, when T_b is still high, thereby facilitating a fall in T_b, leading to further mitochondrial metabolic suppression via passive thermal effects. In support of this notion, Chung et al. (2011) showed that liver mitochondrial metabolism is fully suppressed during early entrance into a torpor bout, when T_b is still 30°C, during hibernation in thirteen-lined ground squirrels. In addition, my own data show that glutamate oxidation rate was lowest in mice sampled early during torpor (T_b > 28°C) and succinate oxidation, though it only gradually declined during torpor, was greatest when T_b was 25°C (Figure 2-3). At lower temperatures, succinate oxidation rates (measured in vitro at 37°C) began to gradually rise. This is intriguing because I have previously suggested that 25°C may be the T_b at which the effects of active suppression of mitochondrial metabolism become negligible compared with passive thermal effects.

The extent of mitochondrial metabolic suppression via passive thermal effects depends on the temperature sensitivity of OxPhos. Mitochondria from torpid animals may be expected to have greater temperature sensitivity than mitochondria from euthermic animals in order to maximize temperature effects. The temperature sensitivity of the ADP phosphorylation component was consistently higher in liver mitochondria from torpid animals compared with euthermic animals in ground squirrels, mice, and hamsters. Chamberlain (2004) showed that tobacco hornworms (an ectothermic insect) have an ADP phosphorylation component that is also temperature-insensitive. On the other hand, Dufour et al. (1996) showed that, in rats (strictly homeothermic mammals), the ADP phosphorylation component is temperature-sensitive, as in torpid heterotherms. Therefore, it would appear that the ADP phosphorylation component of OxPhos may differ not only between endothermic and ectothermic animals, but also between heterothermic and homeothermic endotherms. This may have implications for our understanding of the evolution of endothermy, as well as the evolution of torpor.

The increased temperature sensitivity of the ADP phosphorylation component during torpor is not likely a mechanism to achieve greater energy savings during torpor since, as discussed previously, ADP phosphorylation has little control over respiration rate, particularly at low temperatures (Table 2-1; 2-2). However, ADP phosphorylation has considerable control over $\Delta\Psi_m$, and increasing the temperature sensitivity of this component during torpor may function to minimize changes in $\Delta\Psi_m$ during torpor. In support of this notion, when mitochondria from euthermic animals are cooled to low temperatures, state 3 $\Delta\Psi_m$ drops by 15-20mV, whereas when mitochondria from torpid

animals are cooled to the same low temperatures, state 3 $\Delta\Psi_m$ remains constant (data not shown).

2.4.3 Mitochondrial proton conductance is not a mechanism to suppress mitochondrial respiration during torpor. Proton leak has been shown to be a significant contributor to cellular (Brand et al. 1994), tissue (Rolfe and Brand 1996), and whole-animal oxygen consumption (Rolfe and Brown 1997). Therefore, decreasing IMM proton leakiness during torpor could increase mitochondrial efficiency (Brand et al. 1993) and contribute to energy savings. To date, however, there has been little support for this hypothesis in other hypometabolic models; for example, proton leak was not suppressed in either hibernating frogs (St. Pierre et al. 2000) or estivating snails (Bishop et al. 2002). My data show that proton leakiness was reduced during torpor only in Balb/c mice (and, in fact, when measured at 15°C, proton leakiness was actually higher in torpid Balb/c mice; Figures 2-13; 2-16). In addition, in torpid ground squirrels (Figure 2-10) and torpid hamsters (Brown et al. 2007), proton leakiness was higher compared to euthermic animals. A previous study in 13-lined ground squirrels showed that proton leakiness did not differ between torpid and euthermic animals when fed the same diet used in the present study, but showed lower proton leakiness when fed diets with very high or very low amounts of polyunsaturated fatty acids (Gerson et al. 2008). One reason for the disparity between these two studies might be the type of euthermic animal used as a control. In the present study, interbout euthermic animals were used as controls, whereas Gerson et al. (2008) used summer active animals. Barger et al. (2003) showed no change in proton leakiness in Arctic ground squirrels, but these authors also used cold-acclimated non-hibernating animals as controls. It may be that proton leak

cannot be actively suppressed during torpor because, while it would conserve energy, it would have some other more costly impact.

2.4.4 Mechanisms of active mitochondrial metabolic suppression during torpor in liver. The sites of mitochondrial metabolic suppression that I have identified in this study and in previous work (Brown et al. 2007) are summarized in Table 2-3. In hibernating ground squirrels, succinate oxidation was suppressed during torpor, but glutamate oxidation was not. Moreover, substrate oxidation activity measured using succinate was lower during torpor. Taken together, these data suggest that the dicarboxylate transporter and/or complex II are the site(s) of suppression of liver mitochondrial metabolism during torpor in squirrels as these two sites are unique to succinate oxidation. Previous studies have demonstrated that complex II is inhibited during torpor in hibernating squirrels as a result of an increase in liver oxaloacetate levels, but this accounts for only 25% of the suppression of succinate oxidation (Armstrong et al. 2010). I am not aware of any studies that have examined changes in dicarboxylate transport during hibernation, but it may be a worthwhile site for further investigation because it has been shown to have considerable control over state 3 respiration in rat liver mitochondria (Groen et al. 1982).

The lack of suppression with glutamate during torpor in hibernators suggests that there is no suppression of complex I, complex III, complex IV, ubiquinone, cytochrome c, glutamate transport, or GDH. The lack of suppression with glutamate oxidation further suggests that inhibition of respiration rate with pyruvate, another complex I-linked substrate, which has been seen during torpor in previous studies (Muleme et al. 2006), likely reflects inhibition of pyruvate transport and/or PDH, as

Table 2-3. Summary of the changes in the kinetics of oxidative phosphorylation observed during hibernation and daily torpor. Upward and downward arrows indicate a significantly increased or decreased activity, respectively, of the OxPhos component during torpor compared to euthermia, whereas a horizontal double-arrow indicates no significant difference among metabolic states. Data for ground squirrels and all strains of mice are from the present thesis, whereas data for hamsters (shown for comparison) are from Brown et al. (2007).

	Substrate Oxidation		ADP Phosphorylation	Proton Leak
	State 3	State 4		
Ground Squirrels	↓	↓	↓	↑
Mice				
Balb/c	↓	↑	↓	↓
CD1	↔	↔	↑	↔
C57	↔	↔	↓	↔
Hamsters	↓	↓	↔	↑

these two sites are unique to pyruvate oxidation whereas the remaining sites involved in pyruvate oxidation are shared with glutamate oxidation. Indeed, PDH is inhibited during torpor in hibernators via the upregulation of pyruvate dehydrogenase kinase 4, which phosphorylation, and thereby, deactivates the complex (Buck et al. 2002).

ADP phosphorylation was also suppressed during torpor in grounds squirrels (Figure 2-10). This is consistent with previous work showing that the ANT may be suppressed (Shug et al. 1971; Amerkhanov et al. 1996) and/or have a reduced affinity for adenine nucleotides, the concentration of which may decline (Bronnikov et al. 1990), during torpor. Notwithstanding, the fact that ADP phosphorylation was suppressed is intriguing because this component had little control (12%) over state 3 respiration rate (Table 2-1), consistent with some (Dufour et al. 1996) but not all (Brand et al. 1993; Rossignol et al. 2000) previous studies. Therefore, its inhibition contributes little to the suppression of mitochondrial respiration during torpor, making any benefit of suppressing ADP phosphorylation during torpor unclear. ADP phosphorylation does have considerable control (~50%) over state 3 $\Delta\Psi_m$ (data not shown), and it is possible that inhibition of ADP phosphorylation helps to minimize changes in $\Delta\Psi_m$ during torpor. Because substrate oxidation generates $\Delta\Psi_m$, its suppression causes $\Delta\Psi_m$ to decline; by contrast, because ADP phosphorylation consumes $\Delta\Psi_m$, its suppression tends to cause $\Delta\Psi_m$ to rise. Thus, inhibition of substrate oxidation without simultaneous inhibition of ADP phosphorylation may lead to a decline in $\Delta\Psi_m$. My data show that state 3 $\Delta\Psi_m$ of torpid animals is only 3mV lower than that of euthermic animals when measured at 37°C (Figure 2-10) but would be about 8mV lower in the absence of the simultaneous inhibition of ADP phosphorylation.

The sites of suppression of liver mitochondrial oxidative phosphorylation during torpor in mice differed considerably among the three strains examined (Table 2-3). Balb/c mice show the same pattern of suppression as thirteen-lined grounds squirrels, with suppression of ADP phosphorylation in this strain preventing any significant change in state 3 $\Delta\Psi_m$ but contributing little to suppression of mitochondrial respiration. In C57 mice, similar to dwarf Siberian hamsters (Brown et al. 2007), both glutamate and succinate oxidation were suppressed. While suppression in hamsters seems to result from suppression of substrate oxidation (via glutamate transport, complex I, dicarboxylate transport and/or complex II, but not GDH [see Heldmaier et al. 1999]) and without any contribution of ADP phosphorylation, measurements of substrate oxidation suggest that this component is not suppressed in C57 mice. Instead, this strain shows a unique pattern of suppression in that ADP phosphorylation is suppressed to such a considerable extent that, despite its low level of control over respiration rate, it is sufficient to inhibit mitochondrial metabolism. CD1 mice show liver mitochondrial metabolic suppression only with glutamate, which suggests inhibition of glutamate transport, GDH, and/or complex I. ADP phosphorylation was not suppressed in CD1 mice.

There appears to be no consistent pattern among heterothermic species in terms of the particular sites that are inhibited during torpor, even among strains of the same species (i.e., house mice; Table 2-3). This does not preclude the possibility that the upstream signaling cascade triggered during torpor has been conserved among species. Even if the torpor induction signals are the same in all strains, different mouse strains are known to react differently to the same molecular/physiological signals (Marks et al.

1983; Funkat et al. 2004). Notwithstanding, a number of sites are potential candidates for inhibition in several species, including complex I, complex II, glutamate transport, dicarboxylate transport. Therefore, it may be that only a finite number of sites can be downregulated during torpor to achieve mitochondrial metabolic suppression, but which exact sites are suppressed in any given species has not been under sufficient selective pressure so as to be conserved among species. Moreover, for the most part, more than one site appears to be inhibited during torpor in all species, suggesting that torpor involves a coordinated, multi-site downregulation of mitochondrial metabolism. However, these different sites that are inhibited during torpor are not always suppressed and reversed at the same time. For example, in both Balb/c and C57 mice, ADP phosphorylation appears to be suppressed once T_b has reached 26°C, but substrate oxidation not inhibited until T_b reaches 24°C.

2.4.5 The compromise between torpor and foraging in fasted mice. Daily torpor is undoubtedly part of the energy-saving strategy of fasted mice, which spent about 40% of their time torpid, but were never torpid when fed. Energy savings during fasting could presumably be increased by longer and more frequent torpor bouts; however, torpor precludes foraging. Fasting has been shown to increase both nocturnal (active period; Sakurada et al. 2000) and diurnal (inactive period; Overton and Williams 2004) activity in rodents, likely to facilitate increased foraging. The average torpor bout length observed in this study (5.6 hours) may, therefore, represent a balance between an increased need for energy savings and an increased need to forage.

Moderate reductions in T_b and MR during periods of euthermia in fasted animals could conserve additional energy while still permitting activity and foraging. In the

present study, euthermic animals displayed considerable variation in T_b and MR, sometimes reducing T_b to as low as 34°C, with a corresponding reduction of MR up to 25% compared to fed animals. Interestingly, when T_b and MR were reduced, state 3 respiration rate of liver mitochondria was also reduced, particularly with succinate. Therefore, euthermic fasted animals may periodically reduce mitochondrial respiratory capacity—albeit to a lesser extent than during torpor—in order to further reduce their energy demands without compromising foraging ability.

2.4.6 Summary. During periods of hypometabolism in mammals, mitochondrial metabolism is actively suppressed in several energy-consuming tissues (such as liver and skeletal muscle). The principle site of this suppression is the substrate oxidation component of OxPhos, likely complex I and/or II. This active inhibition of mitochondrial metabolism likely facilitates MR suppression during entrance into torpor, when T_b is still high, whereas passive thermal effects likely maintain low levels of mitochondrial metabolism during steady-state torpor.

2.5 References

Ainscow EK, Brand MD (1999) Quantifying elasticity analysis: how external effectors cause changes to metabolic systems. Biosystems 49: 151-159.

Amerkhanov ZG, Yegorova MV, Markova OV, Mokhova EN (1996) Carboxyatractylate- and cyclosporin A-sensitive uncoupling in liver mitochondria of ground squirrels during hibernation and arousal. Biochem Mol Biol Int 38: 863-870.

Armstrong C, Staples JF (2010) The role of succinate dehydrogenase and oxaloacetate in metabolic suppression during hibernation and arousal. J Comp Physiol B 180: 775-783.

Armstrong RB, Phelps RO (1984) Muscle-fiber type composition of the rat hindlimb. Am J Anat 171: 259-272.

Barger JL, Brand MD, Barnes BM, Boyer BB (2003) Tissue-specific suppression of mitochondrial proton leak and substrate oxidation in hibernating arctic ground squirrels. Am J Physiol Regul Integr Comp Physiol 284: R1306-R1313.

Bhattacharya SK, Thakar JH, Johnson PL, Shanklin DR (1991) Isolation of skeletal muscle mitochondria from hamsters using an ionic medium containing ethylenediaminetetraacetic acid and nagarase. Anal Biochem 192: 344-349.

Bishop T, St. Pierre J, Brand MD (2002) Primary causes of decreased mitochondrial oxygen consumption during metabolic depression in snail cells. Am J Physiol Regul Integr Comp Physiol 282: R372-R382.

Bizeau ME, Willis WT, Hazel JR (1998) Differential responses to endurance training in subsarcolemmal and intermyofibrilar mitochondria. J Appl Physiol 85: 1279-1284.

Brand MD, Chien L-F, Ainscow EK, Rolfe DFS, Porter RK (1994) The causes and functions of mitochondrial proton leak. Biochim Biophys Acta 1187: 132-139.

Brand MD, Harper ME, Taylor HC (1993) Control of the effective P/O ratio of oxidative phosphorylation in liver mitochondria and hepatocytes. Biochem J 291: 739-748.

Bronnikov GE, Vinogradova SO, Mezentseva VS (1990) Changes in kinetics of ATP-synthase and in concentrations of adenine nucleotides in ground squirrel liver during hibernation. Comp Biochem Physiol B 97: 411-415.

Brown JCL, Gerson AR, Staples JF (2007) Mitochondrial metabolism during daily torpor in the dwarf Siberian hamster: role of active regulated changes and passive thermal effects. Am J Physiol Regul Integr Comp Physiol 293: R1833-R1845.

Brustovetsky NN, Egorova MV, Gnutov DY, Gogvadze VG, Mokhova EN, Skulachev VP (1992) Thermoregulatory, carboxyatractyloside-sensitive uncoupling in heart and skeletal muscle mitochondria of the ground squirrel correlates with the level of free fatty-acids. FEBS Lett 305: 15-17.

Brustovetsky NN, Mayevksy EI, Grishina EV, Gogvadze VG, Amerkhanov ZG (1989) Regulation of the rate of respiration and oxidative phosphorylation in liver mitochondria from hibernating ground squirrels, *Citellus undulatus*. Comp Biochem Physiol B 94: 537-541.

Buck MJ, Squire TL, Andrews MT (2002) Coordinate expression of the PDK4 gene: a means of regulating fuel selection in a hibernating mammal. Physiol Genom 8: 5-13.

Chamberlain ME (2004) Top-down control analysis of the effect of temperature on ectotherm oxidative phosphorylation. Comp Evol Physiol 287: R794-R800.

Chen Q, Moghaddas S, Hoppel CL, Lesnefsky EJ (2008) Ischemia defects in the electron transport chain increase the production of reactive oxygen species from isolated heart mitochondria. Am J Physiol Cell Physiol 294: C460-466.

Chung D, Lloyd GP, Thomas RH, Guglielmo CG, Staples JF (2011) Mitochondrial respiration and succinate dehydrogenase are suppressed early during entrance into a hibernation bout, but membrane remodeling is only transient. J Comp Physiol B (In press).

Cogswell AM, Stevens RJ, Hood DA (1983) Properties of skeletal muscle mitochondria isolated from subsarcolemmal and intermyofibrillar regions. Am J Physiol Cell Physiol 264: C383-C389.

Dark J, Miller DR, Zucker I (1994) Reduced glucose availability induces torpor in Siberian hamsters. Am J Physiol Regul Integr Comp Physiol 267: R496-R501.

Dufour S, Rousse N, Canioni P, Diolez P (1996) Top-down control analysis of temperature effect on oxidative phosphorylation. Biochem J 314: 743-751.

Else PL, Hulbert AJ (1981) Comparison of the “mammal machine” and “reptile machine”: energy production. Am J Physiol Regul Integr Comp Physiol 240: R3-R9.

Fedotcheva NJ, Sharyshev AA, Mironova GD, Kondrashova MN (1985) Inhibition of succinate oxidation and K^+ transport in mitochondria during hibernation. Comp Biochem Physiol B 82: 191-195.

Forstner H, Gnaiger E (1983) Calculation of equilibrium oxygen concentration. In: Polarographic oxygen sensors: aquatic and physiological applications. Gnaiger E, Forstner H (eds) Springer: Berlin, Heidelberg, New York.

Funkat A, Massa CM, Jovanovksa V, Proietto J, Andrikopoulos S (2004) Metabolic adaptations of three inbred strains of mice (C57BL/6, DBA/2,192T2) in response to a high-fat diet. J Nutr 134: 3264-3262.

Gehnrich SC, Aprille JR (1988) Hepatic gluconeogenesis and mitochondrial function during hibernation. Comp Biochem Physiol B 91: 11-16.

Geiser F (2004) Metabolic rate and body temperature reduction during hibernation and daily torpor. Annu Rev Physiol 66: 239-274.

Gerson AR, Brown JCL, Thomas R, Bernards MA, Staples JF (2008) Effect of dietary polyunsaturated fatty acids on mitochondrial metabolism in mammalian hibernation. J Exp Biol 211: 2689-2699.

Groen AK, Wanders RJA, Westerhoff HV, van der Meer R, Tager JM (1982) Quantification of the contributions of various steps to the control of mitochondrial respiration. J Biol Chem 2754-2752.

GuppyM, Withers P (1999) Metabolic depression in animals: physiological perspectives and biochemical generalizations. Biol Rev 74: 1-40.

Hafner RP, Brown GC, Brand MD (1990) Analysis of the control of respiration rate, phosphorylation rate, proton leak rate and protonmotive force in isolated mitochondria using the 'top-down' approach of metabolic control theory. Eur J Biochem 188: 313-319.

Halestrap AP (1989) The regulation of matrix volume of mammalian mitochondria in vivo and in vitro and its role in the control of mitochondrial metabolism. Biochim Biophys Acta 973: 355-382.

Heldmaier G, Klingenspor M, Werneyer M, Lampi BJ, Brooks SPJ, Storey KB (1999) Metabolic adjustments during daily torpor in the Djungarian hamster. Am J Physiol Endocrinol Metab 276: E896-E906.

Heldmaier G, Ortmann S, Elvert R (2004) Natural hypometabolism during hibernation and daily torpor in mammals. Resp Physiol Neurobiol 141: 317-329.

Heldmaier G, Steinlechner S (1981) Seasonal pattern and energetic of short daily torpor in the Djungarian hamster, *Phodopus sungorus*. Oecologia 48: 265-270.

Hiebert SM, Fulkerson EK, Lindermayer KT, McClure SD (2000) Effect of temperature on preference for dietary unsaturated fatty acids in the Djungarian hamster (*Phodopus sungorus*). Can J Zool 78: 1361-1368.

Hiebert SM, Hauser K, Ebrahaim AJ (2003) Djungarian hamsters exhibit temperature-dependent dietary fat choice in long days. Physiol Biochem Zool 76: 850-860.

Hoffmann K (1973) The influence of photoperiod and melatonin on testis size, body weight, and pelage colour in Djungarian hamster (*Phodopus sungorus*). J Comp Physiol A 85: 267-282.

Hudson JW, Scott IM (1979) Daily torpor in the laboratory mouse, *Mus musculus* var. albino. Physiol Zool 52: 205-215.

Johansson BW (1994) The hibernator heart – natures model of resistance to ventricular fibrillation. European Section Meeting – International Society for Heart Research 685-688.

Kamo N, Muratsuga M, Hongoh R, Kobatake Y (1979) Membrane potential of mitochondria meausured with an electrode sensitive to tetraphenyl phosphonium and

relationship between proton electrochemical potential and phosphorylation potential in steady state. J Mem Biol 49: 105-121.

Kavanaugh NI, Ainscow EK, Brand MD (2000) Calcium regulation of oxidative phosphorylation in rat skeletal muscle mitochondria. Biochim Biophys Acta 1457: 57-70.

Konarzewski B, Diamond J (1995) Evolution of basal metabolic rate and organ masses in laboratory mice. Evol 49: 1239-1249.

Korzeniewski B, Mazat JP (1996) Theoretical studies on control of oxidative phosphorylation in muscle mitochondria at different energy demands and oxygen concentrations. Acta Biotheoretica 44: 263-269.

Krieger DA, Tate CA, McMillonwood J, Booth FW (1980) Populations of rat skeletal muscle mitochondria after exercise and immobilization. J Appl Physiol 48: 23-28.

Labajova A, Vojtiskova A, Krivakova P, Kofranek J, Drahota Z, Houstek J (2006) Evolution of mitochondrial membrane potential using a computerized device with a tetraphenylphosphonium-selective electrode. Anal Biochem 353: 37-42.

Lombardi A, Lanni A, Moreno M, Brand MD, Goglia F (1998) Effect of 3,5-di-iodo-L-thyroine on the mitochondrial energy-transduction apparatus. Biochem J 330: 521-526.

Lyman CP, Chatfield PO (1950) Mechanisms of arousal in the hibernating hamster. J Exp Zool 114: 491-515.

Marcinkeviciute A, Mildaziene V, Crumm S, Demin O, Hoek JB, Kholodenko B (2000) Kinetics and control of oxidative phosphorylation in rat liver mitochonria after chronic ethanol feeding. Biochem J 348: 519-525.

Marks MJ, Burch JB, Collins AC (1983) Genetics of nicotine response in 4 inbred strains of mice. J Pharm Exp Therapeutics 226: 291-302.

Martin AW, Fuhrman FA (1955) The relationship between summated tissue respiration and metabolic rate in the mouse and dog. Physiol Zool 28: 18-36.

Martin SL, Maniero GD, Carey C, Hand SC (1999) Reversible depression of oxygen consumption in isolated liver mitochondrial during hibernation. Phys Biochem Zool 72: 255-264.

Muleme HM, Walpole AC, Staples JF (2006) Mitochondrial metabolism in hibernation: metabolic suppression, temperature effects, and substrate preferences. Physiol Biochem Zool 79: 474-483.

Opazo JC, Nespolo RF, Bozinovic F (1999) Arousal from torpor in the chilean mouse-opposum (*Thylamys elegans*): does non-shivering thermogenesis play a role? Comp Biochem Physiol A 123: 393-397.

Overton JM, Williams TD (2004) Behavioural and physiologic responses to calorie restrcition in mice. Physiol Behav 81: 749-754.

Pehowich DJ, Wang LCH (1984) Seasonal changes in mitochondrial succinate dehydrogenase activity in a hibernator, *Spermophillus richardsonii*. J Comp Physiol B 154: 495-501.

Reynafarje B, Costa LE, Lehninger AL (1985) O_2 solubility in aqueous media determined by a kinetic method. Anal Biochem 145: 406-418.

Rolfe DFS, Brown GC (1997) Cellular energy utilization and molecular origin of standard metabolic rate in mammals. Physiol Rev 77: 731-759.

Rolfe DFS, Brand MD (1996) Contribution of mitochondrial proton leak to skeletal muscle respiration and to standard metabolic rate. Am J Physiol Cell Physiol 271: C1380-1389.

Rossignol R, Letellier T, Malgat M, Rocher C, Mazat JP (2000) Tissue variation in the control of oxidative phosphorylation: implication for mitochondrial disease. Biochem J 347: 45-53.

Rottenberg H (1984) Membrane potential and surface potential in mitochondria: uptake and binding of lipophilic cations. J Memb Biol 81: 127-138.

Sakurada S, Shido O, Sugimoto N, Hiratsuka Y, Yoda T, Kanosue K (2000) Autonomic and behavioural thermoregulation in starved rats. J Physiol 526: 417-424.

Servais S, Couturier K, Koubi H, Rouanet JL, Desplanches D, Sornay-Mayet MH, Sempore B, Lavoie JM, Favier R (2003) Effect of voluntary exercise on H_2O_2 release by subsarcolemmal and intermyofibrilar mitochondria. Free Rad Biol Med 35: 24-32.

Shug AL, Ferguson S, Shrago E, Burlington RF (1971) Changes in respiratory control and cytochromes in liver mitochondria during hibernation. Biochim Biophys Acta 226: 309-312.

South FE (1960) Hibernation, temperature, and rates of oxidative phosphorylation by heart mitochondria. Am J Physiol 198: 463-466.

St. Pierre J, Brand MD, Boutillier RG (2000) The effect of metabolic depression on proton leak rate in mitochondria from hibernating frogs. J Exp Biol 203: 1469-1476.

Stoner HB (1973) The role of the liver in non-shivering thermogenesis in the rat. J Physiol 232: 285-296.

Storey KB (1997) Metabolic regulation in mammalian hibernation: enzyme and protein adaptations. Comp Biochem Physiol A 118: 1115-1124.

Suozzi A, Malatesta M, Zancanaro C (2009) Subcelluar distribution of lipid metabolism during the euthermia-hibernation-arousal cycle. J Anat 214: 956-962.

Takaki M, Nakahara H, Kawatani Y, Utsumi K, Suga H (1997) No suppression of respiratory function of mitochondria isolated from the hearts of anaesthetized rats with high-dose pentobarbital sodium. Jap J Physiol 47: 87-92.
Vaughan DK, Gruber AR, Michalski ML, Seidling J, Schlink S (2006) Capture, care, and captive breeding of 13-lined ground squirrels, *Spermophilus tridecemLineatus.* Lab Animal 35: 1-9.

Wu BJ, Else PL, Storlien LH, Hulbert AJ (2001) Molecular activity of Na^+/K^+-ATPase from different sources is related to the packing of membrane lipids. J Exp Biol 204: 4271-4280.

Wu BJ, Hulbert AJ, Storlien LH, Else PL (2004) Membrane lipids and sodium pumps of cattle and crocodiles: an experimental test of the membrane pacemaker theory of metabolism. Am J Physiol Regul Integr Comp Physiol 287: R633-R641.

Yoshida Y, Holloway GP, Ljubicic V, Hatta H, Spriet LL, Hood DA, Bonen A (2007) Negligible direct lactate oxidation in subsarcolemmal and intermyofibrillar mitochondria obtained from red and white rat skeletal muscle. J Physiol 582: 1317-1335.

CHAPTER 3

Changes in mitochondrial reaction oxygen species (ROS) production during hibernation and daily torpor

3.1 Introduction

In hibernating animals, blood flow is reduced to a number of tissues for several days during torpor (Bullard and Funkhouser 1962; Frerichs et al. 1994) such that these tissues would be considered clinically ischemic. Subsequently, during spontaneous arousals from torpor, blood flow to most tissues increases again, and these tissues become reperfused (Johansen 1961; Bullard and Funkhouser 1962; Osborne et al. 2005). While blood flow patterns during daily torpor have not been studied, indirect evidence suggests that daily heterotherms also experience ischemia for several hours during torpor followed by reperfusion during arousal (Tan et al. 2005).

In homeothermic mammals, ischemia-reperfusion (IR) is usually associated with considerable tissue injury (de Groot and Rauen 2007). On the other hand, when IR (or physiologically-similar states) occurs in heterothermic animals, either naturally (i.e., during torpor) or artificially (e.g., via hypothermia or induced blood flow restriction), no injury occurs; that is, heterothermic animals appear to be resistant to the deleterious effects of IR (Zhou et al. 2001; Kurtz et al. 2006; Dave et al. 2006; Christian et al. 2008). One main contributor to IR tissue injury is ROS production. There are several sources of ROS production during ischemia and reperfusion, including xanthine oxidase, NADPH oxidase, and peroxynitrate production (Montalvo-Jave et al. 2008),

but one of the principle sources of ROS production during IR is mitochondrial oxidative phosphorylation (Piantadosi and Zhang 1996; Becker et al. 1998; Hoerter et al. 2004). During ischemia, the mitochondrial ETC becomes over-reduced because of the lack of oxygen, the terminal electron acceptor. During the subsequent reperfusion, when oxygen returns to normal levels, over-reduced ETC complexes quickly transfer electrons to oxygen, favouring ROS production. Therefore, it seems likely that heterothermic animals may employ mechanisms to minimize mitochondrial ROS production during ischemia (i.e., torpor) and/or reperfusion (i.e., arousal), and/or reduce the potential for ROS production to cause significant tissue damage, thereby conveying resistance to IR.

In addition to showing resistance to IR, numerous studies suggest that heterotherms live longer than similarly-sized homeotherms. Edible dormice, which undergo hibernation, as well as extended periods of summer dormancy (Bieber and Ruf 2009) and daily torpor (Fietz et al. 2004), live up to 9 years in captivity (Krystufek et al. 2005, and references therein) while comparably-sized homeothermic rodents typically have a much shorter lifespan (~ 5-6 years; Speakman et al. 2005). Among bats, hibernating species live 6 years longer than non-hibernators on average (Wilkinson and South 2002). Moreover, within a given heterothermic species, individuals showing longer periods of torpor also have longer lifespans. Lyman et al. (1981) showed a positive correlation between percentage of lifespan spent in hibernation and age at death in Turkish hamsters. In both Brandt's bats and little brown bats, males have longer hibernation seasons and live longer than females (Podlutsky et al. 2005). Finally, fat-tailed dwarf lemurs living in dry forests, which hibernate for 7 months, have a nearly 2-

fold higher life expectancy than conspecifics living in rainforests, which hibernate for only 5 months (Lahann and Dausmann 2011). While reduced predation rates during torpid seasons may contribute to the relationship between torpor and longevity (Turbill et al. 2011; but see also Sommer et al. 2009), torpor may also slow down the rate of processes that contribute to aging, thereby increasing longevity.

One widely-accepted theory of aging (despite some recent opposition [Buffenstein et al. 2008; Gems and Doonan 2009; Lapointe and Hekimi 2010]) is the free radical theory (Harman 1956; Schriner et al. 2005; Sanz et al. 2006). This theory proposes that aging is the result of a progressive accumulation of ROS-induced oxidative damage to proteins, DNA, and membrane phospholipids. Furthermore, it predicts that long lifespan is achieved by processes that alleviate oxidative damage. Consistent with this notion, a number of studies have demonstrated that the rate of accumulation of oxidative damage is slower in longer-lived species (or individuals) than shorter-lived species (or individuals; Sohal et al. 1993; Sohal et al. 1995; Barja and Herrero 2000). The main source of ROS in animals is the mitochondria (Turrens 2003); therefore, it seems likely that heterothermic animals employ mechanisms to alleviate mitochondrial ROS production and/or its damaging effects during torpor, thereby increasing lifespan.

Thus, heterothermic mammals demonstrate two phenotypes (IR injury resistance and long lifespan), both of which may be mediated by minimizing ROS production and/or its damaging effects. In general, there are three ways that heterothermic species could minimize ROS-induced oxidative damage: i) reduce ROS production rates; ii) increase ROS degradation rates by increasing antioxidant levels; and/or iii) better repair

ROS-induced oxidative damage after it occurs. Most research investigating how heterothermic mammals might prevent ROS-induced oxidative damage during torpor and/or arousal has focused on the role of antioxidants. A number of studies have shown increased levels of at least some antioxidants during torpor and/or arousal in some tissues of hibernating animals (Buzadzic et al. 1990; Toien et al. 2002; Ma et al. 2004; Eddy et al. 2005; Osbourne and Hashimoto 2006; Okamoto et al. 2006; Ohta et al. 2006; Morin and Storey 2007; Page et al. 2009; Ni and Storey 2010). Moreover, transcription factors that broadly regulate antioxidant expression are also upregulated in several tissues during torpor in hibernating animals (Morin et al. 2008). By contrast, to my knowledge, no studies have measured mitochondrial ROS production during torpor in any hibernator or daily heterotherm. A few studies have estimated cellular ROS production rates in heterotherms via indirect methods, including uric acid levels, and these studies suggest that ROS production increases during torpor and/or arousal (Okamoto et al. 2006; Osborne and Hashimoto 2006), at least in some tissues.

Therefore, the objective of this chapter of my thesis was to measure and compare rates of mitochondrial ROS production among metabolic states in hibernation (in ground squirrels) and daily torpor (in dwarf Siberian hamsters and mice). Given that heterothermy is associated with IR injury resistance and long lifespan, both of which may be mediated via alleviation of ROS production, I hypothesize that ROS production is reduced in mitochondria isolated from torpid compared to euthermic animals. As with mitochondrial respiration rate, there are two mechanisms by which ROS production may be reduced in torpid mitochondria: active, regulated inhibition and/or passive thermal effects. Therefore, I measured mitochondrial ROS production rates over a range

of physiologically-relevant temperatures in order to assess the potential contribution of each mechanism.

3.2 Experimental Procedures

3.2.1 Animals. Thirteen-lined ground squirrels (*Ictidomys tridecemlineatus*), house mice (*Mus musculus*; Balb/c strain only), and dwarf Siberian hamsters (*Phodopus sungrous*) were maintained under the same conditions as described in Chapter 2. Ground squirrels were sampled when summer active, interbout euthermic, or torpid, as described in Chapter 2. Mice and hamsters were sampled when euthermic or torpid according to the definitions outlined in Chapter 2.

3.2.2 Mitochondrial isolation and respiration rate. Euthermic animals were euthanized with Euthanyl, and torpid animals were euthanized via cervical dislocation in order to prevent arousal, as described in Chapter 2. For ground squirrels, mice, and hamsters, the liver was immediately removed and transferred to ice-cold liver homogenization buffer, and mitochondria were isolated for each species as described in Chapter 2. Skeletal muscle tissue from both hind limbs of ground squirrels was also excised and washed in ice-cold skeletal muscle homogenization buffer. Purified mitochondria were isolated as described in Chapter 2. In addition, for hamsters, the whole heart was removed and transferred to ice-cold heart homogenization buffer, and crude mitochondria were obtained as described in Chapter 2. Mitochondrial state 4 respiration rates were measured in all tissues examined at 37°C, as well as 10°C and 25°C (for ground squirrels) and 15°C and 26°C (for hamsters and mice) using temperature-controlled polarographic O_2 meters as described in Chapter 2.

3.2.3 Mitochondrial ROS production. Mitochondrial ROS production was measured as H_2O_2 release (see Chapter 1). ROS production was measured under state 4 conditions at 10, 25 and 37°C (ground squirrels) or 15, 26, and 37°C (hamsters and mice) according to an assay procedure modified from Barja (1998; see also Brown et al. 2009). For ground squirrels, both glutamate- and succinate-fueled ROS production were measured in each mitochondrial preparation, but in hamsters and mice, either glutamate- or succinate-fueled ROS production (but not both) was measured in each mitochondrial preparation because of low mitochondrial yield due to small liver size. Substrates and inhibitors were added to the same concentrations used for mitochondrial respiration (Chapter 2; all concentrations are the final concentration of the compound in the centrifuge tube during ROS production measurements). In a 1.7mL centrifuge tube, a reaction mixture (1.5mL total) was prepared by adding the following reagents in the following order: buffer (145mM KCl, 30mM HEPES, 5mM KH_2PO_4, 3mM $MgCl_2$, 0.1mM EGTA, 0.1% bovine serum albumin, pH 7.4 at 37°C), mitochondria (~0.1 mg protein mL^{-1}), horseradish peroxidase (4 U mL^{-1}), and homovanillic acid (4 mM). Glutamate and malate, or succinate and rotenone, were added to stimulate basal ROS production. Two reaction mixtures were prepared: one was immediately immersed in ice (0 min incubation) and one was incubated for 20-60 min (depending on substrate and temperature) then immersed in ice to stop any further ROS production. Rates of ROS production were determined by linear regression between these two points. Substrate-free controls were performed to allow for correction for endogenous ROS production. Endogenous ROS production was negligible, even in the presence of ETC inhibitors. Duplicate 225μL samples from each centrifuge tube were added to 75μL of

glycine buffer (0.1M glycine, 25mM EDTA, pH 12 at room temperature) in 96-well black plates, and the fluorescence of the dimer produced from homovanillic acid in the presence of H_2O_2 and horseradish peroxidase was measured at 310nm excitation and 420nm emission (SpectraMax M2e, Molecular Devices, Sunnyvale CA). The glycine buffer increased the pH of the sample to 10, which produces maximal fluorescence of the dimer (Ruch et al., 1983). In parallel, maximal mitochondrial ROS production at complex I and complex III was measured by adding rotenone or antimycin A (5 µg mL^{-1}, dissolved in ethanol) to glutamate- and succinate-fueled respiration, respectively. Fluorescence values were converted to rates of H_2O_2 release using a standard curve generated by the production of known amounts of H_2O_2 by glucose oxidase with glucose as substrate, a reaction which was linear over at least 10 min. Rates of mitochondrial H_2O_2 release were linear over the time course examined.

Mitochondrial H_2O_2 release rate and state 4 respiration rates for individual preparations were used to calculate the percentage free radical leak (FRL), which is a measure of the proportion of electrons that produce $O_2^{-}\cdot$ (and subsequently H_2O_2) compared to the total number of electrons which pass through the ETC (Barja et al., 1994), according the following equation:

$$FRL = 100\left(\frac{H_2O_2 \;\; production \;\; rate}{2 \bullet O_2 \;\; consumption \;\; rate}\right)$$

(Equation 3-1).

3.2.4 Data analysis. Unless otherwise indicated, data presented are mean ± SEM. Basal and maximal ROS production, as well as FRL, were analyzed using a

general linear model in SAS 9.2 with metabolic state, temperature, and species (where applicable; mice and hamsters were analyzed together) as factors in the analysis. Non-significant interactions were dropped from the model. FRL was arcsine transformed prior to analysis. Q_{10} values were calculated with data from all temperatures using a 2-parameter exponential equation, and Q_{10} values for ROS production and respiration rate were compared using a general linear model with type (ROS vs. respiration), metabolic state, and species (where applicable).

3.3 Results

3.3.1 Liver mitochondrial ROS production measured at 37°C. Mitochondrial ROS production rate was measured under basal and maximal conditions (i.e., in the absence and presence of ETC inhibitors acting downstream of the ROS-production sites, respectively), and basal ROS production was used to calculate FRL. FRL could not be calculated for summer active animals because mitochondrial respiration rate was not measured for these animals, but it was estimated using the assumption that respiration rate does not differ between summer and interbout euthermia in liver mitochondria (Armstrong and Staples 2010), and I will comment on it briefly in these results for comparative purposes.

In ground squirrels, with glutamate as substrate, basal ROS production was 87% lower in mitochondria from interbout euthermic animals compared to both summer active and torpid animals, which did not differ from each other (Figure 3-1A), when measured at 37°C. FRL was reduced to a similar degree, suggesting that lower ROS production in interbout euthermic animals did not result from a reduction of

mitochondrial respiration rate (Figure 3-1B). Maximal ROS production was also 22% lower in interbout euthermic animals than summer active animals, but it was 33% higher in torpid animals than summer animals (Figure 3-1C). With succinate, basal ROS production measured at 37°C did not differ among the three metabolic states (Figure 3-1D), but FRL was 27% higher in torpid animals compared to interbout euthermic animals and my estimate for summer active animals (Figure 3-1E) because state 4 respiration rate is reduced in torpid animals but ROS production is not. By contrast, maximal ROS production was 35% lower in torpid animals compared to either summer active or interbout euthermic animals, which did not differ from each other (Figure 3-1F).

Basal ROS production with glutamate did not differ between torpid and euthermic animals in either mice or hamsters (Figure 3-2A) when measured at 37°C, but, with succinate, basal ROS production was 26-43% higher in torpid animals than euthermic animals in both species (Figure 3-2B). Differences in basal ROS production were also reflected in my calculations of FRL, which did not differ between metabolic states with glutamate (Figure 3-2C), but were 1.6-2.6-fold higher in torpid animals than euthermic animals with succinate (Figure 3-2D). In contrast to basal ROS production, maximal ROS production with glutamate was 31% and 19% lower in torpid animals than euthermic controls in both mice and hamsters, respectively (Figure 3-2E), but showed a species-specific response with succinate, being 58% higher in torpid hamsters than euthermic hamsters, but not different between metabolic states in mice (Figure 3-2F).

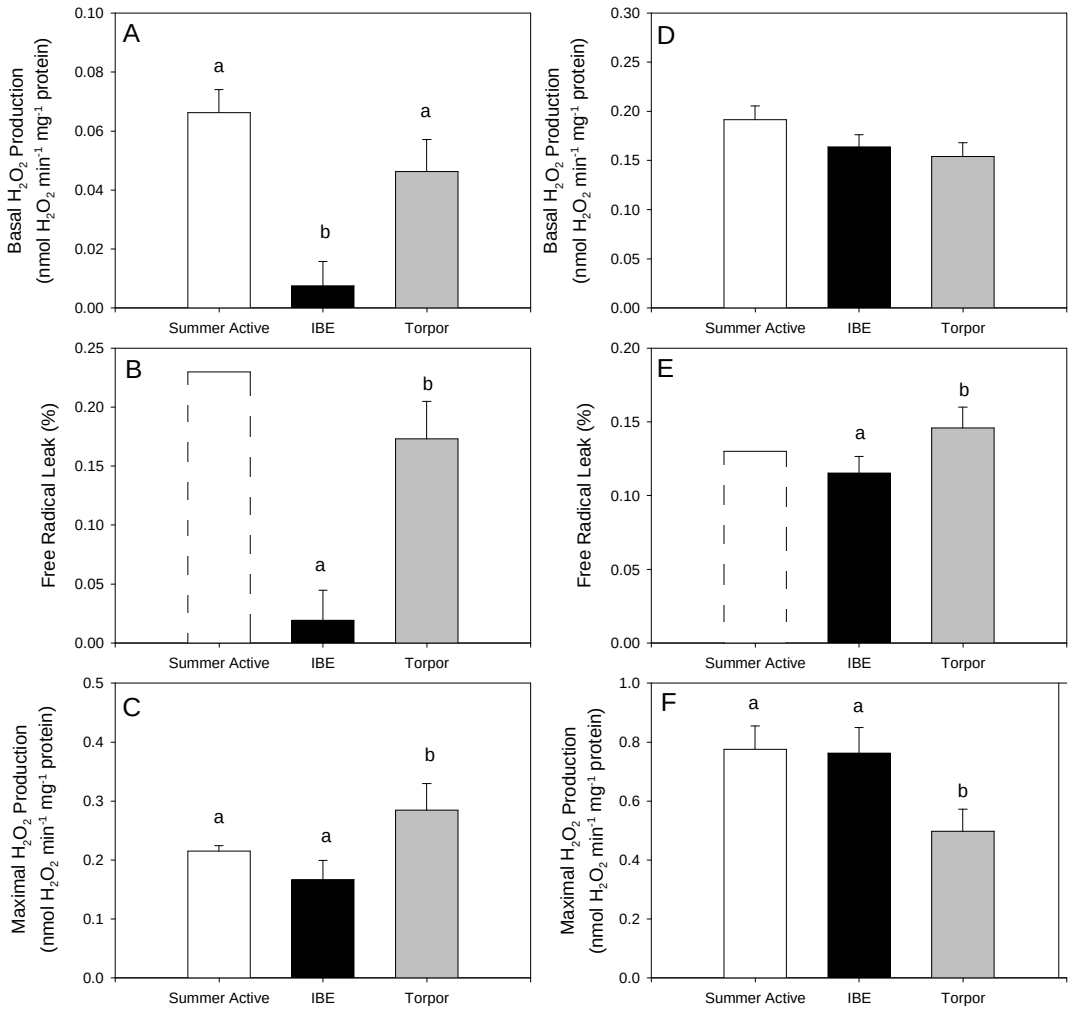

Figure 3-1. Liver mitochondrial reactive oxygen species (ROS) production and free radical leak measured at 37°C during summer, interbout euthermia (IBE), and torpor in thirteen-lined ground squirrels. ROS production was measured with glutamate (left-hand panels) or succinate (right-hand panels). Data shown are mean ± SEM. N=8 for summer active and torpor, N=5 for interbout euthermia. Values for bars with different letters are significantly ($P < 0.05$) different from each other. Dashed lines for free radical leak from summer active animals indicate that these data are estimates.

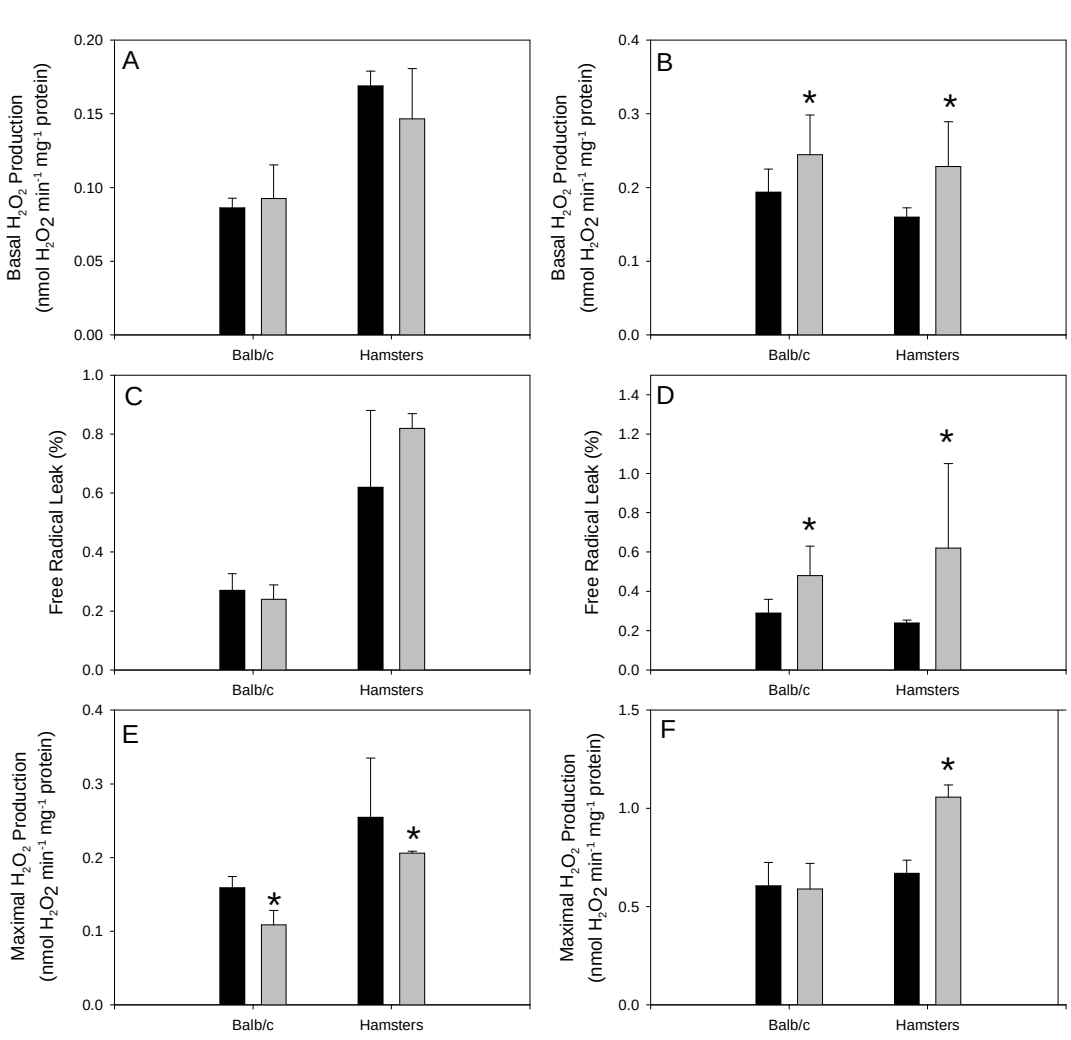

Figure 3-2. Liver mitochondrial reactive oxygen species (ROS) production measured at 37°C in torpid and euthermic mice (Balb/c strain) and hamsters. ROS production was measured with glutamate (left-hand panels) and succinate (right-hand panels). Black bars represent euthermic animals, and grey bars represent torpid animals. Data shown are mean ± SEM. For euthermic Balb/c mice, N=5 for glutamate, N=6 for succinate. For torpid Balb/c mice, N=3 for glutamate, N=5 for succinate. For hamsters, N=3 in all conditions. *, $P < 0.05$ compared to euthermic animals of the same species.

3.3.2 Effects of temperature on liver mitochondrial ROS production. In ground squirrels, with glutamate (Figure 3-3A), basal ROS production declined with temperature in torpid and summer active animals, but not interbout euthermic animals, where mitochondria produced ROS at low rates regardless of temperature. In addition, differences in basal ROS production rate observed at 37°C were not seen at either 10°C or 25°C. FRL with glutamate (Figure 3-3B) did not decline with temperature in mitochondria from either torpid or interbout euthermic animals, and remained higher in interbout euthermia than torpor at all temperatures. By contrast, estimated FRL in summer active animals appears to decline with temperature, showing levels comparable to torpid animals at 37°C and 25°C but comparable to interbout euthermic animals at 10°C. Similar to basal ROS production, differences in maximal ROS production observed at 37°C also did not persist at either 10°C or 25°C with glutamate (Figure 3-3C). Also similar to basal ROS production, maximal ROS production with glutamate declined with temperature in mitochondria from summer active and torpid animals, but not interbout euthermic animals.

With succinate, basal ROS production declined with temperature, but did not differ among metabolic states at any temperature (Figure 3-3D). FRL also declined with temperature, and remained higher in mitochondria from torpid animals than either interbout euthermic or summer active animals at all temperatures (Figure 3-3E). Similarly, maximal ROS production also declined with temperature, and remained lower in torpid animals than either summer active or interbout euthermic animals at all temperatures (Figure 3-3F).

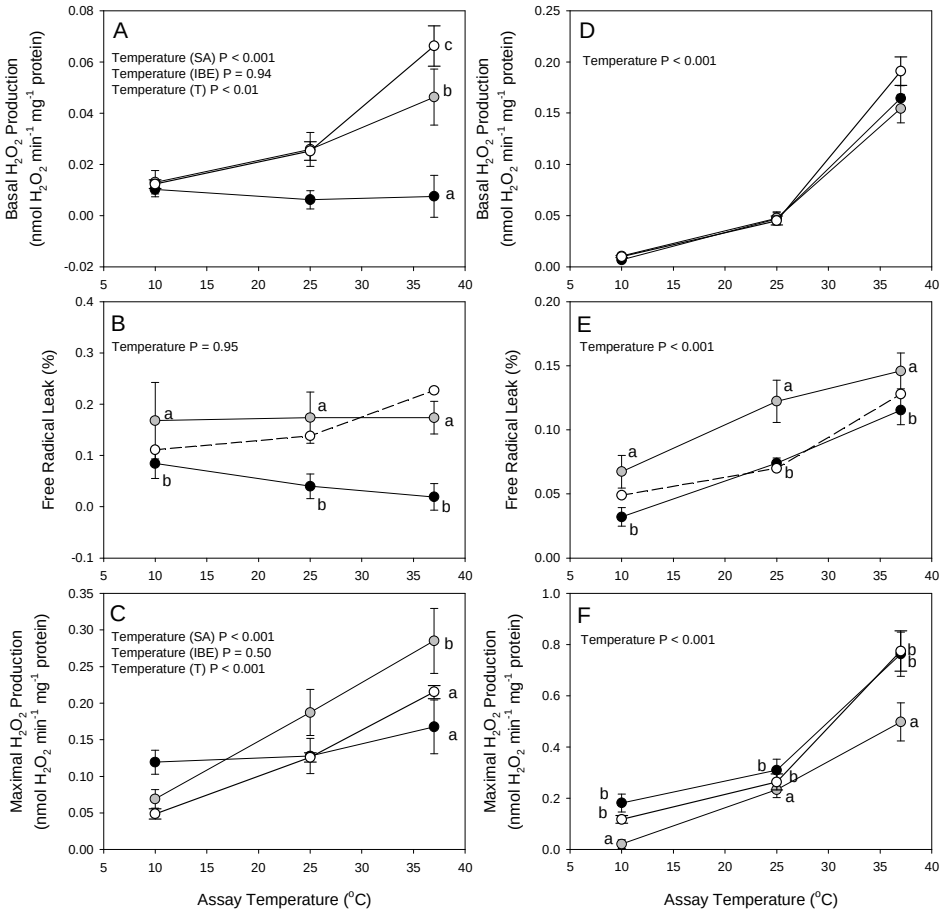

Figure 3-3. Effect of assay temperature on liver mitochondrial ROS production in summer active (SA), interbout euthermic (IBE), and torpid (T) ground squirrels. ROS production was measured with glutamate (left-hand panels) or succinate (right-hand panels). Data for 37°C is the same as in Figure 3-1. Data shown are mean ± SEM. N=8 for summer active and torpor, N=5 for interbout euthermia. Temperature effects are indicated by P values shown in each panel. At each temperature, differences among metabolic states are indicated by letters, where values with different letters are significantly ($P < 0.05$) different from each other. White, black, and grey symbols represent summer active, interbout euthermia, and torpor, respectively. FRL values for summer active animals are estimates only, as indicated by the dashed lines.

In mice and hamsters, basal ROS production (Figure 3-4A,B) and FRL (Figure 3-4C,D) declined with temperature in both species when glutamate fueled respiration, but did not differ between torpid and euthermic animals. Similarly, maximal ROS production (Figure 3-4E,F) also declined with temperature in both species, but was lower in torpid animals in both species at all temperatures. When succinate fueled respiration rate, basal ROS production (Figure 3-5A,B) and FRL (Figure 3-5C,D) both declined with temperature in mice and hamsters, and, in both species, was higher in torpid animals than euthermic animals at all temperatures. As with both basal ROS production and FRL, maximal ROS production (Figure 3-5E,F) also declined with temperature. Differences in maximal ROS production between metabolic states, however, was both temperature- and species-specific. In mice, maximal ROS production did not differ between torpid and euthermic mice regardless of temperature; in hamsters, on the other hand, maximal ROS production was higher during torpor at both 37°C and 25°C, but not 10°C.

3.3.3 Skeletal muscle ROS production in hibernating ground squirrels. When measured at 37°C, with glutamate, basal ROS production in skeletal muscle was nearly 50% higher in torpid animals than interbout euthermic animals (Figure 3-6A), but no difference was observed when succinate fueled respiration (Figure 3-6B). However, FRL did not differ among metabolic states regardless of the substrate used (Figure 3-6C,D), suggesting that higher ROS production with glutamate in torpid animals simply reflected higher state 4 respiration rates. Maximal ROS production rate was 57% lower in torpid animals when glutamate fueled respiration (Figure 3-6E), but no difference

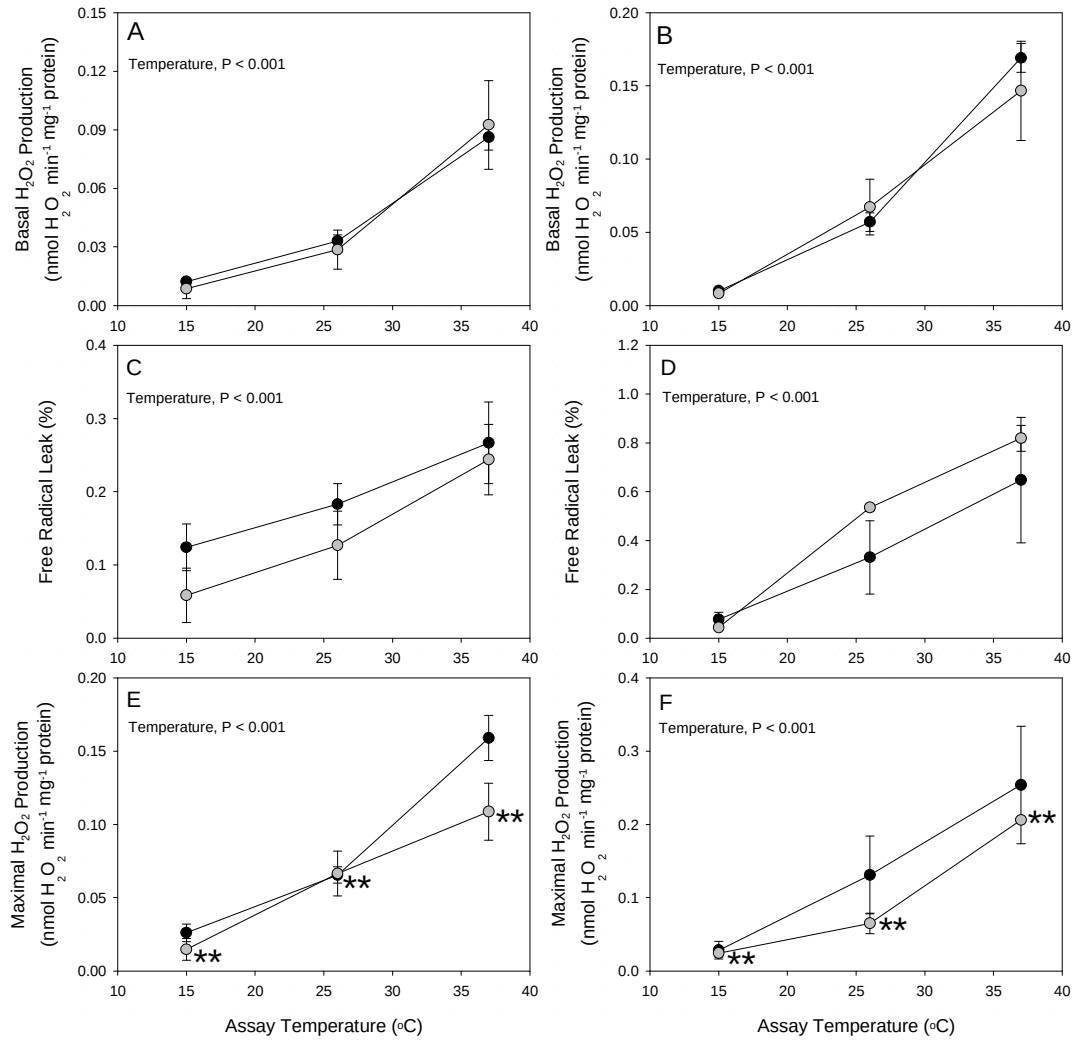

Figure 3-4. Effect of assay temperature on liver mitochondrial ROS production in euthermic and torpid mice and hamsters with glutamate. The left-hand panels show ROS production for mice, and the right-hand panels show ROS production for hamsters. Data for 37°C is the same as in Figure 3-2. Black and grey symbols represent euthermic and torpid animals, respectively. Data shown are mean ± SEM. N=5 for euthermic mice, N=3 for torpid mice, N=3 for all hamsters. P values for temperature effects are shown in each panel. At each temperature, differences between metabolic states are indicated by symbols. **, $P < 0.01$ vs. euthermic animals.

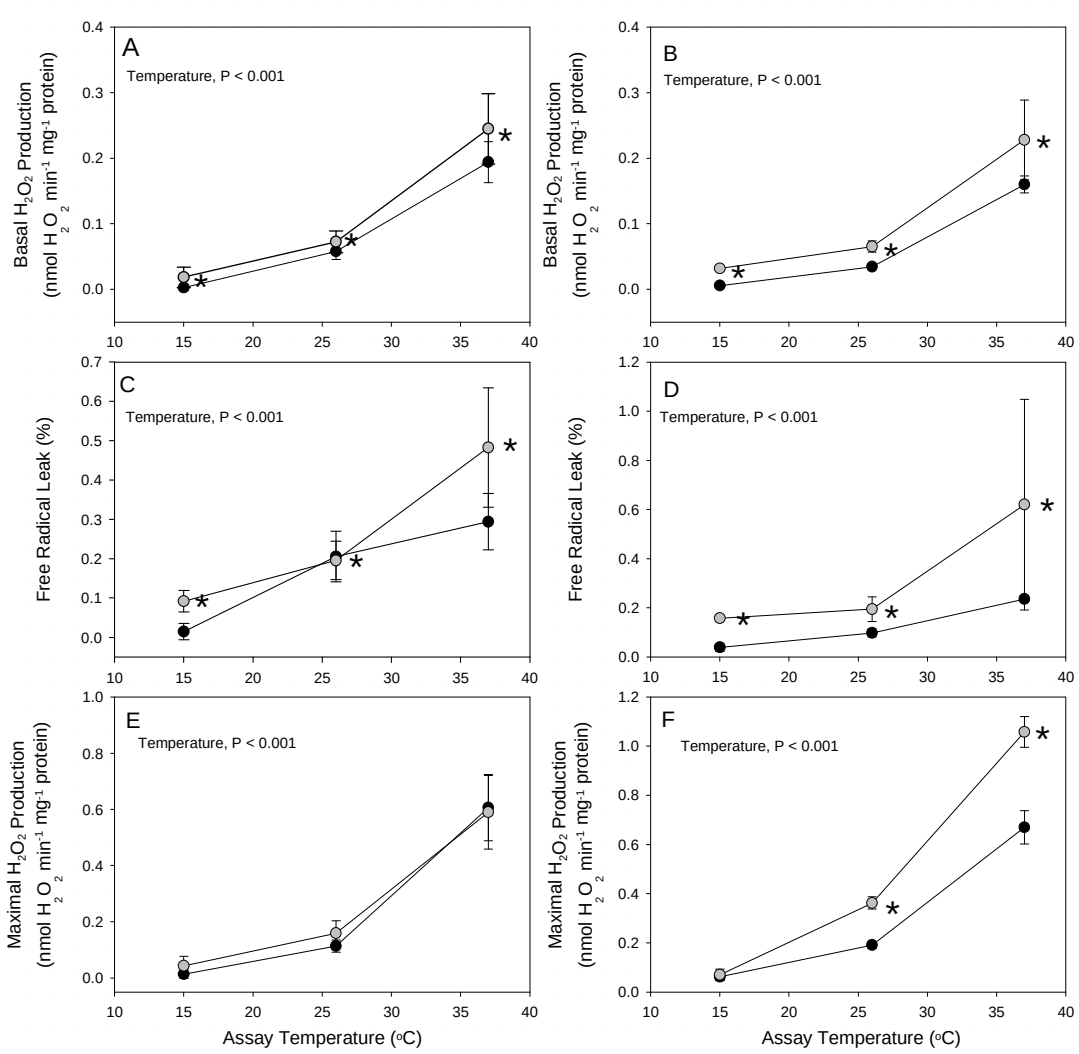

Figure 3-5. Effect of assay temperature on liver mitochondrial ROS production in euthermic and torpid mice and hamsters with succinate. The left-hand panels show ROS production for mice; the right-hand panels show ROS production for hamsters. Data for 37°C is the same as in Figure 3-2. Black and grey symbols represent euthermic and torpid animals, respectively. Data shown are mean ± SEM. N=6 for euthermic mice, N=5 for torpid animals, N=3 for all hamsters. P values for temperature effects are shown in each panel. At each temperature, differences among metabolic states are shown using symbols. *, $P < 0.05$ vs. euthermic animals.

was observed with succinate (Figure 3-6F). The differences (or lack thereof) observed at 37°C were also observed at 10°C and 25°C with both glutamate (Figure 3-7A-C) and succinate (Figure 3-7D-F), suggesting that differences among metabolic states were not temperature-dependent. As temperature declined, basal ROS production and FRL declined with temperature regardless of the metabolic state or substrate used; however, while maximal ROS production with glutamate declined with temperature in both torpid and interbout euthermic animals, maximal ROS production with succinate did not in either metabolic state.

3.3.4 Heart mitochondrial ROS production during daily torpor in hamsters. Basal ROS production of heart mitochondria was 2.4 and 2-fold higher in torpid animals than euthermic animals with glutamate (Figure 3-8A) or succinate (Figure 3-8B), respectively, when measured at 37°C. FRL did not differ between metabolic states with glutamate (Figure 3-8C) but was higher in torpid animals (by nearly 3-fold) when succinate fueled respiration (Figure 3-8D). Maximal ROS production rate did not differ between torpid and euthermic animals regardless of the substrate used (Figure 3-8E,F).

Higher rates of basal ROS production with both glutamate (Figure 3-9A) and succinate (Figure 3-9B) in mitochondria from torpid animals persisted at both 25°C and 10°C. FRL with glutamate did not differ from between metabolic states at any temperature (Figure 3-9C), but FRL with succinate was higher in torpid animals at all temperatures (Figure 3-9D). Maximal ROS production never differed among metabolic states, regardless of the substrate used (glutamate, Figure 3-9E; succinate, Figure 3-9F). Basal ROS production declined with temperature in torpid and euthermic animals with both glutamate and succinate, and FRL declined with temperature in both metabolic

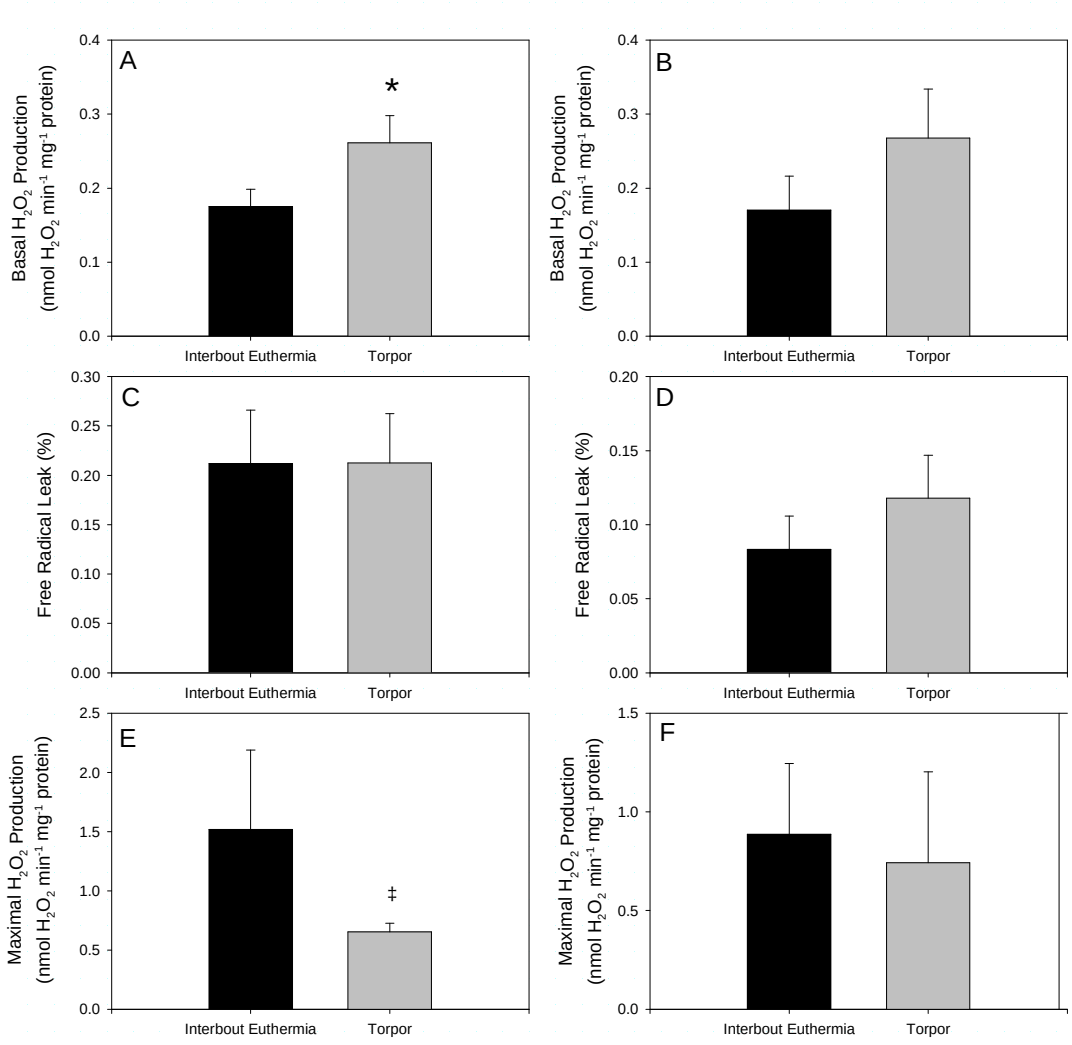

Figure 3-6. Skeletal muscle mitochondrial reactive oxygen species (ROS) production measured at 37°C during interbout euthermia and torpor in hibernating thirteen-lined ground squirrels. ROS production was measured with glutamate (left-hand panels) and succinate (right-hand panels). Data shown are mean ± SEM. N=5 for interbout euthermia, N=8 for torpor. *, $P < 0.05$; ‡, $P < 0.10$ compared to interbout euthermia.

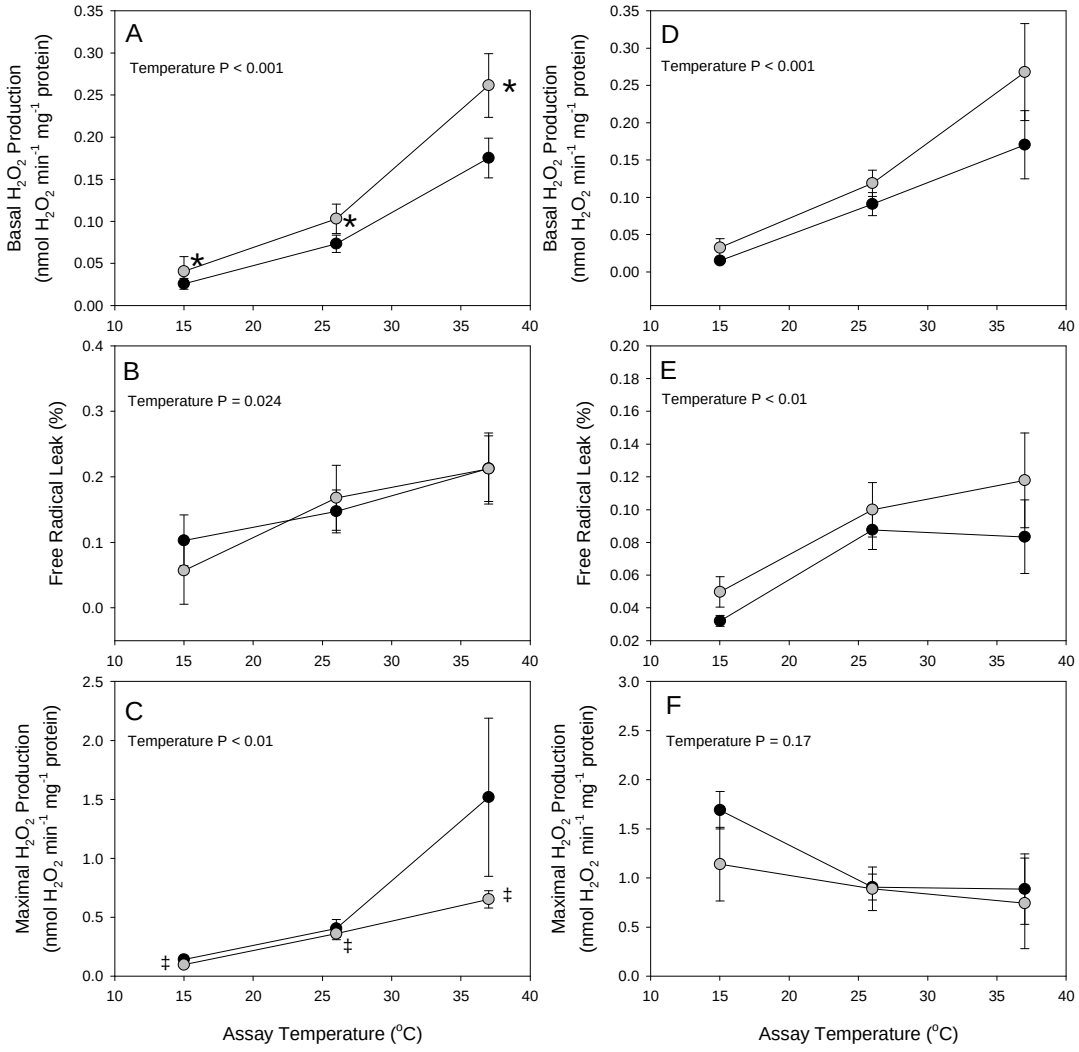

Figure 3-7. Effect of assay temperature on skeletal muscle mitochondrial ROS production in interbout euthermic and torpid ground squirrels. ROS production was measured with glutamate (left-hand panels) or succinate (right-hand panels). Data for 37°C is the same as in Figure 3-6. Data shown are mean ± SEM. N=5 for interbout euthermia, N=8 for torpor. Temperature effects are indicated by P values shown in each panel. At each temperature, differences among metabolic states are indicated by symbols. *, $P < 0.05$; ‡, $P < 0.10$ vs. interbout euthermic animals. Black, and grey symbols represent interbout euthermia and torpor, respectively.

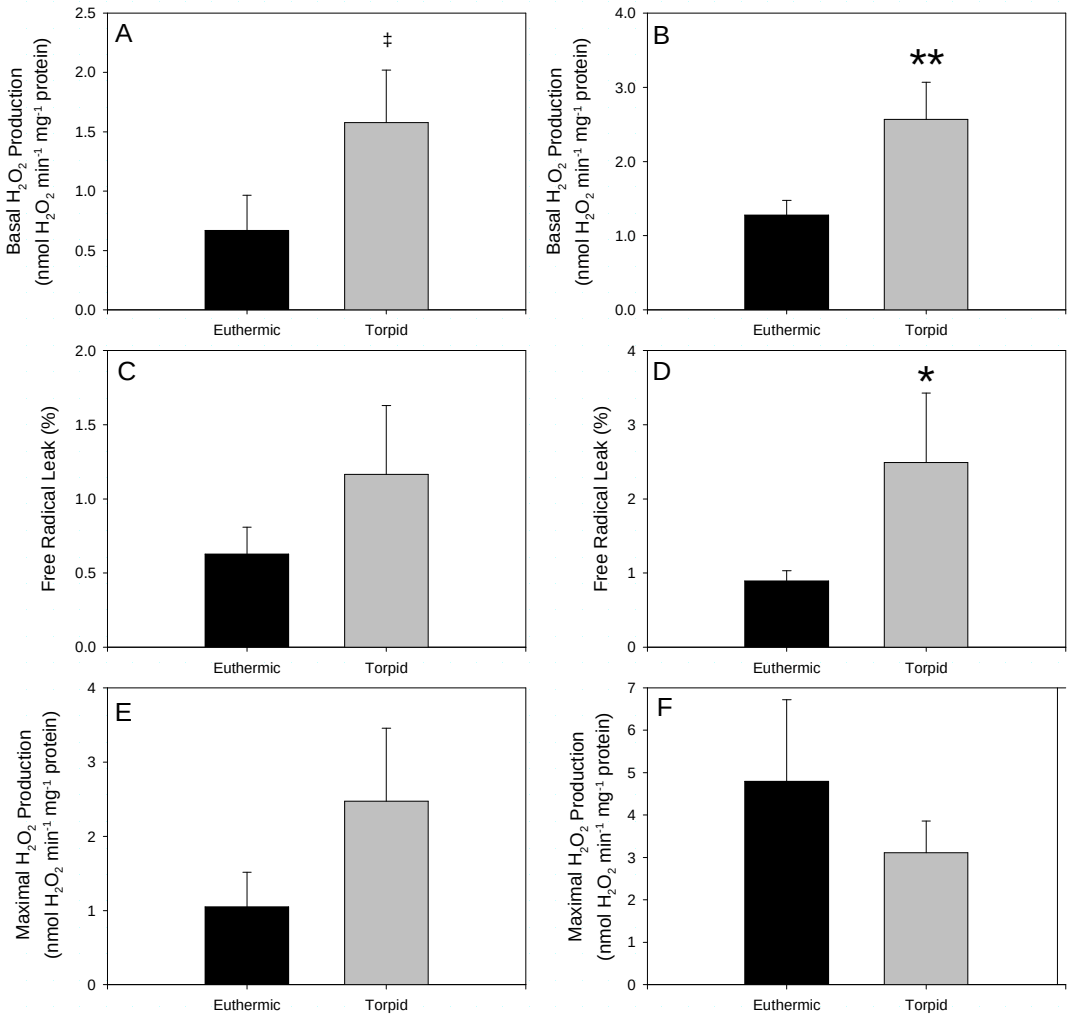

Figure 3-8. Heart mitochondrial reactive oxygen species (ROS) production measured at 37°C during euthermia and torpor in hamsters. ROS production was measured with glutamate (left-hand panels) and succinate (right-hand panels). Data shown are mean ± SEM. N=3. **, $P < 0.01$; *, $P < 0.05$; ‡, $P < 0.10$ compared to interbout euthermia.

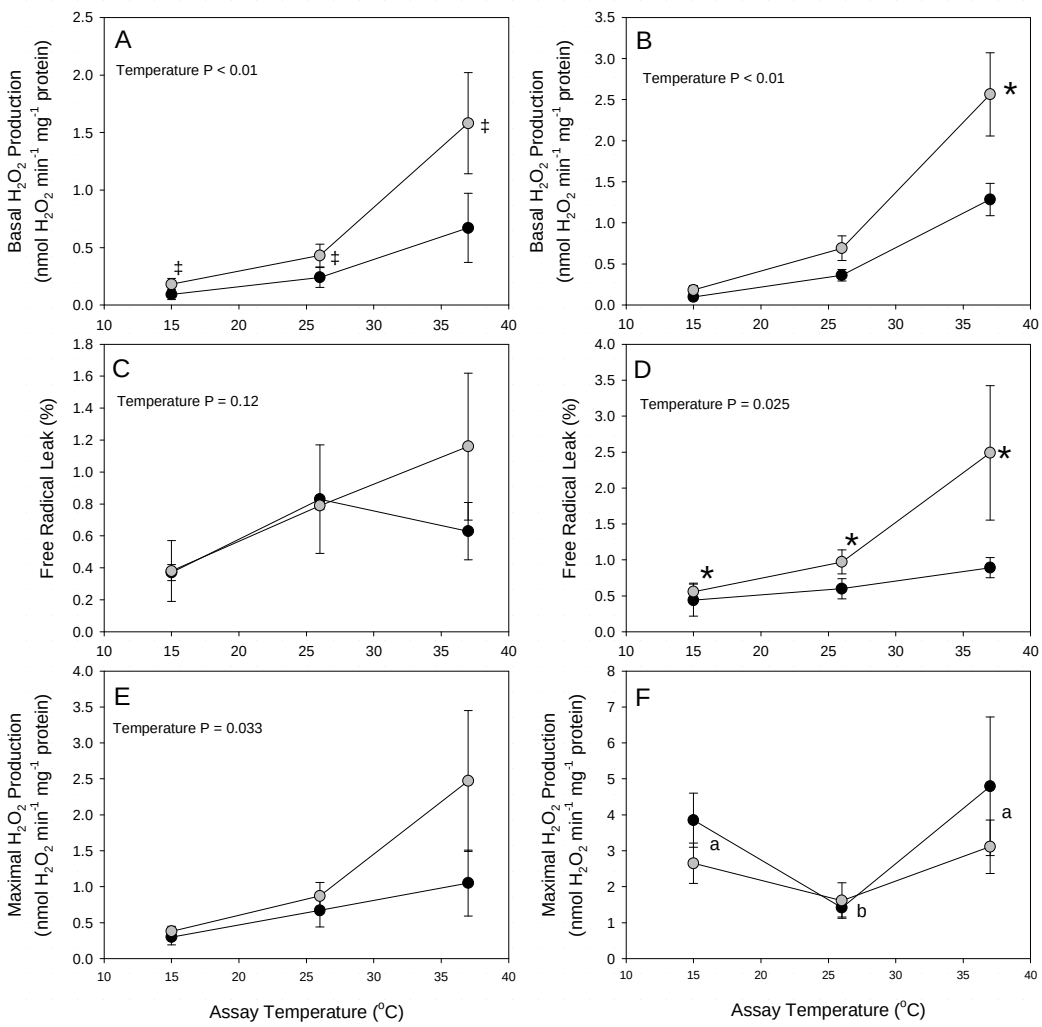

Figure 3-9. Effect of assay temperature on heart mitochondrial ROS production in euthermic and torpid hamsters. ROS production was measured with glutamate (left-hand panels) and succinate (right-hand panels). Data for 37°C is the same as in Figure 3-8. Data shown are mean ± SEM. N=3. P values for temperature effects are shown in each panel except F, where values with different letters are significantly ($P < 0.05$) different. At each temperature, differences between metabolic states are shown using symbols. *, $P < 0.05$; ‡, $P < 0.10$ compared to euthermic animal

Table 3-1. Q_{10} values for state 4 respiration rate and ROS production rate of liver and skeletal mitochondria isolated from ground squirrels during summer, interbout euthermia (IBE), and torpor. N=8 for summer active and torpor, N=5 for interbout euthermia. **, P < 0.01; *, P < 0.05; ‡, P < 0.10 vs. respiration rate in the same tissue and metabolic state. Differences among metabolic states are shown using letters, where values with different letters are significantly (P < 0.05) different from each other.

	Glutamate					
	Respiration Rate			ROS Production Rate		
	Summer Active	IBE	Torpor	Summer Active	IBE	Torpor
Liver	1.72 ± 0.14	1.54 ± 0.12	1.43 ± 0.09	2.15 ± 0.12 * a	1.15 ± 0.15 b	1.79 ± 0.14 c
Skeletal Muscle	---	1.48 ± 0.087	1.49 ± 0.08	---	2.15 ± 0.27 **	2.05 ± 0.13 **

	Succinate					
	Respiration Rate			ROS Production Rate		
	Summer Active	IBE	Torpor	Summer Active	IBE	Torpor
Liver	2.29 ± 0.21	2.03 ± 0.06	2.42 ± 0.39	3.39 ± 0.26 **	3.01 ± 0.27 **	2.75 ± 0.13 **
Skeletal Muscle	---	1.77 ± 0.07	1.65 ± 0.09	---	2.15 ± 0.34 ‡	1.98 ± 0.21 ‡

Table 3-2. Q_{10} values for state 4 respiration rate and ROS production rate of liver mitochondria isolated from euthermic and torpid mice. For glutamate, N=5 for euthermia, N=3 for torpor. For succinate, N=6 for euthermia, N=5 for torpor. **, $P < 0.01$ vs. respiration rate in the same metabolic state with the same substrate. There were no differences between euthermic and torpid animals in any case.

	Respiration Rate		ROS Production Rate	
	Euthermia	Torpor	Euthermia	Torpor
Glutamate	1.72 ± 0.13	1.50 ± 0.03	2.45 ± 0.17 **	4.67 ± 2.56 **
Succinate	1.75 ± 0.16	1.92 ± 0.29	3.96 ± 0.87 **	3.52 ± 0.61 **

Table 3-3. Q_{10} values for state 4 respiration rate and ROS production rate of liver and heart mitochondria isolated from euthermic and torpid dwarf Siberian hamsters. N=3 in all cases. * P < 0.01 vs. respiration rate measured in the same tissue and metabolic state. There were no differences between metabolic states in any case.

	Glutamate			
	Respiration Rate		ROS Production	
	Euthermia	Torpor	Euthermia	Torpor
Liver	1.38 ± 0.13	1.15 ± 0.05	2.91 ± 0.24 **	2.27 ± 0.19 **
Heart	2.40 ± 0.03	1.99 ± 0.20	2.47 ± 0.11	3.50 ± 1.46

	Succinate			
	Respiration Rate		ROS Production	
	Euthermia	Torpor	Euthermia	Torpor
Liver	1.90 ± 0.12	1.72 ± 0.36	4.29 ± 0.72 **	2.80 ± 0.40 **
Heart	2.17 ± 0.22	1.92 ± 0.30	3.25 ± 0.21 **	3.51 ± 0.60 **

states with succinate (and nearly so with glutamate). Maximal ROS production also declined with temperature when glutamate fueled respiration, but an interesting response to temperature was noted with succinate. In both torpid and euthermic animals, maximal ROS production with succinate declined between 37°C and 25°C, but increased between 25°C and 10°C.

3.3.5 Temperature-sensitivity of mitochondrial respiration rate and ROS production. In general, Q_{10} values for ROS production were higher than for respiration rate in mitochondria from ground squirrels (Table 3-1), mice (Table 3-2), and hamsters (Table 3-3). There are only two exceptions: Q_{10} values for ROS production and respiration rate did not differ in ground squirrel liver mitochondria from interbout euthermic and torpid animals when glutamate fueled respiration, or in hamster heart mitochondria with glutamate.

3.4 Discussion

3.4.1 Liver and heart mitochondrial ROS production at complex III is higher during torpor. In both hibernators and daily heterotherms, at all assay temperatures, liver and heart mitochondria from torpid animals had higher levels of FRL (and sometimes basal ROS production) compared to mitochondria from euthermic animals when succinate was used to fuel respiration (Figures 3-3E, 3-5D, 3-9D). In the presence of rotenone, which inhibits reverse electron flow to complex I (see Chapter 1), all ROS production with succinate is derived from complex III. Therefore, it appears that liver and heart mitochondria from torpid animals leak electrons from complex III more readily than euthermic mitochondria. In skeletal muscle, FRL with succinate showed no

difference between euthermia and torpor, although the trend was toward higher FRL in torpid animals (Figure 3-7E).

ROS production at complex III is sensitive to $\Delta\Psi_m$ (Korshunov et al. 1997); however, $\Delta\Psi_m$ was not consistently higher in torpid animals in this study (Figure 2-10C, 2-13) or previous work in our lab (Brown et al. 2007). In addition, Barger et al. (2003) showed a decrease in $\Delta\Psi_m$ during torpor in Arctic ground squirrels. Therefore, $\Delta\Psi_m$ is not likely responsible for the increased electron leakiness of complex III during torpor. Rather, the most likely contributing factor is an increase in the degree of reduction of complex III during torpor. The degree of reduction of complex III is a function of the rate at which electrons arrive at the ROS-producing site within complex III (i.e., Q_o) compared to rate at which they leave this site. When electrons arrive at the complex III ROS-producing site faster than they leave, the site is more likely to be reduced at any given time, which increases the likelihood of ROS production.

The data in this study support the notion that the degree of complex III reduction increases during torpor in liver and heart mitochondria. When antimycin A was added to succinate-fueled mitochondria, the ROS-producing site Q_o of complex III becomes fully reduced and produces ROS at a maximal rate. For the most part, maximal ROS production with succinate was not higher in torpid animals in this study (Figures 3-3F, 3-5E,F, 3-7F, 3-9F). Therefore, when the degree of complex III reduction is the same (i.e., fully reduced), torpid mitochondria do not produce ROS at higher rates than euthermic mitochondria. Thus, higher FRL with succinate under basal conditions must reflect an increase in the degree of complex III reduction in torpid animals.

Complex III reduction state would increase in torpor if some site(s) downstream of the complex III ROS-production site (e.g., cytochromes b_H and b_L, cytochrome c, complex IV) were inhibited. Expression of some subunits of complex IV have been shown to be upregulated during hibernation, which might rule out a role for this complex, though complex IV activity was not assessed (Hittel and Storey 2002). Muleme et al. (2006) showed that electron flux through complex IV is reduced during torpor (but also arousal) in ground squirrels, which could promote ROS production at complex III during torpor. Petrosillo et al. (2003) showed that cardiolipin, an IMM-specific phospholipid (Schlame et al. 2000), is lost during ischemia, leading to impaired complex III activity and increased ROS production from this site; however, Chung et al. (2011) have shown that cardiolipin content does not change during torpor, at least in ground squirrel liver mitochondria. Pasdois et al. (in press) showed that heart mitochondria isolated following ischemia showed a 2-fold higher rate of mitochondrial ROS production than mitochondria isolated prior to ischemia as a result of the loss of cytochrome c, which caused the remaining cytochrome c (and likely also upstream ETC components) to become more reduced. I am not aware of any studies that have examined changes in cytochrome c content in mitochondria during torpor, if loss of cytochrome c plays some role in increasing ROS production during torpor, supplementation of mitochondria with exogenous cytochrome c should reduce ROS production to a greater extent in mitochondria isolated from torpid animals compared to euthermic controls. It is intriguing that changes in ROS production of torpid mitochondria show parallels to changes in ROS production resulting from ischemia.

Although heterothermic animals show resistance to IR injury, mitochondria may still suffer some ischemia-induced impairments.

With few exceptions (e.g., Gehnrich and Aprille 1988; Muleme et al. 2006), most investigations of mitochondrial respiration during torpor, including the present study, have suggested that upstream components of the ETC (i.e., complex I and II) but not downstream components (i.e., complex III and IV, cytochrome c) are inhibited during torpor, which is at odds with my inferences based on changes in ROS production. Studies examining the control of mitochondrial respiration by individual ETC complexes may reconcile these contradictions. Complex III and IV levels in mitochondria have been shown to be in excess compared to other ETC complexes (Schwerzmann et al. 1989), and Rossignol et al. (2000) showed that, in both liver and heart, complex III and IV have little control over respiration compared to other ETC complexes. Therefore, inhibition of either complex III or IV could occur during torpor, causing increased ROS production at complex III, without reducing mitochondrial respiration rate. Therefore, studies of mitochondrial respiration rate alone with commonly-used substrates like glutamate and succinate may not yield a complete picture of the changes occurring in mitochondrial OxPhos during torpor.

3.4.2 ROS production at complex I is reduced during interbout euthermia in hibernators. Liver basal ROS production and FRL with glutamate were both considerably lower in interbout euthermic animals than summer active animals (Figure 3-1A,B) despite that mitochondrial respiration rates likely do not differ between these two euthermic states in liver (Armstrong et al. 2010; Chung et al. 2011). This significant reduction in basal ROS production and FRL was only partially alleviated by

rotenone, which fully reduces complex I and leads to maximal ROS production at this site. This suggests that, while the capacity of complex I may be moderately suppressed during interbout euthermia compared to summer, the degree of complex I reduction is considerably lower during interbout euthermia than summer in liver mitochondria and drastically limits ROS production from this site during interbout euthermia (and possibly also during the preceding arousal). This difference is not simply a seasonal effect, as basal ROS production rates and FRL of torpid animals were more comparable to those of summer active animals despite being acclimated to the same environmental conditions as interbout euthermic animals.

As mentioned in the introduction to this chapter, during arousal, the tissues of hibernating animals become reperfused following hours or days of ischemia. In homeothermic species, reperfusion is associated with a burst of ROS production that causes considerable oxidative damage to reperfused tissues. Heterothermic species undergo repeated periods of reperfusion (during each arousal from torpor) yet do not appear to suffer much oxidative damage, particularly in liver (Orr et al. 2009). This suggests that some mechanism likely limits ROS-induced damage during arousal.

There is convincing evidence that ascorbate dynamics may play a role in degrading ROS during arousal from torpor in hibernators (Drew et al. 1999; Ma et al. 2004). During torpor, plasma ascorbate levels increase significantly, and tissue ascorbate levels are quite low; however, during arousal, the opposite pattern is observed, as plasma ascorbate moves into various tissues and is thought to degrade any ROS produced. The present study moves our understanding forward, and suggests that simultaneous suppression of complex I ROS production and a decrease in its degree of

reduction may be another contributing mechanism. How the degree of reduction of complex I is kept low during interbout euthermia is not known, but there will likely be considerable interest in elucidating this mechanism because it may have applications to medicine for preventing tissue damage IR injury during, for example, stroke and organ transplantation. Whether a similar suppression of complex I ROS production occurs during arousal from daily torpor could not be elucidated in this study but warrants further investigation.

3.4.3 Low body temperature during torpor reduces mitochondrial ROS production and may alleviate ROS production during arousal. A decline in assay temperature from 37°C to 10-15°C reduced basal ROS production by 71-96% in all tissues studied regardless of metabolic state (Figures 3-3A,D, 3-5A,B, 3-7A,D, 3-9A,B). Therefore, although torpor increases electron leak from some sites of the ETC, this should be more than compensated for by low T_b during torpor. On the whole, then, ROS production should be reduced during torpor, consistent with my hypothesis, and this may help to explain both IR injury resistance and longevity in heterothermic mammals.

Changes in mitochondrial oxygen consumption do not always lead to parallel changes in mitochondrial ROS production (Barja 2007), but lower rates of mitochondrial respiration with temperature might lower ROS production by decreasing electron flux through ROS-producing sites. However, the predominant mechanism for lower ROS production at low temperatures is a decrease in the degree of reduction of both complex I and III at low temperature. By and large, mitochondrial FRL was lower at low temperatures in all tissues and species regardless of metabolic state (Figure 3-3B,E, 3-5C,D, 3-7B,E, 3-9C,D), suggesting that a smaller proportion of electrons leak

from the ETC (leading to ROS production) at low temperatures, likely because the ETC is more oxidized at low temperatures. Keeping the mitochondrial ETC oxidized via passive thermal effects during torpor may be an important mechanism for preventing ROS production during the subsequent reperfusion during arousal. Kil et al. (1996) showed that mild hypothermia in rat brains during ischemia reduced ROS damage during subsequent reperfusion, perhaps by a similar mechanism.

The reason that ETC complexes are more oxidized at low temperatures appears to be that mitochondrial ROS production is more temperature-sensitive than respiration rate. There are two reasons why ROS production might be more temperature-sensitive than respiration rate. First, mitochondrial ROS production is influenced by even small changes in $\Delta\Psi_m$ (Korshunov et al. 1997; Votyakova and Reynolds 2001). My data (not shown), as well as data from others (Dufour et al. 1996; Chamberlain 2004), suggest that state 4 $\Delta\Psi_m$ typically declines with temperature because proton leakiness (which consumes $\Delta\Psi_m$) is less temperature-sensitive than substrate oxidation (which generates $\Delta\Psi_m$). This would alleviate ROS production but would actually stimulate substrate oxidation, leading to differences in temperature sensitivity between ROS production and oxygen consumption. Second, all ETC components may not be uniformly temperature-sensitive. In particular, if ETC components upstream of ROS-producing sites are more temperature-sensitive than ROS-production sites downstream, as temperature declines, electrons will leave ROS-production sites faster than they arrive, keeping the sites more oxidized. In support of this contention, complexes I and II are more temperature-sensitive than complexes III and IV between 5°C and 35°C in rat hearts (Lemieux et al. 2010).

To my knowledge, no previous studies have examined temperature effects on mitochondrial ROS production in any mammalian species, but three previous studies did examine temperature effects in several ectothermic animals and showed different results to the present study. In the mantle tissue of an intertidal mud clam (Abele et al. 2002) and the gill tissue of an Antarctic bivalve (Heise et al. 2003), there was no change in FRL between 5 and 25°C or 1 and 12°C, respectively. Moreover, in body wall tissue of a lugworm (Keller et al. 2004), FRL was higher at 1°C compared to 10°C in both summer- and winter-acclimated animals. Therefore, temperature affects mitochondrial ROS production in a fundamentally different way in endotherms and ectotherms, though the reason for this difference is unclear. It might be worthwhile to determine how temperature affects ROS production in homeotherms to determine whether temperature effects in heterotherms are representative of mammals in general, or whether heterothermic animals show unique response to temperature.

Therefore, in support of my hypothesis, my data suggest that mitochondrial ROS production is reduced during torpor. Low assay temperatures, which should reflect low T_b during torpor, reduce mitochondrial ROS production via temperature effects that slow down electron flux through the ETC and leads to the oxidation of its components. During arousal, the increased oxidation state of the ETC during torpor may alleviate any burst in mitochondrial ROS production as blood flow returns to tissues and oxygen levels rise. In addition, in hibernators, mitochondrial ROS production from complex I may be actively suppressed during arousal and interbout euthermia, at least in liver, further alleviating any mitochondrial ROS production during the hibernation season. Therefore, if plasma and tissues levels of ROS are higher during arousal, as some

previous studies suggest (Okamoto et al. 2006; Obsborne and Hashimoto 2006), either it is derived from sources other than the mitochondria (e.g., xanthine oxidase, NADPH oxidase), or, despite reductions in mitochondrial ROS production, the antioxidant capacity remains overwhelmed.

3.5 References

Abele D, Heise K, Portner HO, Puntarulo S (2002) Temperature-dependence of mitochondrial function and production of reactive oxygen species in the intertidal mud clam *Mya arenaria*. J Exp Biol 205: 1831-1841.

Armstrong C, Staples JF (2010) The role of succinate dehydrogenase and oxaloacetate in metabolic suppression during hibernation and arousal. J Comp Physiol B 180: 775-783.

Barger JL, Brand MD, Barnes BM, Boyer BB (2003) Tissue-specific suppression of mitochondrial proton leak and substrate oxidation in hibernating arctic ground squirrels. Am J Physiol Regul Integr Comp Physiol 284: R1306-R1313.

Barja G (1998) Mitochondria free radical release and aging in mammals and birds. Ann. NY Acad. Sci. 854: 224-238.

Barja G (2007) Mitochondrial oxygen consumption and reactive oxygen species production are independently modulated: implications for aging studies. Rej Res 10: 215-224.

Barja, G., Cadenas, S., Rojas, C., Perez-Campo, R., Lopez-Torres, M (1994) Low mitochondrial free radical release per unit O_2 consumption can explain the simultaneous presence of high longevity and high aerobic metabolic rate in birds. Free Radic. Res. 21: 317-328.

Barja G, Herrero A (2000) Oxidative damage to mitochondrial DNA is inversely related to maximum lifespan in the heart and brain of mammals. FASEB J 14: 312-318.

Becker LB, vanden Hoek TL, Shao Z-H, Li C-Q, Schumacker PT (1998) Generation of superoxide in cardiomyocytes during ischemia before reperfusion. Am J Physiol Heart Circ Physiol 277: H2240-H2246.

Bieber C, Ruf T (2009) Summer dormancy in edible dormice (*Glis glis*) without energetic constraints. Naturwissenschaften 96: 165-171.

Brown JCL, Gerson AR, Staples JF (2007) Mitochondrial metabolism during daily torpor in the dwarf Siberian hamster: role of active regulated changes and passive thermal effects. Am J Physiol Regul Integr Comp Physiol 293: R1833-R1845.

Brown JCL, McClelland GB, Faure PA, Klaiman JM, Staples JF (2009) Examining the mechanisms responsible for lower ROS release rates in liver mitochondria from the long-lived house sparrow (*Passer domesticus*) and big brown bat (*Eptesicus fuscus*) compared to the short-lived mouse (*Mus musculus*). Mech Ageing Dev 130: 467-476.

Buffenstein R, Edrey YH, Yang T, Mele J (2008) The oxidative stress theory of aging : embattled or invisible? Insights from non-traditional model organisms. AGE 30: 99-109.

Bullard RW, Funkhouser GE (1962) Estimated regional blood flow by rubidium 86 distribution during arousal from hibernation. Am J Physiol 203: 266-270.

Buzadzic B, Spasic M, Saicic ZS, Radojicic R, Petrovic VM, Halliwell B (1990) Antioxidant defenses in the ground squirrel *Citellus citellus* – the effect of hibernation. Free Rad Biol Med 9: 407-413.

Chamberlain ME (2004) Top-down control analysis of the effect of temperature on ectotherm oxidative phosphorylation. Comp Evol Physiol 287: R794-R800.

Christian SL, Ross AP, Zhao HWW, Kristenson HJ, Zhan XH, Rasley BT, Bickler PE, Drew KL (2008). Arctic ground squirrel (*Spermophilus parryii)* hippocampal neurons tolerate prolonged oxygen-glucose deprivation and maintain baseline ERK1/2 and JNK activation despite drastic ATP loss. J Cereb Blood Flow Metab 28: 1307-1319.

Chung D, Lloyd GP, Thomas RH, Guglielmo CG, Staples JF (2011) Mitochondrial respiration and succinate dehydrogenase are suppressed early during entrance into a hibernation bout, but membrane remodeling is only transient. J Comp Physiol B (In press).

Dave KR, Prado R, Raval AP, Drew KL, Perez-Pinzon MA (2006) The Arctic ground squirrel brain is resistant to injury from cardiac arrest during euthermia. Stroke 37: 1261-1265.

deGroot H, Rauen U (2007) Ischemia-reperfusion injury: processes in pathogenetic networks: a review. Transplant Proc 39: 481-484.

Drew KL, Osborne PG, Frerichs KU, Hu Y, Koren RE, Hallenbeck JM, Rice ME (1999) Ascorbate and glutathione regulation in hibernating ground squirrels. Brain Res 851: 1-8.

Dufour S, Rousse N, Canioni P, Diolez P (1996) Top-down control analysis of temperature effect on oxidative phosphorylation. Biochem J 314: 743-751.

Eddy SF, McNally JD, Storey KB (2005) Up-regulation of a thioredoxin peroxidase-like protein, proliferation-associated gene, in hibernating bats. Arch Biochem Biophys 435: 103-111.

Fietz J, Schlund W, Dausmann KH, Regelmann M, Heldmaier G (2004) Energetic constraints on sexual activity in the male edible dormouse (*Glis glis*). Oecologia 138: 202-209.

Frerichs KU, Kennedy C, Sokoloff L, Hallenbeck JM (1994) Local cerebral blood flow during hibernation, a model of natural tolerance to "cerebral ischemia". J Cerebral Blood Flow Metab 14: 193-205.

Gehnrich SC, Aprille JR (1988) Hepatic gluconeogensis and mitochondiral function during hibernation. Comp Biochem Physiol B 91: 11-16.

Gems D, Doonan R (2009) Antioxidant defence and aging in *C. elegans*. Cell Cycle 8: 1-7.

Harman D (1956) Aging: a theory based on free-radical and radiation chemistry. J Gerontol 11: 298-300.

Heise K, Puntarulo S, Portner HO, Abele D (2003) Production of reactive oxygen species by isolated mitochondria of the Antarctic bivalve *Laternula elliptica* (King and Broderip) under heat stress. *Comp Biochem Physiol C* 134: 79-90.

Hittel DS, Storey KB (2002) Differential expression of mitochondrial-encoded genes in a hibernating mammal. J Exp Biol 205: 1625-1631.

Hoerter J, Gonzalez-Barraso M, Couplan E, Mateo P, Gelly C, Cassard-Doulcier A-M, Diolez P, Bouillard F (2004) Mitochondiral uncoupling protein 1 expressed in the heart of transgenic mice protects against ischemia-reperfusion damage. Circulation 110: 528-533.

Johansen K (1961) Distribution of blood in the arousing hibernator. Acta Physiol Scand 52: 379-386.

Keller M, Sommer AM, Portner HO, Abele D (2004) Seasonality of energetic functioning and production of reactive oxygen species by lugworm (*Arenicola marina*) mitochondria exposed to acute temperature changes. J Exp Biol 207: 2529-2538.

Kil HY, Zhang J, Piantadosi CA (1996) Brain temperature alters hydroxyl radical production during cerebral ischemia/reperfusion in rats. J Cereb Blood Flow Metab 16: 100-106.

Korshunov SS, Skulachev VP, Starkov AA (1997) High protonic potential actuates a mechanism of production of reactive oxygen species in mitochondria. FEBS Lett 416: 15-18.

Krystufek B, Pistotnik M, Casar KS (2005) Age determination and age structure in the edible dormouse *Glis glis* based on incremental bone lines. Mammal Rev 35: 210-214.

Kurtz CC, Lindell SL, Mangino MJ, Carey HV (2006) Hibernation confers resistance to intestinal ischemia-reperfusion injury. Am J Physiol Gastro Liver Phys 291: G895-G901.

Lahann P, Dausmann KH (2011) Live fast, die young: flexibility of life history traits in the fat-tailed dwarf lemur (*Cheirogaleus medius*). Behav Ecol Sociobiol 65: 381-390.

Lapointe J, Hekimi S (2010) When a theory of aging ages badly. Cell Mol Life Sci 67: 1-8.

Lemieux H, Tardif J-C, Blier PU (2010) Thermal sensitivity of oxidative phosphorylation in rat heart mitochondria: does pyruvate dehydrogenase dictate the response to temperature? J Therm Biol 35: 105-111.

Lyman CP, O'Brien RC, Greene GC, Papafrangos ED (1981) Hibernation and longevity in the Turkish hamster *Mesocricetus brandti*. Science 212: 668-670.

Ma YL, Rice ME, Chao ML, Rivera PM, Zhao HW, Ross AP, Zhu X, Smith MA, Drew KL (2004) Ascorbate distribution during hibernation is independent of ascrobate redox state. Free Rad Biol Med 37: 511-520.

Montalvo-Jave EE, Tattersfield TE, Ortega-Salgado JA, Pina E, Geller DA (2008) Factors in the pathophysiology of the liver ischemia-reperfusion injury. J Surg Res 147: 153-159.

Morin P, Ni Z, McMullen DC, Storey KB (2008) Expression of Nrf2 and its downstream targets in hibernating ground squirrels, *Spermophilus tridecemLineatus.* Mol Cell Biochem 312: 121-129.

Morin P, Storey KB (2007) Antioxidant defense in hibernation: cloning and expression of peroxiredoxins from hibernating ground squirrels, *Spermophilus tridecemLineatus*. Arch Biochem Biophys 461: 59-65.

Muleme HM, Walpole AC, Staples JF (2006) Mitochondrial metabolism in hibernation: metabolic suppression, temperature effects, and substrate preferences. Physiol Biochem Zool 79: 474-483.

Ni Z, Storey KB (2010) Heme oxygenase expression and Nrf2 signaling during hibernation in ground squirrels. Can J Physiol Pharm 88: 379-387.

Ohta H, Okamoto I, Hanaya T, Arai S, Ohta T, Fukuda S (2006) Enhanced antioxidant defense due to extracellular catalase activity in Syrian hamster during arousal from hibernation. Comp Biochem Physiol C 143: 484-491.

Okamoto I, Kayano T, Hanaya T, Arai S, Ikeda M, Kurimoto M (2006) Up-regulation of an extracellular superoxide dismutase-like activity in hibernating hamsters subjected to oxidative stress in mid- to late arousal from torpor. Comp Biochem Physiol C 144: 47-56.

Orr AL, Lohse LA, Drew KL, Hermes-Lima M (2009) Physiological oxidative stress after arousal from hibernation in Arctic ground squirrel. Comp Biochem Physiol A 153: 213-221.

Osbourne PG, Hashimoto M (2006) Brain antioxidant levels in hamsters during hibernation, arousal and centothermia. Behav Brain Res 168: 208-214.

Osborne PG, Sato J, Shuke N, Hashimoto M (2005) Sympathetic alpha-adrenergic regulation of blood flow and volume in hamsters arousing from hibernation. Am J Physiol Regul Integr Comp Physiol 289: R554-R562.

Page MM, Peters CW, Staples JF, Stuart JA (2009) Intracellular antioxidant enzymes are not globally upregulated during hibernation in the major oxidative tissues of the 13-lined ground squirrel *Spermophilus tridecemLineatus*. Comp Biochem Physiol A 152: 115-122.

Pasdois P, Parker JE, Griffiths EJ, Halestrap AP (2011) The role of oxidized cytochrome c in regulating mitochondrial reactive oxygen species production and its perturbation in ischaemia. Biochem J (In press).

Petrosillo G, Ruggiero FM, Di Venosa N, Paradies G (2003) Decreased complex III activity in mitochondria isolated from rat heart subjected to ischemia and reperfusion: role of reactive oxygen species and cardiolipin. FASEB J 17: 714-716.

Piantadosi CA, Zhang J (1996) Mitochondrial generation of reactive oxygen species after brain ischemia in the rat. Stroke 27: 327-332.

Podlutsky AJ, Khritankov AM, Ovodov ND, Austad SN (2005) J Gerontol 60: 1366-1368.

Rossignol R, Letellier T, Malgat M, Rocher C, Mazat J-P (2000) Tissue variation in the control of oxidative phosphorylation: implication for mitochondrial diseases. Biochem J 347: 45-53.

Ruch W, Cooper PH, Baggiolini M (1983) Assay of H_2O_2 production by macrophags and neutrophils with homovanillic acid and horseradish peroxidase. J Imm Meth 63: 347-357.

Sanz A, Pamploma R, Barja G (2006) Is the mitochondria free radical theory of aging intact? Antiox Redox Signal 8: 582-599.

Schlame M, Rua D, Greenberg ML (2000) The biosynthesis and functional role of cardiolipin. Prog Lipid Res 39: 257-288.

Schriner SE, Linford NJ, Martin GM, Treuting P, Ogburn CE, Emond M, Coskun PE, Ladiges W, Wolf N, Van Remmen H, Wallace DC, Rabinovitch PS (2005) Extension of murine lifespan by overexpression of catalase targeted to mitochondria. Science 308: 1909-1911.

Schwerzmann K, Hoppeler H, Kayar SR, Weibel ER (1989) Oxidative capacity of muscle and mitochondria: correlation of physiological, biochemical, and morphometric characteristics. PNAS 86: 1583-1587.

Sohal RS, Ku HH, Agarwal S (1993) Biochemical correlates of longevity in two closely related rodent species. Biochem Biophys Res Comm 196: 7-11.

Sohal RS, Sohal BH, Orr WC (1995) Mitochondrial superoxide and hydrogen peroxide generation, protein oxidative damage, and longevity in different species of flies. Free Rad Biol Med 19: 499-504.

Sommer RS, Niederle M, Labes R, Zoller H (2009) Bat predation by the barn owl *Tyto alba* in a hibernation site of bats. Folia Zool 58: 98-103.

Speakman JR (2005) Body size, energy metabolism, and lifespan. J Exp Biol 208: 1717-1730.

Tan D-X, Manchester LC, Sainz RM, Mayo JC, Leon J, Reiter RJ (2005) Physiological ischemia/reperfusion phenomena and their relation to endogenous melatonin production. Endocrine 27: 149-157.

Toien O, Drew KL, Chao ML, Rice ME (2001) Ascrobate dynamics and oxygen consumption during arousal from hibernation in Arctic ground squirrels. Am J Physiol Regul Comp Integr Physiol 281: R572-R583.

Turbill C, Bieber C, Ruf T (2011) Hibernation is associated with increased survival and the evolution of slow life histories among mammals. Proc Roy Soc B (In press)

Turrens JF (2003) Mitochondrial formation of reactive oxygen species. J Physiol 552: 335-344.

Votyakova TV, Reynolds IJ (2001) $\Delta\Psi_m$-dependent and independent production of reactive oxygen species by rat brain mitochondria. J Neurochem 79: 266-277.

Wilkinson GS, South JM (2002) Life history, ecology, and longevity in bats. Aging Cell 1: 124-131.

Zhou F, Zhu X, Castellani RJ, Stimmelmayr R, Perry G, Smith MA, Drew KL (2001) Hibernation, a model of neuroprotection. Am J Pathol 158: 2145-2151.

CHAPTER 4

Mitochondrial metabolic suppression and reactive oxygen species (ROS) production during euthermic fasting in mice and dwarf Siberian hamsters

4.1 Introduction

Many mammals in seasonal environments likely experience periods of fasting brought about by food shortage and/or environmental conditions that preclude foraging. During fasting, animals must rely entirely upon endogenous energy reserves, and one of the most important physiological responses that occurs during fasting is a significant suppression of mass-specific resting MR (up to 30%; Rixon and Stevenson 1957; Munch et al. 1993; Fuglei and Oritsland 1999) that occurs with core T_b falling no more than a few degrees (Markussen and Oritsland 1986; Sakurada et al. 2000). How this MR suppression during fasting is achieved is not well understood, but, as outlined in Chapter 2 for hibernation and daily torpor, a role for mitochondrial metabolic suppression is feasible, given that mitochondria are responsible for ~90% of whole-animal oxygen consumption and have considerable control over cellular energy demands (Rolfe and Brown 1997).

Few previous studies have examined changes in mitochondrial respiration rates and/or oxidative phosphorylation kinetics in fasted mammals compared to fed controls. Liver mitochondrial state 3 and 4 respiration rates were up to 20% lower in fasted rats than fed controls (Sorensen et al. 2006), but, in that study, fed animals were actually fasted overnight, which could have affected mitochondrial properties. By contrast, DiMarco and Hoppel (1975) found no difference in either state 3 or 4 liver

mitochondrial respiration in fasted rats compared to fed controls. Bezaire et al. (2001) and Cadenas et al. (1999) found no effect of fasting on state 4 respiration or proton leakiness in skeletal muscle mitochondria mice and rats, respectively. Iossa et al. (2001) also found no difference in state 4 respiration in skeletal muscle but observed higher protein leakiness in fasted animals. Mollica et al. (2006) showed that neither state 3 nor state 4 respiration rates were lower in skeletal muscle of fasted rats, but proton leakiness was higher. Therefore, it remains unclear whether mitochondrial metabolic suppression characterizes fasting in mammals, and, to my knowledge, no single study has fully examined the effects of fasting on all three components of OxPhos, as most previous work has focused on proton leak. Thus, the first objective of this chapter of my thesis was to determine whether mitochondrial respiration is actively suppressed in liver of euthermic mice and dwarf Siberian hamsters fasted for ~40 hours compared to animals fed ad libitum. In addition, I wanted to determine which components of OxPhos were responsible for any suppression observed.

Mice and hamsters were chosen as the comparative models for this fasting study for three reasons. First, both of these species are small, having little capacity for endogenous energy storage yet a high mass-specific metabolic rate. Therefore, they should both be especially prone to the effects of fasting. Second, mice and hamsters are comparably-sized rodents, yet they respond to fasting in considerably different ways. Dwarf Siberian hamsters do not undergo torpor when fasted, except under extreme conditions of body mass loss (>25%; Ruby and Zucker 1992), whereas, house mice undergo torpor when fasted soon after food is withheld (Hudson and Scott 1979). Given that daily torpor likely contributes significantly to a reduction of energy expenditure

during fasting in mice, I would predict that hamsters either have higher rates of body mass loss during fasting than mice or, if mitochondrial metabolic suppression is a mechanism of MR suppression, then the extent of mitochondrial metabolic suppression during euthermic fasting should be greater in hamsters than mice to compensate for the lack of torpor expression in hamsters. The third reason for comparing mice and hamsters is that, in Chapter 2, I demonstrated active mitochondrial metabolic suppression in liver and skeletal muscle in torpor in daily heterotherms and hibernators, where MR is suppressed up to 70% and 95% compared to BMR. My interpretation of these observations is that active mitochondrial metabolic suppression is a mechanism contributing to MR reduction during torpor. However, active mitochondrial metabolic suppression merely correlates with MR suppression in torpor, and there is no direct evidence of a causal link between active mitochondrial metabolic suppression and MR reduction. By examining mitochondrial respiration during fasting in mice and hamsters, I can determine whether active mitochondrial metabolic suppression occurs in other hypometabolic states, even without simultaneous torpor expression.

In addition to any effects on mitochondrial respiration, fasting, like torpor, may also have effects on mitochondrial ROS production. Calorie restriction (typically 40% of ad libitum feeding) has been the subject of much experimentation since McKay and Crowell (1934) showed that calorie-restricted rats lived longer than ad libitum-fed controls. A role for oxidative stress in explaining the calorie restriction phenotype became well-established in the early 1990s, as a number of studies reported that damage to DNA, proteins, and lipids were reduced in calorie-restricted animals compared to ad libitum fed controls (Sohal et al. 1994; Lass et al. 1998; Gredilla et al. 2001; Lopez-

Torres et al. 2002). Several studies showed that reduced rates of mitochondrial ROS production in a number of tissues of calorie-restricted animals may be a contributing mechanism to the slower accumulation of oxidative damage and the longevity of calorie-restricted-animals (Gredilla et al. 2001; Bevilacqua et al. 2005).

By comparison, only a single study has previously investigated how more severe food restriction (i.e., fasting) affects mitochondrial ROS production. Sorensen et al. (2006) showed that fasting increased ROS production from complex III in rats by increasing the degree of reduction of the ETC. Therefore, the third objective of this chapter of my thesis was to measure liver mitochondrial ROS production during fasting by comparing fed animals to 40h-fasted animals. In addition, I have attempted to correlate changes in ROS production with changes observed in OxPhos.

4.2 Experimental Procedures

4.2.1 Animals and fasting protocol. This project was approved by the local Animal Use Subcommittee (protocol 2008-055-06) and conformed to the guidelines of the Canadian Council on Animal Care. Female Balb/c and CD1 mice, 2-3 months old, were obtained from Charles River Laboratories. Male hamsters (*Phodopus sungorus*), 1 month old, were obtained from Dr. Katherine Wynne-Edwards (Queen's University, Kingston, Ontario, Canada). Animals were maintained in our facilities at the University of Western Ontario for at least 2 months prior to sampling. Animals inhabited cages (30 x 18 x 13 cm) filled with bedding and nesting material. Mice consumed water and standard rodent chow (ProLab RMH 3000, LabDiet) ad libitum, and were maintained at 20 ± 1°C on a 12-hour photoperiod. Hamsters consumed water and modified rodent

chow containing 5.5 mg linoleic acid g^{-1} diet (Gerson et al. 2008) ad libitum, and were maintained on a 14-hour photoperiod to prevent spontaneous daily torpor. In both mice and hamsters, T_b was monitored as described in Chapter 2.

Two days prior to sampling, food (but not water) was removed from fasted mice and hamsters, whereas fed animals were allowed to continue ad libitum feeding. Fasting induced torpor in mice, but mice were sampled when euthermic. As I had found T_b effects on mitochondrial metabolism of euthermic animals when T_b was below 36°C (see Chapter 2), euthermic fasted mice were sampled only when T_b was greater than 36°C. No fasting-induced torpor was observed in any hamster.

4.2.2 Mitochondrial isolation, respiration rate, kinetics of oxidative phosphorylation, and ROS production. All animals were killed by anaesthetic overdose (Euthanyl, 270mg mL^{-1}, 0.2 mL 100 g^{-1}). The liver was immediately removed, weighed, and transferred to ice-cold homogenization buffer, and mitochondria were isolated via differential centrifugation using the method described for mice and hamsters in Chapter 2. Mitochondrial respiration rates were measured using temperature-controlled polarographic O_2 meters (Rank Brothers), and $\Delta\Psi_m$ was measured using TPP^+-sensitive electrodes (World Precision Instruments), as described for mice and hamsters in Chapter 2. OxPhos kinetics were measured at 37°C using succinate. In addition, glutamate-fueled state 3 and 4 respiration rates were measured. Both procedures were described in Chapter 2 for mice and hamsters. Mitochondrial ROS production (measured as H_2O_2 release rate) was measured at 37°C using peroxidase and homovanillic acid, as described in Chapter 3. FRL was calculated using the equation from Barja et al. (1994).

4.2.3 Data analysis. Data are presented as means ± SEM. Differences in whole-animal characteristics, mitochondrial respiration rate, ROS production rate, and FRL between metabolic states were determined using a general linear model, with species and metabolic state as factors. Non-significant interactions were dropped from the models. These analyses were completed using SAS 9.2. Differences in OxPhos kinetics between fed and fasted animals were determined using a custom-designed algorithm in Microsoft Excel 2003 (Appendix A), and control coefficients were calculated as described in Hafner et al. (1990; see also Appendix A). Data for mice and hamsters were analyzed independently for these kinetic analyses. P values reported indicate differences in the kinetic curves only at state 3 and 4 respiration.

4.3 Results

4.3.1 Effect of fasting on whole-animal characteristics. Prior to the fasting experiment, there was no difference in body mass between those animals that were subsequently fasted and those that remained fed ad libitum, although there were differences in body mass among species, being highest in dwarf Siberian hamsters and lowest in Balb/c mice (Figure 4-1A). Fasting duration did not differ among species (41.4 h ± 3.4 across all species), and body mass declined by about 10% per day in both mouse strains during fasting, but declined only 5% in hamsters (Figure 4-1B). Mass-specific daily caloric intake did not differ among species (Figure 4-1C) despite that mice were kept at 20°C and fed a standard rodent diet (3.36 kcal g^{-1}), whereas hamsters were kept at 15°C and fed a diet enriched in linoleic acid (3.58 kcal g^{-1}; Gerson et al. 2008). In addition, in both mice and hamsters, fasting caused T_b to decline 1-2°C during

both the scotophase and photophase (Figure 4-1D). At sampling, liver mass was 30-40% lower in fasted mice compared to fed mice, but no difference was seen in hamsters (Figure 4-1E). As a result, the hepatosomatic index (liver mass/body mass; HSI) also declined during fasting in mice but not hamsters; interestingly, when fed, HSI was higher in mice than hamsters but fell to the level of hamsters in fasted mice (Figure 4-1F).

4.3.2 Liver mitochondrial respiration and oxidative phosphorylation kinetics measured during fasting. State 3 respiration fueled by glutamate was 22-31% lower in fasted animals than fed animals in both strains of mice and hamsters (Figure 4-2A). State 4 respiration, on the other hand, did not differ between fed and fasted animals (Figure 4-2B). Moreover, neither state 3 (Figure 4-2C) nor state 4 (Figure 4-2D) respiration rate with succinate differed between fed and fasted animals in either mice or hamsters.

Substrate oxidation activity at state 3 $\Delta\Psi_m$ values differed between fed and fasted animals only in Balb/c mice (Figure 4-3A), where it was higher in fasted animals; at state 4 $\Delta\Psi_m$ values, on the other hand, substrate oxidation activity did not differ between fed and fasted animals in Balb/c mice, but was lower in both CD1 mice (Figure 4-3B) and hamsters (Figure 4-3C). ADP phosphorylation activity was lower in fasted animals in both Balb/c mice (Figure 4-4A) and hamsters (Figure 4-4C), and showed a similar trend in CD1 mice (Figure 4-4B) but failed to achieve statistical significance. Interestingly, in both mouse strains, IMM proton leakiness was higher in fasted animals compared to fed animals (Figure 4-5A,B), but did not differ between fed and fasted hamsters (Figure 4-5C).

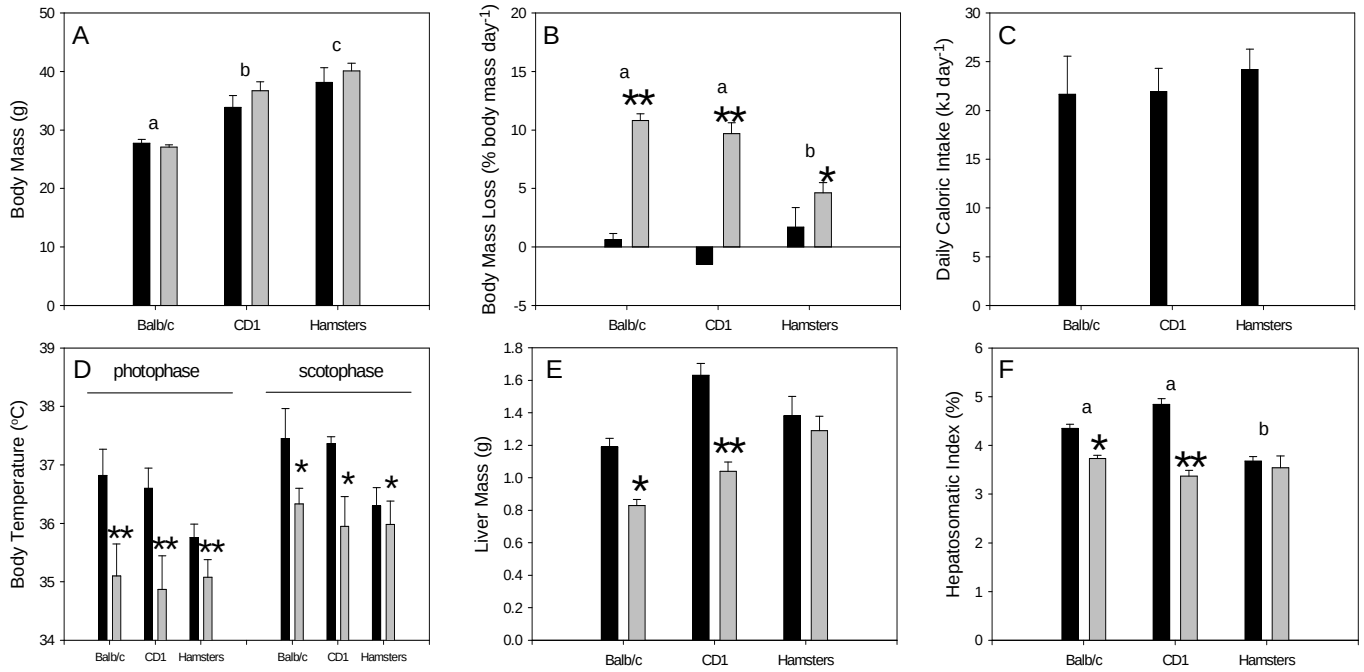

Figure 4-1. Whole-animal fasting responses in mice and hamsters. Black and grey bars represent fed and fasted groups respectively. Body mass measured prior to fasting (A). Body mass loss (B), caloric intake (C), and body temperature (D) measured during the experiment. Liver mass (E) and hepatosomatic index (F) measured at sampling. Data shown are mean ± SEM. N=4 for fed and fasted mice in both strains, N=8 for fed and fasted hamsters. Between-species effects shown with letters; species with common letters do not differ. Within-species effects shown using symbols; *, $P < 0.05$; **, $P < 0.01$ vs. fed animals.

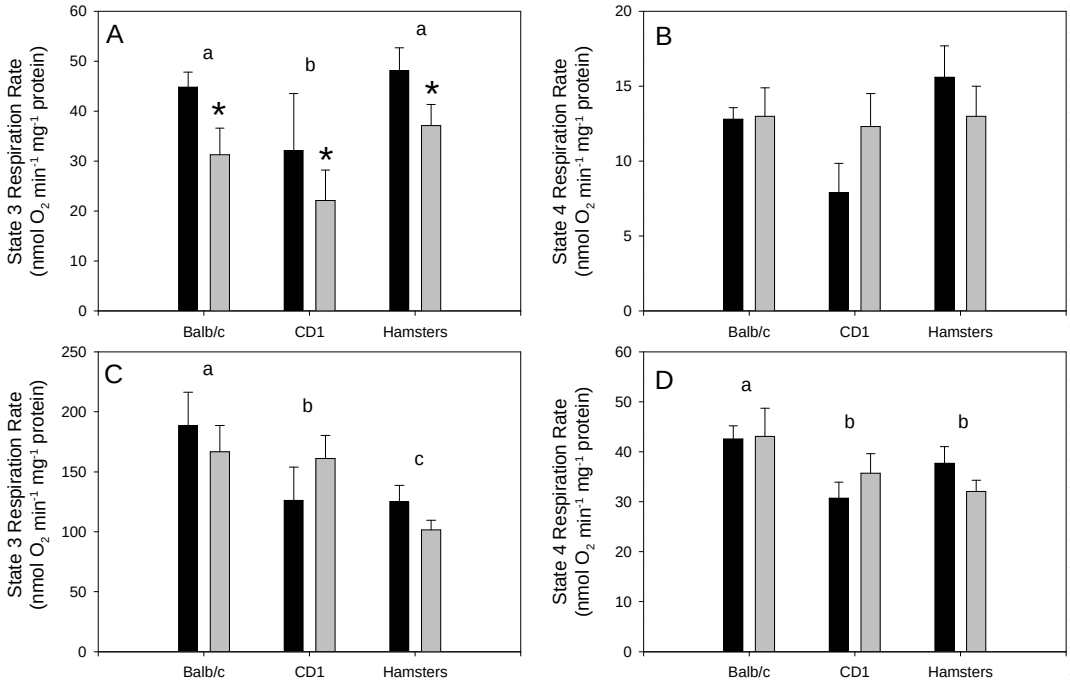

Figure 4-2. Effect of fasting on liver mitochondrial respiration rates measured at 37°C for mice (Balb/c, CD1) and hamsters. Black and grey bars represent fed and fasted animals, respectively. *A,B.* Glutamate-fueled respiration rates. *C,D.* Succinate-fueled respiration rates. Data shown are mean ± SEM. N=4 for fed and fasted mice in both strains, N=8 for fed and fasted hamsters. *, $P < 0.05$ compared to fed animals. Differences among species are shown using letters, where species that do not share a common letter are significantly ($P < 0.05$) different.

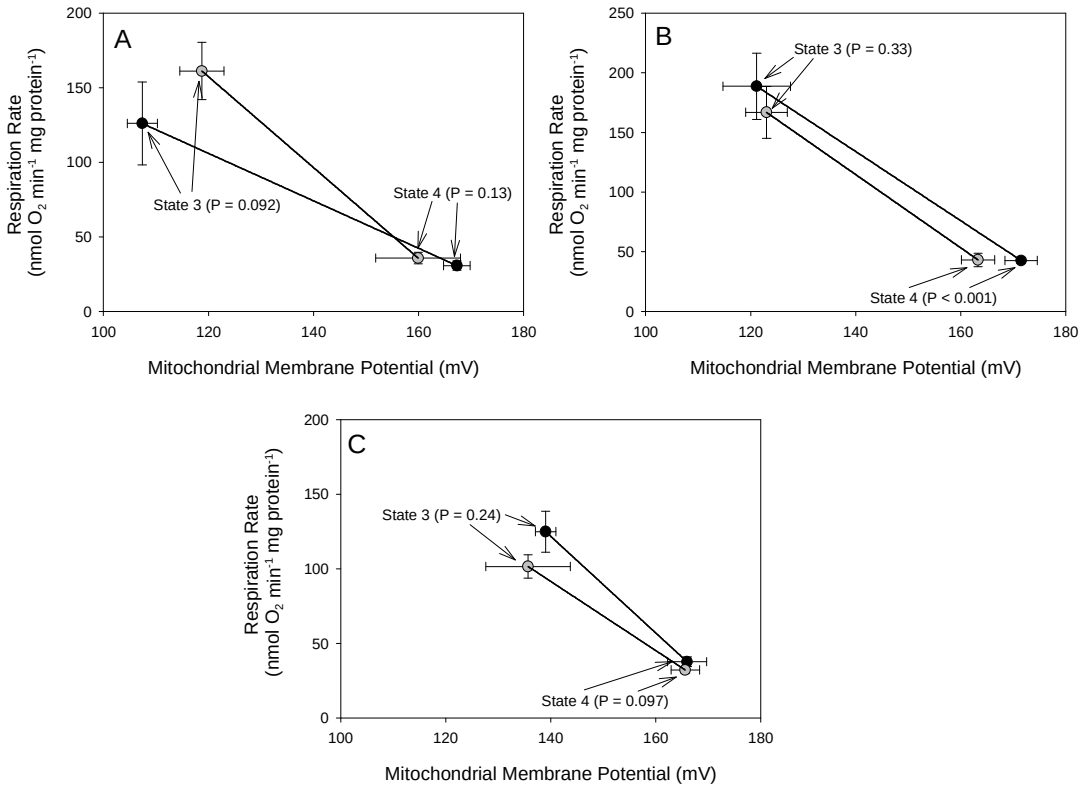

Figure 4-3. Effect of fasting on liver mitochondrial substrate oxidation kinetics in mice and hamsters. Black and grey symbols represent fed and fasted animals, respectively. *A.* Balb/c mice. *B.* CD1 mice. *C.* Hamsters. Data shown are mean ± SEM. N=4 for fed and fasted mice in both strains, N=8 for fed and fasted hamsters. Within each species/strain, kinetic differences between fed and euthermic fasted animals were determined using a custom-designed algorithm (see Experimental Procedures). P-values indicate whether the two curves differ only at the level of respiration rate indicated, not along the entire length of the curve.

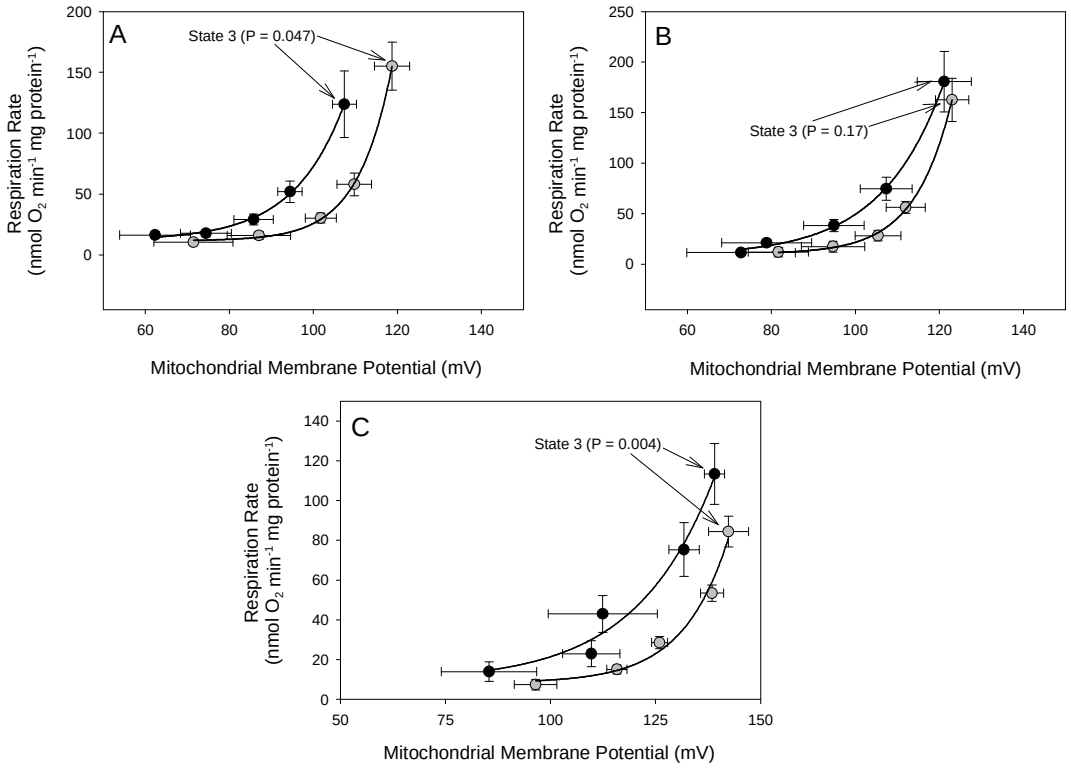

Figure 4-4. Effect of fasting on liver mitochondrial ADP phosphorylation kinetics in mice and hamsters. Black and grey symbols represent fed and fasted animals, respectively. *A.* Balb/c mice. *B.* CD1 mice. *C.* Hamsters. Data shown are mean ± SEM. N=4 for fed and fasted mice in both strains, N=8 for fed and fasted hamsters. Within each species/strain, kinetic differences between fed and euthermic fasted animals were determined using a custom-designed algorithm (see Experimental Procedures). P-values indicate whether the two curves differ only at the level of respiration rate indicated, not along the entire length of the curve.

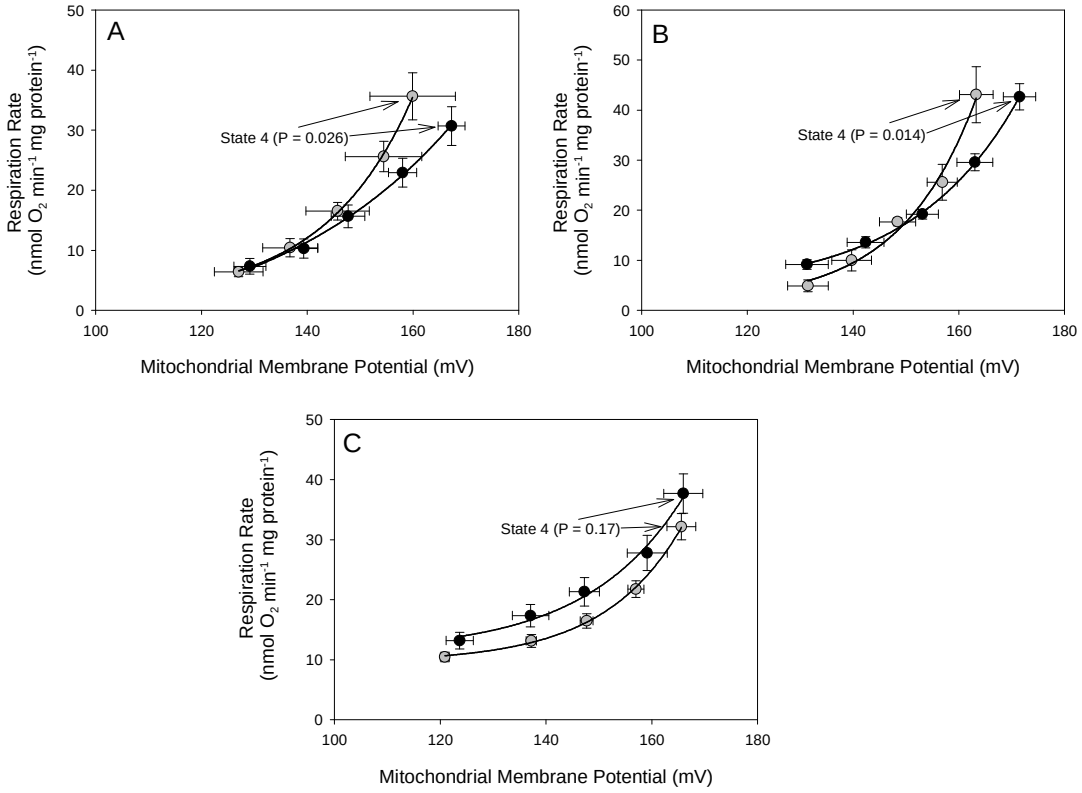

Figure 4-5. Effect of fasting on liver mitochondrial proton leak kinetics in mice and hamsters. Black and grey symbols represent fed and fasted animals, respectively. *A.* Balb/c mice. *B.* CD1 mice. *C.* Hamsters. Data shown are mean ± SEM. N=4 for fed and fasted mice in both strains, N=8 for fed and fasted hamsters. Within each species/strain, kinetic differences between fed and euthermic fasted animals were determined using a custom-designed algorithm (see Experimental Procedures). P-values indicate whether the two curves differ only at the level of respiration rate indicated, not along the entire length of the curve.

Table 4-1 summarizes the distribution of control of OxPhos in fed and fasted animals. In both mouse strains, substrate oxidation had the majority of the control over state 3 respiration rate in fed animals, and fasting led to little change in this pattern. By contrast, in hamsters, while substrate oxidation had the majority of control in fed animals as well, it had less control than in fed mice. Moreover, when hamsters were fasted, the control exerted by substrate oxidation increased considerably, while that of ADP phosphorylation declined concomitantly. With regards to state 4 respiration, in all species, proton leak had most of the control, though the extent of its control tended to decline during fasting, particularly in CD1 mice and hamsters.

4.3.3 Liver mitochondrial ROS production during fasting in mice and hamsters. In liver, basal ROS production rates (measured in the absence of ETC inhibitors acting downstream of ROS-producing sites) with both glutamate (Figure 4-6A) and succinate (Figure 4-6B) did not differ between fed and fasted animals in either strain of mice or hamsters. Similarly, FRL also did not differ between fed and fasted animals in either species with either substrate (Figure 4-6C,D). However, maximal ROS production was up to 40% and 57% lower with glutamate (Figure 4-6E) and succinate (Figure 4-6F), respectively, in all species.

Table 4-1. Distribution of control over liver mitochondrial respiration by the three components of oxidative phosphorylation at 37°C in fed and fasted mice (Balb/c and CD1 strains) and dwarf Siberian hamsters. Overall control coefficients for state 3 (A) and state 4 (B) were calculated using the mean values of membrane potential and respiration rate from kinetic curves in Figures 4-3, 4-4, and 4-5, as well as the equations described in the Materials and Methods.

A.	Balb/c		CD1		Hamsters	
	Fed	Fasted	Fed	Fasted	Fed	Fasted
Substrate Oxidation	0.92	0.85	0.80	0.85	0.65	0.78
ADP Phosphorylation	0.10	0.14	0.19	0.15	0.32	0.18
Proton Leakiness	-0.02	0.01	0.01	0.0	0.03	0.04

B.	Balb/c		CD1		Hamsters	
	Fed	Fasted	Fed	Fasted	Fed	Fasted
Substrate Oxidation	0.40	0.40	0.40	0.48	0.30	0.40
ADP Phosphorylation	0	0	0	0	0	0
Proton Leakiness	0.60	0.60	0.60	0.52	0.70	0.60

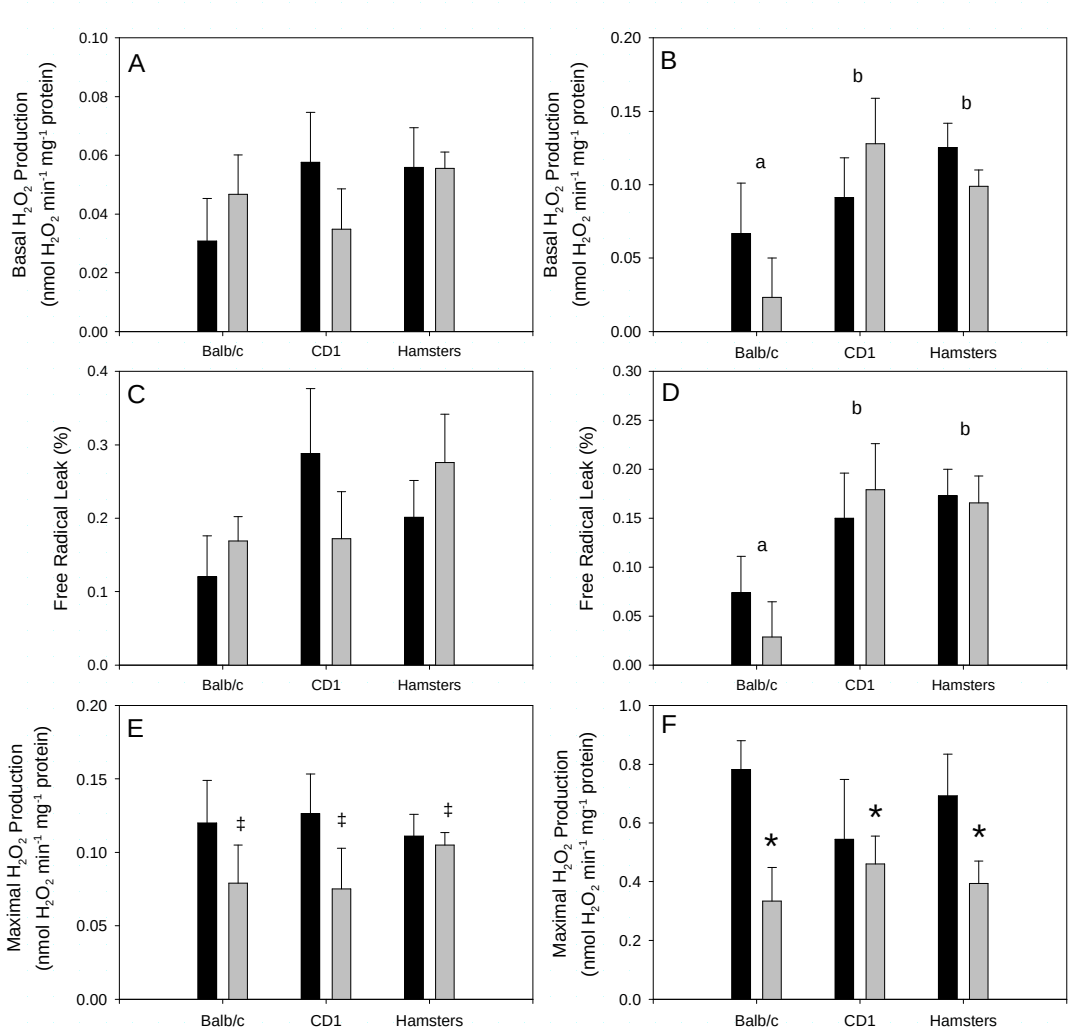

Figure 4-6. Effect of fasting on liver mitochondrial ROS production measured at 37°C in mice (Balb/c, CD1) and hamsters. Black and grey bars represent fed and fasted animals, respectively. Mitochondrial respiration was fueled by glutamate (left-hand panels) or succinate (right-hand panels). Data shown are mean ± SEM. N=4 for fed and fasted mice in both strains, N=8 for fed and fasted hamsters. ‡, $P < 0.10$; *, $P < 0.05$, compared to fed animals. Differences among species are shown using letters, where species that do not share a common letter are significantly ($P < 0.05$) different.

4.4 Discussion

4.4.1 Liver mitochondrial metabolic suppression characterizes hypometabolism in mammals. Liver mitochondrial state 3 respiration rate measured at 37°C was suppressed during euthermic fasting in both mice and hamsters with glutamate but not succinate. This suggests that glutamate transport, GDH, and/or complex I are likely sites of suppression of mitochondrial metabolism during fasting, as these are unique to glutamate oxidation, whereas other components of the ETC are also shared with succinate oxidation. It also supports the notion that hypometabolism—whether during euthermic fasting or torpor—may be achieved, in part, by liver mitochondrial metabolic suppression. In addition, during torpor in both hibernators and daily heterotherms, animals are necessarily fasted for hours to days (and months), and it is possible that the extent of active mitochondrial metabolic suppression observed in liver during torpor (in Chapter 2) represents only part of the total extent of active suppression that occurs. That is to say, it is possible that effects of fasting and torpor on mitochondrial metabolic suppression are additive, and the total extent of suppression achieved during hibernation or daily torpor may be greater than observed in Chapter 2, though testing this hypothesis would be difficult.

While active suppression of mitochondrial respiration during fasting is consistent with the hypothesis that mitochondrial metabolic suppression contributes to MR suppression during all hypometabolic states, it would appear that common mechanisms are not involved in bringing about mitochondrial inhibition during both torpor and fasting. For example, in the present study, glutamate oxidation was suppressed during fasting in Balb/c mice (Figure 4-2), but glutamate oxidation was not

suppressed during torpor in this same strain (Figure 2-2). At the same time, while succinate oxidation was not suppressed during fasting in any species/strain (Figure 4-2), it was suppressed during torpor in both Balb/c mice and hamsters (Figure 2-2; Brown et al. 2007). Nevertheless, the sites that were suggested above to be involved in inhibition of glutamate oxidation (glutamate transporter, GDH, and/or complex I) during fasting were all suggested as possible sites of inhibition during torpor in these species as well. This suggests that, while there may be variation in the precise mechanisms employed to suppress mitochondrial metabolism during hypometabolic periods, only certain sites are ever inhibited.

ADP phosphorylation activity was also suppressed in liver during euthermic fasting in mice and hamsters, although it contributed little to suppression of mitochondrial respiration. ADP phosphorylation was not suppressed during daily torpor, except in Balb/c mice (Chapter 2), where it also made little contribution to mitochondrial metabolic suppression, but it was suppressed during torpor in hibernating animals, though, again, it played only a minimal role in suppression of mitochondrial respiration. The role of ADP phosphorylation inhibition during euthermic fasting is unclear, though, as discussed for torpor, it may play some role in maintaining $\Delta\Psi_m$. Proton leakiness was increased during fasting in mice in the present study (Figure 4-5). Increased proton leak during fasting has been reported previously in some (Iossa et al. 2001; Mollica et al. 2006) but not all studies (Bezaire et al. 2001). It was also higher during daily torpor in hamsters (Brown et al. 2007) and ground squirrels (Figure 2-10). Therefore, reducing proton leakiness is not likely a principle mechanism for suppressing mitochondrial metabolism during either fasting or torpor.

4.4.2 Fasting reduces ROS production capacity but simultaneously increases the degree of reduction of the mitochondrial ETC. Neither basal ROS production nor FRL increased in liver mitochondria from fasted mice or hamsters, in contrast to observations in rats. Sorensen et al. (2006) observed higher rates of basal ROS production in fasted rats compared to fed controls, and Domenicali et al. (2001) showed that levels of malondialdehyde (an indicator of oxidative damage to fatty acids) were higher in liver of rats during fasting. These differences among rodent species might reflect a differential response to fasting between heterothermic and strictly homeothermic mammals. The difference between the present study and previous work seems to relate to changes in mitochondrial ROS production capacity during fasting. Sorenson et al. (2006) showed no change in maximal ROS production rates with fasting, whereas the present study showed lower maximal ROS production rates at both complex I and III with fasting. The reason the lower maximal ROS production rate in the present study was not reflected in measurements of basal ROS production or FRL is likely that the degree of ETC reduction is simultaneously increased; thus, under basal conditions, mitochondria are operating more closely to their maximal capacity. The data from Sorenson et al. (2006) also suggest an increase in ETC reduction state during fasting, which, in the absence of suppressed ROS production capacities, leads to higher rates of basal ROS production and FRL. Thus, there are similarities in the fasting response among rats, mice, and hamsters (in terms of the degree of ETC reduction) but there are also differences (in terms of ROS production capacity).

As discussed in the previous chapter, the degree of reduction of the ETC reflects the relative rate at which electrons arrive at and leave sites of ROS production;

therefore, during fasting, electrons must be leaving sites of ROS production more slowly than they arrive. This suggests that sites downstream of both complex I and III must be inhibited during fasting. Again, as with torpor, respiration data in the present thesis do not suggest any sites downstream of either complex I or III are inhibited during torpor; however, as discussed in the previous chapter, some downstream sites (e.g., cytochrome c, complex IV) could be inhibited during fasting, which would cause the upstream components of the ETC to become more reduced without necessarily affecting mitochondrial respiration because cytochrome c and complex IV have little control over mitochondrial respiration. Therefore, my data suggest that both torpor and fasting may be characterized by mitochondrial metabolic suppression of the ETC downstream of the ubiquinone pool which causes an increase in ETC reduction state, though only in torpor does this lead to higher rates of mitochondrial ROS production under basal conditions. In both cases, this downstream ETC suppression site has no impact on mitochondrial respiration rate.

By comparison to fasting, long-term (> 6 months) calorie restriction and alternate day fasting (ADF) both lower basal complex I ROS production in other species by decreasing the degree of reduction of complex I (Gredilla et al. 2001; Lopez-Torres et al. 2002; Hagopian et al. 2005). Therefore, it would appear that fasting and calorie restriction change the degree of reduction of the mitochondrial ETC in opposite ways. Why moderate forms of food restriction like 40% calorie restriction should have the complete opposite effect of fasting (rather than no effect or a blunted effect in the same direction) is not entirely clear, especially given both fasting and calorie restriction lead to similar changes in gene expression in mice (Bauer et al. 2004). One contributing

factor may be that neither MR (Masoro 2005) nor liver mitochondrial respiration rate (Gredilla et al. 2001; Lopez-Torres et al. 2002) or ATP production rate (Drew et al. 2003) are depressed in calorie restriction, except perhaps in quite long-term studies with older animals (Lambert et al. 2004; Hagopian et al. 2005).

4.4.3 The fasting response differs in hamsters and mice at the organismal level. Despite being housed under somewhat different conditions, and showing a significant difference in body mass, the hamsters and mice used in this study had the same daily energy expenditure, as inferred from food consumption data; however, when fasted, the rate of body mass loss was 55% lower in hamsters compared with mice. I had predicted that hamsters might have higher rates of body mass loss, since they do not undergo daily torpor and they do not appear to suppress mitochondrial metabolism during fasting more than mice. It is possible that hamsters save additional energy via mechanisms other than suppression of liver mitochondrial metabolism, but I do not believe that this is the case. The body mass of the hamsters used in the present study was, on average, 8 g higher compared to mice, but liver mass did not differ between the two species. This latter observation suggests that the higher body mass of hamsters does not reflect a larger body size per se, but rather a higher body fat content. Consistent with this observation, the total fat content of mice is reported to be 4 g (Reed et al. 2007), whereas the total fat content of hamsters is reported to be ~12 g (Bartness and Wade 1985), which reflects the difference in body mass observed between our two experimental species. Assuming that the energy content of body fat is 9.4 kcal g^{-1} (Pike and Brown 1984), hamsters have enough fat to survive for nearly 5 days, whereas mice have only enough fat to survive for less than two days. Therefore, over the 40 hour

period of fasting used in the present study, hamsters could utilize fat nearly exclusively, whereas mice would likely have to utilize other substrates (i.e., carbohydrates, proteins) to complement their fat use. Consistent with this hypothesis, liver mass declined during fasting in mice, likely representing glycogen depletion, which occurs quickly in fasted small rodents (Mosin 1982), whereas liver mass did not decline during fasting in hamsters, likely reflecting glycogen sparing. This differential substrate utilization could explain the difference in rate of body mass loss. Since fat is more than twice as energy dense as lean mass, if hamsters use predominantly fat when fasted, whereas mice use both fat and lean mass, even if both species have the same energy expenditure rates, body mass will decline at a faster rate in mice. This observation that the amount of pre-fasting fat storage might correlate with fasting endurance is consistent with previous work in penguins, where Gentoo penguins (which have only 9% body fat) fast only a few days whereas King penguins (which have 30% body fat) are known to fast for weeks to months (Cherel et al. 1993). It can perhaps be inferred that the extent of energy savings that can be achieved during euthermic fasting is constant across species, and differences in fasting endurance are largely driven by the quantity of fat reserves.

The differential substrate utilization may also explain why mice undergo daily torpor when fasted, as soon as 8 hours after fasting begins, whereas hamsters do not. Mice have less available endogenous energy and, therefore, may have a greater need for energy savings during periods of fasting. While hamsters could presumably save energy via daily torpor as well, the fact that these animals do not undergo torpor likely supports the notion that daily torpor has costs (Deboer and Tobler 1994; Wojciechwoski and Jefimow 2006) and, therefore, is not employed unless necessary. Consistent with this

hypothesis, studies that have shown daily torpor in food-restricted long-day acclimated hamsters (Ruby and Zucker 1992) have demonstrated that torpor occurs only after more than 25% of body mass is lost. Given that about 30% of body mass in hamsters is fat, it is likely that once the 25% body mass loss threshold is surpassed, the hamsters' endogenous energy storage levels are sufficiently low to necessitate daily torpor. Consistent with this notion, Bae et al. (2003) have shown that moderate food restriction can elicit torpor in juvenile dwarf Siberian hamsters, which may reflect that these animals likely have smaller fat reserves than adults, more akin to mice.

4.4.4 Summary. Liver mitochondrial metabolism is suppressed during euthermic fasting in both mice and hamsters, and the site of this suppression is likely glutamate transporters, GDH, or complex I. This finding supports the notion that mitochondrial metabolic suppression contributes to MR suppression during mammalian hypometabolism. As during torpor, suppression of mitochondrial metabolism also increases the reduction state of the ETC, suggesting that fasting may increase oxidative stress, unlike CR, which has been shown previously to reduce ETC reduction state and alleviated oxidative stress. Finally, higher levels of body fat in hamsters may reduce the rate of body mass loss and glycogen depletion during fasting, and may explain why hamsters, unlike mice, do not undergo torpor in response to fasting.

4.5 References

Bae HH, Larkin JE, Zucker I (2003) Juvenile Siberian hamsters display torpor and modified locomotor activity and body temperature rhythms in response to reduced food availability. Physiol Biochem Zool 76: 858-867.

Barja, G., Cadenas, S., Rojas, C., Perez-Campo, R., Lopez-Torres, M (1994) Low mitochondrial free radical release per unit O_2 consumption can explain the simultaneous

presence of high longevity and high aerobic metabolic rate in birds. Free Radic. Res. 21: 317-328.

Bartness TJ, Wade GN (1985) Photoperiodic control of seasonal body weight cycles in hamsters. Neurosci Biobehav Rev 9: 599-612.

Bauer M, Hamm AC, Bonaus M, Jacob A, Jaekel J, Schorle H, Pankratz MJ, Katzenberger JD (2004) Starvation response in mouse liver shows strong correlation with life-span-prolonging processes. Physiol Genom 17: 230-244.

Bevilacqua L, Ramsey JJ, Hagopian K, Weindruch R, Harper M-E (2004) Long-term caloric restriction increases UCP3 content but decreases proton leak and reactive oxygen species production in rat skeletal muscle mitochondria. Am J Physiol Endocrinol Metab 289: E429-E438.

Bezaire V, Hofmann W, Kramer JKG, Kozak LP, Harper M-E (2001) Effects of fasting on muscle mitochondrial energetics and fatty acid metabolism in *Ucp3(-/-)* and wild-type mice. Am J Physio Endocrinol Metab 281: E975-E982.

Brown JCL, Gerson AR, Staples JF (2007) Mitochondrial metabolism during daily torpor in the dwarf Siberian hamster: role of active regulated changes and passive thermal effects. Am J Physiol Regul Integr Comp Physiol 293: R1833-R1845.

Cadenas S, Buckingham JA, Samec S, Seydoux J, Din N, Dulloo AG, Brand MD (1999) UCP2 and UCP3 rise in starved rat skeletal muscle but mitochondrial proton conductance is unchanged. FEBS Lett 462: 257-260.

Cherel Y, Freby F, Gilles J, Robin J-P (1993) Comparative fuel metabolism in Gentoo and King penguins: adaptation to brief versus prolonged fasting. Polar Biol 13: 263-269.

Deboer T, Tobler I (1994) Sleep EEG after daily torpor in the Djungarian hamster: similarity to the effects of sleep deprivation. Neurosci Lett 166: 35-38.

DiMarco JP, Hoppel C (1975) Hepatic mitochondrial function in ketogenic states. J Clin Invest 55: 1237-1244.

Domenicali M, Caraceni P, Vendemiale G, Grattagliano I, Nardo B, Dall'Agata M, Santoni B, Trevisani F, Cavallari A, Altomare E, Bernardi M (2001) Food deprivation exacerbates mitochondrial oxidative stress in rat liver exposed to ischemia-reperfusion injury. J Nutr 131: 105-110.

Drew B, Phaneuf S, Dirks A, Selman C, Gredilla R, Lezza A, Barja G, Leeuwenburgh C (2003) Effects of aging and caloric restriction on mitochondrial energy production in gastrocnemius muscle and heart. Am J Physiol Regul Integr Comp Physiol 284: R474-R480.

Fuglei E, Oritsland NA (1999) Seasonal trends in body mass, food intake and resting metabolic rate, and induction of metabolic depression in arctic foxes (*Alopex lagopus*) at Svalbard. J Comp Physiol B 169: 361-369.

Gerson AR, Brown JCL, Thomas R, Bernards MA, Staples JF (2008) Effects of polyunsaturated fatty acids on mitochondrial metabolism in mammalian hibernation. J Exp Biol 211: 2689-2699.

Gredilla R, Barja G, Lopez-Torres M (2001) Effect of short-term caloric restriction on H_2O_2 production and oxidative DNA damage in rat liver mitochondria and location of the free radical source. J Bioenerg Biomembr 33: 279-287.

Hagopian K, Harper M-E, Ram JJ, Humble SJ, Weindruch R, Ramsey JJ (2005) Long-term calorie restriction reduces proton leak and hydrogen peroxide production in liver mitochondria. Am J Physiol Endocrinol Metab 288: E674-E684.

Hudson JW, Scott IM (1979) Daily torpor in the laboratory mouse, Mus musculus var. albino. Phys Zool 52: 205-215.

Iossa S, Lionetti L, Mollica MP, Crescenzo R, Botta M, Samec S, Dulloo AG, Liverini G (2001) Differences in proton leak kinetics, but not in UCP3 protein content, in subsarcolemmal and intermyofibrillar skeletal muscle mitochondria from fed and fasted rats. FEBS Lett 505: 53-56.

Lambert AJ, Wang B, Yardley J, Edwards J, Merry BJ (2005) The effect of aging and caloric restriction on mitochondrial protein density and oxygen consumption. Exp Gerontol 39: 289-295.

Lass A, Sohal BH, Weindruch R, Forster MJ, Sohal RS (1998) Calorie restriction prevents age-associated accrual of oxidative damage to mouse skeletal muscle. Free Rad Biol Med 25: 1089-1097.

Lopez-Torres M, Gredilla R, Sanz A, Bajra G (2002) Influence of aging and long-term caloric restriction on oxygen radical generation and oxidative DNA damage in rat liver mitochondria. Free Rad Biol Med 32: 882-889.

Markussen NH, Oritsland NA (1986) Metabolic depression and heat balance in starving Wistar rats. Comp Biochem Physiol A 84: 771-776.

Masoro EJ (2005) Overview of caloric restriction and ageing. Mech Ageing Dev 126: 913-922.

McKay CM, Crowell MF (1934) Prolonging the lifespan. Sci Mon 39: 405-414.

Mollica MP, Lionetti L, Crescenzo R, D'Andrea E, Ferraro M, Liverini G, Iossa S (2006) Heterogeneous bioenergetic behavior of subsarcolemmal and intermyofibrillar mitochondria in fed and fasted rats. Cell Mol Life Sci 63: 358-366.

Mosin AF (1982) Some physiological and biochemical features of starvation and refeeding in small wild rodents (Microtinae). Comp Biochem Physiol A 71: 461-464.

Munch IC, Markussen H, Oritsland NA (1993) Resting oxygen consumption in rats during food restriction, starvation and refeeding. Acta Physiol Scand 148: 335-340.

Pike RL, Brown ML (1984) Nutrition: an integrated approach. 3rd ed. Wiley: New York.

Reed DR, Bachmanov AA, Tordoff MG (2007) Forty mouse strain survey of body composition. Physiol Behav 91: 593-600.

Rixon RH, Stevenson JAF (1957) Factors influencing survival of rats in fasting. Am J Physiol 188: 332-336.

Rolfe DFS, Brown GC (1997) Cellular energy utilization and molecular origin of standard metabolic rate in mammals. Physiol Rev 77: 731-759.

Ruby NF, Zucker I (1992) Daily torpor in the absence of the suprachiasmitc nucleus in Siberian hamsters. Am J Physiol Regul Integr Comp Physiol 263: R353-R362.

Sakurada S, Shido O, Sugimoto N, Hiratsuka Y, Yoda T, Kanosue K (2000) Autonomic and behavioural thermoregulation in starved rats. J Physiol 526: 417-424.

Sohal RS, Agarwal S, Candas M, Forster MJ, Lai H (1994) Effect of age and calorie restriction on DNA oxidative damage in different tissues of C57BL/6 mice. Mech Ageing Dev 76: 215-224.

Sorensen M, Sanz A, Gomez J, Pamplona R, Portero-Otin M, Gredilla R, Barja G (2006) Effects of fasting on oxidative stress in rat liver mitochondria. Free Rad Res 40: 339-347.

Wojciechowski MS, Jefimow M (2006) Is torpor only an advantage? Effect of thermal environment on torpor use in the Siberian hamsters (*Phodopus sungorus*). J Physiol Pharmacol 57: 83-98.

CHAPTER 5

General Discussion and Perspectives

5.1 My thesis and beyond: what are the big ideas?

5.1.1 Active, regulated mitochondrial metabolic suppression plays an important role in reducing metabolic rate during mammalian hypometabolism. My thesis demonstrates that the oxidative capacity of liver and skeletal muscle mitochondria is actively suppressed as much as 70% during periods of torpor and fasting in mammals, conditions where MR is reduced by 30-99% compared to resting levels. These observations are consistent with previous work (Fedotcheva et al. 1985; Gehnrich and Aprille 1988; Brustovetsky et al. 1989; Martin et al. 1999; Barger et al. 2003; Muleme et al. 2006; Sorensen et al. 2006; Brown et al. 2007; Gerson et al. 2008; Armstrong et al. 2010; Chung et al. 2011) and have led me to conclude that actively reduced mitochondrial oxidative capacity is one mechanism that contributes significantly to the suppression of MR during hypometabolic periods in mammals. Liver and skeletal muscle are responsible for up to 12% and 26% of BMR, respectively, in small mammals (Martin and Fuhrman 1955), and mitochondrial respiration is thought to be responsible for as much as 90% of MR (Rolfe and Brown 1997). Therefore, active mitochondrial metabolic suppression in the tissues so far examined has the potential to account for up to 16% of the reduction in MR observed during hypometabolism (see Table 5-1 for details). Therefore, in the present thesis, I have established that mitochondrial metabolic suppression characterizes mammalian hypometabolism, and I have elucidated some of

the mechanisms involved, particularly inhibition of complex I and II. Studies of mitochondria from other metabolically-active tissues, such as brain, kidney, and gut, which together account for an additional 20% of BMR (Martin and Fuhrman 1955), are now needed to help us to better appreciate the full potential contribution of active mitochondrial metabolic suppression to the overall suppression of MR during hypometabolism and whether similar mechanisms are involved in bringing about this metabolic suppression in all tissues.

To date, all previous studies of mitochondrial metabolism during hypometabolism in mammals had examined only one hypometabolic state (i.e., torpor or fasting, but never both) in any given species. One novel aspect of this thesis was that it demonstrated that active mitochondrial metabolic suppression occurs during various kinds of hypometabolism (i.e., both daily torpor and fasting) within the same species. This is important because it lends strength to the conclusion that mitochondrial metabolic suppression contributes to MR suppression per se in mammals. However, despite this novel approach to examining the role of mitochondrial metabolic suppression to MR reduction, I must remain cognizant to the fact the that lower rates of mitochondrial respiration from hypometabolic animals observed in the present study may yet be a consequence of other changes that occur during hypometabolism, and mitochondrial metabolic suppression itself may, in fact, play no role in reducing MR. Mitochondrial membrane composition has been to shown to change during both hibernation (Armstrong et al. 2010; Chung et al. 2011) and fasting (Sorensen et al. 2006), and whole liver phospholipid composition changes during daily torpor (JCL Brown, unpublished results). Membrane phospholipid composition is known to affect

the activity of membrane-bound enzymes (Wu et al. 2001; 2004), and changes in membrane composition have been shown to correlate with mitochondrial respiration during metabolic depression in lungfish (Frick et al. 2010). Therefore, mitochondria from hypometabolic animals could have slower mitochondrial respiration rates merely because of the effects of changes in membrane composition during hypometabolism. Consistent with this notion, Gerson et al. (2008) showed that modulation of mitochondrial membrane phospholipid composition could alleviate the occurrence of liver mitochondrial metabolic suppression during torpor without affecting the extent of MR suppression. However, as I have proposed that active mitochondrial metabolic suppression plays its most significant role during entrance into torpor, when T_b is still high, it may have been the rate of MR decline that would have differed in Gerson et al. (2008) rather than torpid MR, though this was not examined.

In reality, it may be quite difficult to establish a definitive causal role for mitochondrial metabolic suppression in the reduction of MR during hypometabolism. Armstrong et al. (2010) showed that OAA levels in liver increased during torpor in hibernating ground squirrels, and OAA binding to complex II suppressed its activity and accounted for about 25% of the suppression of mitochondrial respiration during torpor. While this provides evidence that some component of mitochondrial OxPhos is directly modified during torpor, it remains possible that increased levels of OAA in liver and its subsequent binding to complex II is the indirect result of changes in the activity of the many enzymes that affect OAA levels in mitochondria (Marco et al. 1974). Blackstone et al. (2005) reported that inhaled H_2S caused a depression of MR and T_b in mice, reminiscent of natural torpor, and MR and T_b returned to resting levels

when H_2S was removed. H_2S is a known inhibitor of ETC complex IV (Cooper and Brown 2008), and so the observations of Blackstone et al. (2005) support the principle that reversible mitochondrial metabolic suppression can be a mechanism for reversible MR suppression. Volpato et al. (2008) further showed that H_2S depresses MR in mice even in the absence of a change in T_b (i.e., even when T_a is 35°C), suggesting that mitochondrial inhibition can even be a mechanism for active MR suppression. Unfortunately, more recent studies have shown that H_2S actually stimulated metabolism in piglets (Li et al. 2008). Whether this reflects that piglets are comparatively large animals, or that the links between mitochondrial and whole-animal metabolism are stronger in heterothermic animals, remains to be determined.

While studies of isolated mitochondria have provided valuable information about how and the extent to which mitochondrial metabolism is reduced during hypometabolism, whether these results can be extrapolated to the in vivo condition is unclear. Isolated mitochondria are studied under conditions that may not completely reflect the cellular environment. In particular, respiration rates of isolated mitochondria are measured using saturating concentrations of respiratory substrates, as well as air-saturated levels of oxygen, in order to assess changes in maximal rates of mitochondrial respiration. However, cellular substrate concentrations are likely not saturating (Iles et al. 1985; Lewandowski et al. 1996), and oxygen levels in the cell are thought to be considerably lower than air-saturation (Chen et al. 1995). All of these factors may affect measurements of mitochondrial respiration. In fact, recent work by Reynafarje and Ferriera (2008) has suggested that oxygen concentration may be one of the most important determinants of mitochondrial respiration rate and ATP synthesis capacity,

and Gnaiger and Kuznetsov (2002) suggest that control of mitochondrial respiration shifts towards complex IV at low oxygen levels, accounting for the stoichiometric "excess" of this ETC complex in some tissues (Schwerzmann et al. 1989). Moreover, substrate concentrations and oxygen levels may change during hypometabolism, a factor which has been ignored in studies of isolated mitochondria. Therefore, while studies like mine provide definitive evidence that mitochondrial metabolism is inhibited during periods of hypometabolism, future studies of isolated mitochondria in hibernation and daily torpor should focus on examining the effect of substrate and oxygen levels on mitochondrial metabolism, and assess whether the changes in mitochondrial metabolism that I have demonstrated during hypometabolism still have an observable impact on mitochondrial respiration under conditions that better reflect the cellular environment.

5.1.2. Food consumption rates affect mitochondrial ETC reduction state. My thesis clearly shows that the degree of reduction of the mitochondrial ETC increases during fasting in small rodents, as was observed in rats by Sorensen et al. (2006). This observation contrasts previous work (Gredilla et al. 2001; Bevilacqua et al. 2005) showing that 40% (though neither 8.5% nor 25%; Gomez et al. 2007) calorie restriction decreased the degree of reduction of the mitochondrial ETC. These observed changes in mitochondrial ETC reduction state during calorie restriction and fasting are consistent with observations that 40% calorie restriction reduces oxidative damage to tissues compared to ad libitum feeding (Sohal et al. 1994; Lass et al. 1998; Gredilla et al. 2001; Lopez-Torres et al. 2002) whereas fasting increases oxidative damage instead

(Domenicali et al. 2001). They have also been the basis for much of the research examining the practicality of calorie-restricted diets in humans (Hursting et al. 2003).

The term calorie restriction may be misleading in that it implies that ad libitum feeding rates in rodents are “normal”. In fact, ad libitum feeding is not normal and produces animals that are essentially obese (Roe 1981; Weindruch 1996). If we consider calorie-restricted diets as the “normal” rate of food intake instead, then it can be concluded that normal rates of feeding minimize oxidative stress, whereas both ad libitum feeding and fasting lead to deleterious body weight changes and increased oxidative stress. Interestingly, the notion that there may be links between body weight, aging, and disease are only beginning to be explored in detail (Ahima 2009) despite some early research (e.g., Pariza 1987). Many authors have reported that calorie restriction has negative effects on growth and reproduction, and, on this basis, it is believed that calorie-restricted diets cannot be used in practice as an approach to reduce disease incidence or aging rates in humans. However, it may be instead that animals must continuously match their energy intake to their energy demands in order to simultaneously optimize reproduction/growth and survival. That is, chronic calorie restriction may not be feasible because animals must increase their food intake (to levels more comparable to ad libitum feeding) during periods of reproduction and/growth in order to meet their increased energy demands. While this may result in animals paying a cost in terms of oxidative stress, this cost is likely offset by the selective benefits of larger body size and/or offspring production.

5.1.3 Alleviation of oxidative stress may have contributed to the evolution of hibernation and daily torpor in small mammals. The evolution of hibernation and daily

torpor remains a contentious issue. Some authors believe that these phenomena are ancestral traits in the mammalian lineage, given their widespread occurrence and phenotypic similarity in protherians, metatherians, and eutherians, and even some birds (Augee and Gooden 1992), as well as their occurrence in quite primitive mammals (Lovegrove et al. 1999). Other authors (e.g., Harris et al. 2004) believe that hibernation and daily torpor are derived traits that represent a specialized environmental adaptation and possibly a paedomorphic trait. Still others (e.g., Geiser 2008) show that torpor may be an ancestral trait in marsupials but a derived character in placental mammals. Regardless of whether mammalian torpor is ancestral or derived, the selective pressures that drove the evolution of mammalian torpor are not fully understood. Geiser (1998) suggested that, whatever the particular selective pressure, body size plays an important role in whether a species uses torpor or not, with torpor occurring most frequently in small mammals.

The most common explanation for the lack of torpor expression in large mammals is based on energetics because most authors implicitly accept that energy conservation was the primary selective pressure that drove the evolution of hibernation and daily torpor, although Humphries et al. (2003) suggests that there is little empirical evidence to support this notion. Small mammals have higher mass-specific BMR than large animals, but the minimal MR than can be achieved during torpor is the same in all mammals regardless of body mass (Heldmaier et al. 2004). Therefore, the extent of energy savings that can be achieved in large animals is thought to be much smaller than the energy savings that can be achieved in small mammals, which is why large mammals seldom use torpor.

A recent study by Geiser and Turbill (2009) suggested that strictly homeothermic mammals were more prone to past extinction, suggesting that hibernation and daily torpor are beneficial traits whose loss of expression in some mammals has been detrimental to their fitness. Extinction is most common in large mammals (Cardillo et al. 2005), and most large mammals do not undergo daily torpor or hibernation. Therefore, it seems reasonable to suggest that large mammals may be more susceptible to extinction because they do not undergo torpor. This suggests that large animals do not undergo torpor not simply because the benefits may be comparatively small—as would be predicted if energetics were the main selective pressure driving the evolution of torpor—but because the costs may be comparatively high. I believe my data are consistent with this prediction. Mitochondrial ROS production likely declines during torpor largely due to passive thermal effects as T_b falls, given that low temperature greatly reduced mitochondrial ROS production in all tissues, but when mitochondrial ROS production was measured at 37°C, it was higher in torpid animals, particularly at complex III. In small mammals, inhibition of MR leads to a concomitant large decline in T_b because the surface area-to-volume ratio is quite large; by contrast, in large mammals, a similar MR inhibition may lead to only a small drop in T_b, if any, because the surface area-to-volume ratio is quite small. Therefore, while small mammals can take advantage of passive thermal effects on ROS production, large mammals cannot, and, in fact, large mammals may actually face higher levels of oxidative stress during torpor because of higher rates of mitochondrial ROS production. Therefore, large animals may, indeed, face higher costs during torpor—in terms of oxidative stress—than small mammals, which may preclude the use of torpor in large

Table 5-1. Potential contribution of mitochondrial metabolic suppression to basal metabolic rate (BMR) reduction during hypometabolism. For each tissue, the maximal suppression of state 3 respiration rate observed is indicated for each species. Below this value, in parentheses, is this suppression multiplied by the % contribution to BMR of the particular tissue, which indicates the extent to which suppression of this tissue could reduce metabolism below basal levels. For each species, the sum of these values in parentheses appears in the total column. Below this value, in parentheses, is the proportion of total suppression of BMR (90% in hibernation; 70% in daily torpor; and 30% in fasting) that is represented by the total mitochondrial metabolic suppression observed. Data for all strains of mice were combined.

	Liver	Skeletal Muscle	Heart	Total
% BMR	12	26	0.5	38.5
Hibernation				
Ground Squirrels	70% (8%)	32% (8%)	--	16% (16%)
Daily Torpor				
Mice	31% (4%)	--	--	4% (5%)
Hamsters	70% (8%)	--	-100% (-0.5%)	7.5% (10%)
Euthermic Fasting				
Mice	25% (3%)	--	--	3% (10%)
Hamsters	25% (3%)	--	--	3% (10%)

mammals. Indeed, there is some support for the notion that potential oxidative damage may prevent the expression of torpor (Frank and Storey 1995).

5.2 References

Ahima RS (2009) Connecting obesity, aging and diabetes. Nature Med 15: 996-997.

Armstrong C, Staples JF (2010) The role of succinate dehydrogenase and oxaloacetate in metabolic suppression during hibernation and arousal. J Comp Physiol B 180: 775-783.

Augee ML, Gooden BA (1992) Monotreme hibernation – some afterthoughts. In: Platypus and echidna. Augee ML (ed) Royal Zoological Society New South Wales: Syndey.

Barger JL, Brand MD, Barnes BM, Boyer BB (2003) Tissue-specific suppression of mitochondrial proton leak and substrate oxidation in hibernating arctic ground squirrels. Am J Physiol Regul Integr Comp Physiol 284: R1306-R1313.

Bevilacqua L, Ramsey JJ, Hagopian K, Weindruch R, Harper M-E (2005) Long-term caloric restriction increases UCP3 content but decreases proton leak and reactive oxygen species production in rat skeletal muscle mitochondria. Am J Physiol Endocrinol Metab 289: E429-E438.

Blackstone E, Morrison M, Roth MB (2005) H_2S induces a suspended animation-like state in mice. Science 308: 518-521.

Brown JCL, Gerson AR, Staples JF (2007) Mitochondrial metabolism during daily torpor in the dwarf Siberian hamster: role of active regulated changes and passive thermal effects. Am J Physiol Regul Integr Comp Physiol 293: R1833-R1845.

Brustovetsky NN, Mayevksy EI, Grishina EV, Gogvadze VG, Amerkhanov ZG (1989) Regulation of the rate of respiration and oxidative phosphorylation in liver mitochondria from hibernating ground squirrels, *Citellus undulatus*. Comp Biochem Physiol B 94: 537-541.

Cardillo M, Mace GM, Jones KE, Bielby J, Bininda-Emonds ORP, Sechrest W, Orne CDL, Purvis A (2005) Multiple causes of high extinction risk in large mammal species. Science 309: 1239-1241.

Chen Q, Fischer A, Reagan JD, Yan L-J, Ames BN (1995) Oxidative damage and senescence of human diploid fibroblast cells. PNAS 92: 4337-4341.

Chung D, Lloyd GP, Thomas RH, Guglielmo CG, Staples JF (2011) Mitochondrial respiration and succinate dehydrogenase are suppressed early during entrance into a hibernation bout, but membrane remodeling is only transient. J Comp Physiol B (In press).

Cooper CE, Brown GC (2008) The inhibition of mitochondrial cytochrome oxidase by the gases carbon monoxide, nitric oxide, hydrogen cyanide and hydrogen sulfide: chemical mechanism and physiological significance. J Bioenerg Biomembr 40: 533-539.

Domenicali M, Caraceni P, Vendemiale G, Grattagliano I, Nardo B, Dall'Agata M, Santoni B, Trevisani F, Cavallari A, Altomare E, Bernardi M (2001) Food deprivation exacerbates mitochondrial oxidative stress in rat liver exposed to ischemia-reperfusion injury. J Nutr 131: 105-110.

Fedotcheva NJ, Sharyshev AA, Mironova GD, Kondrashova MN (1985) Inhibition of succinate oxidation and K^+ transport in mitochondria during hibernation. Comp Biochem Physiol B 82: 191-195.

Frank CL, Storey KB (1995) The optimal depot fat composition for hibernation by golden-mantled ground squirrels (*Spermophilus lateralis*). J Comp Physiol 164: 536-542.

Frick NT, Bystriansky JS, Ip YK, Chew SF, Ballantyne JS (2010) Cytochrome c oxidase is regulated by modulations in protein expression and mitochondrial membrane phospholipid composition in estivating African lungfish. Am J Physiol Regul Integr Comp Physiol 298: R608-R616.

Gehnrich SC, Aprille JR (1988) Hepatic gluconeogenesis and mitochondrial function during hibernation. Comp Biochem Physiol B 91: 11-16.

Geiser F (1998) Evolution of daily torpor and hibernation in birds and mammals: importance of body size. Clin Exp Pharm Physiol 25: 736-740.

Geiser F (2008) Ontogeny and phylogeny of endotehrmy and torpor in mammals and birds. Comp Biochem Physiol A 150: 176-180.

Geiser F, Turnbill C (2009) Hibernation and daily torpor minimize mammalian extinctions. Naturwissenschaften 96: 1235-1240.

Gerson AR, Brown JCL, Thomas R, Bernards MA, Staples JF (2008) Effects of polyunsaturated fatty acids on mitochondrial metabolism in mammalian hibernation. J Exp Biol 211: 2689-2699.

Gnaiger E, Kuznetsov AV (2002) Mitochondrial respiration at low levels of oxygen and cytochrome c. Biochem Soc Trans 30: 252-258.

Gredilla R, Barja G, Lopez-Torres M (2001) Effect of short-term caloric restriction on H_2O_2 production and oxidative DNA damage in rat liver mitochondria and location of the free radical source. J Bioenerg Biomembr 33: 279-287.

Harris MB, Olson LE, Milsom WK (2004) The origin of mammalian heterothermy: a case for perpetual youth? In: Life in the cold: mechanisms, adaptation, and application. University of Alaska Fairbanks: Alaska.

Heldmaier G, Ortmann S, Elvert R (2004) Natural hypometabolism during hibernation and daily torpor in mammals. Resp Physiol Neurobiol 141: 317-329.

Humphries MM, Thomas DW, Kramer DL (2003) The role of energy availability in mammalian hibernation: a cost-benefit approach. Physiol Biochem Zool 76: 165-179.

Hursting SD, Lavigne JA, Berrigan D, Perkins SN, Barrett JC (2003) Calorie restriction, aging, and cancer prevention: mechanisms of action and applicability to humans. Ann Rev Med 54: 131-152.

Iles RA, Stevens AN, Griffiths JR, Morris PG (1985) Phosphorylation status of liver by ^{31}P-n.m.r. spectroscopy, and its implications for metabolic control. Biochem J 229: 141-151.

Lass A, Sohal BH, Weindruch R, Forster MJ, Sohal RS (1998) Calorie restriction prevents age-associated accrual of oxidative damage to mouse skeletal muscle mitochodnria. Free Rad Biol Med 25: 1089-1097.

Lewandowski ED, Doumen C, White LT, LaNoue KF, Damico LA, Yu X (1996) Muliplet structure of ^{13}C NMR signal from glutamate and direct detection of tricarboxylate acid (TCA) cycle intermediates. MRM 35: 149-154.

Li J, Zhang G, Cai S, Redington AN (2008) Effect of inhaled hydrogen sulfide on metabolic responses in anesthetized, paralyzed, and mechanically ventilated piglets. Ped Crit Care Med 9: 110-112.

Lopez-Torres M, Gredilla R, Sanz A, Barja G (2002) Influence of aging and long-term caloric restriction on oxygen radical generation and oxidative DNA damage in rat liver mitochondria. Free Rad Biol Med 32: 882-889.

Lovegrove BG, Lawes MJ, Roxburgh L (1999) Confirmation of plesiomorphic daily torpor in mammals: the round-eared elephant shrew *Macroscelides proboscideus* (Macroscelidea). J Comp Physiol B 169: 453-460.

Marco R, Pestana A, Sebastian J, Sols A (1974) Oxaloacetate metabolic crossroads in liver: enzyme compartmentation and regulation of gluconeogenesis. Mol Cell Biochem 3: 53-63.

Martin AW, Fuhrman FA (1955) The relationship between summated tissue respiration and metabolic rate in the mouse and dog. Phys Zool 28: 18-34.

Martin SL, Maniero GD, Carey C, Hand SC (1999) Reversible depression of oxygen consumption in isolated liver mitochondrial during hibernation. Phys Biochem Zool 72: 255-264.

Muleme HM, Walpole AC, Staples JF (2006) Mitochondrial metabolism in hibernation: metabolic suppression, temperature effects, and substrate preferences. Physiol Biochem Zool 79: 474-483.

Pariza MW (1987) Dietary fat, calorie restriction, ad libitum feeding, and cancer risk. Nutr Rev 45: 1-7.

Reynafarje BD, Ferreira J (2008) Oxidative phosphorylation: kinetic and thermodynamic correlation between electron flow, proton translocation, oxygen consumption, and ATP synthesis under close to in vivo concentrations of oxygen. Int J Med Sci 5: 143-151.

Roe FJC (1981) Are nutritionists worried about the epidemic of tumours in laboratory animals? Proc Nutr Sci 40: 57-65.

Rolfe DFS, Brown GC (1997) Cellular energy utilization and molecular origin of standard metabolic rate in mammals. Physiol Rev 77: 731-759.

Schwerzmann K, Hoppeler H, Kayar SR, Weibel ER (1989) Oxidative capacity of muscle and mitochondria: correlation of physiological, biochemical, and morphometric characteristics. PNAS 86: 1583-1587.

Sohal RS, Agarwal S, Candas M, Forster MJ, Lai H (1994) Effect of age and calorie restriction on DNA oxidative damage in different tissues of C57BL/6 mice. Mech Ageing Dev 76: 215-224.

Sorensen M, Sanz A, Gomez J, Pamplona R, Portero-Otin M, Gredilla R, Barja G (2006) Effects of fasting on oxidative stress in rat liver mitochondria. Free Rad Res 40: 339-347.

Volpato GP, Searles R, Yu B, Scherrer-Crosbie M, Bloch KD, Ichinose F, Zapol WM (2008) Inhaled hydrogen sulfide: a rapidly reversible inhibitor of cardiac and metabolic function in the mouse. Anesthesiology 108: 659-668.

Weindruch R (1996) The retardation of aging by caloric restriction: studies in rodents and primates. Toxicol Pathol 24: 742-745.

Wu BJ, Else PL, Storlien LH, Hulbert AJ (2001) Molecular activity of Na^+/K^+-ATPase from different sources is related to the packing of membrane lipids. J Exp Biol 204: 4271-4280.

Wu BJ, Hulbert AJ, Storlien LH, Else PL (2004) Membrane lipids and sodium pumps of cattle and crocodiles: an experimental test of the membrane pacemaker theory of metabolism. Am J Physiol Regul Integr Comp Physiol 287: R633-R641.

APPENDIX A

A quantitative approach to top-down elasticity analysis

A.1 Calculating coefficients for top-down elasticity analysis

A.1.1. Flux control coefficients. Cells often carry out chemical reactions via a series of intermediate steps called metabolic pathways. Each intermediate step in a metabolic pathway has the potential to influence the rate at which the overall chemical reaction takes places, and this can be described quantitatively as the flux control coefficient for that step. Given that every metabolic pathway must be completely controlled by the intermediate steps of which it is comprised, the sum of the flux control coefficients for all the intermediate steps of any metabolic pathway is, by definition, equal to 1 (Fell 1992). Intermediate steps whose flux control coefficient is closer to 1 have more control over the overall reaction rate than intermediate steps whose flux control coefficient is closer to zero.

OxPhos is an example of a metabolic pathway. Under state 3 conditions, the overall reaction—which is the oxidation of a reduced substrate for the production of ATP—is carried out by two components (i.e., two intermediate steps), substrate oxidation and ADP phosphorylation, though proton leak also contributes to some small extent even under state 3 conditions. Under state 4 conditions, the overall reaction—which is the oxidation of a reduced substrate leading to the production of heat—is also carried out by two components, substrate oxidation and proton leak. Therefore, the

control of both state 3 and 4 respiration rate can be determined by calculating the flux control coefficients of substrate oxidation, ADP phosphorylation, and proton leak.

According to the connectivity theorem (Fell 1992), flux control coefficients can be calculated from the elasticity coefficients of each component of OxPhos. For any given component of OxPhos, the elasticity coefficient represents how sensitive that component of OxPhos is to changes in the concentration of its substrate or product. Generally, the more sensitive a component is to changes in substrate/product concentration, the lower its flux control coefficient. In the case of OxPhos, our kinetic curves permit us to determine elasticity coefficients for all components of OxPhos with regards to $\Delta\Psi_m$, which is the substrate for ADP phosphorylation and proton leak, and the product of substrate oxidation. Elasticity coefficients are calculated according to the equation in Hafner et al. (1990):

$$\varepsilon^{i}_{\Delta\Psi m} = (\partial J_i / \partial \Delta\Psi_m) \times (\Delta\Psi_m / J_i), \qquad \text{(Equation A-1)}$$

where $\partial J_i / \partial \Delta\Psi_m$ is the first-derivative of the kinetic curve for OxPhos component *i* (where *i* can be substrate oxidation, ADP phosphorylation, or proton leak) at the state 3 or state 4 point on the curve (i.e., whichever respiratory state is being considered), and $\Delta\Psi_m$ and J_i are observed values for mitochondrial membrane potential and activity of OxPhos component *i* under the same respiratory conditions.

Using the calculated elasticity coefficients, flux control coefficients for each component of OxPhos can be calculated according to Hafner et al. (1990):

$$C_s^{O2} = (J_p \times \varepsilon^p_{\Delta\Psi m} + J_l \times \varepsilon^l_{\Delta\Psi m}) / (J_p \times \varepsilon^p_{\Delta\Psi m} + J_l \times \varepsilon^l_{\Delta\Psi m} - J_s \times \varepsilon^s_{\Delta\Psi m});$$

$$C_p^{O2} = J_p \times [(1- C_s^{O2})/J_s];$$

$$C_l^{O2} = J_l \times [(1- C_s^{O2})/J_s], \qquad \text{(Equations A2-4)}$$

where C_s^{O2}, C_p^{O2}, and C_l^{O2} are flux control coefficients for substrate oxidation, ADP phosphorylation, and proton leak, respectively, and J_s, J_p, and J_l are the observed activities of these same OxPhos components under either state 3 or 4 conditions (i.e., for whichever state the flux control coefficients are being calculated).

A.1.2. Integrated elasticity coefficients. As can be seen from measurements of kinetic curves (for example, see Figure 1-7), one of the principle factors that determines the activity of any component of OxPhos is Δp, often estimated by measurements of $\Delta\Psi_m$. Δp is the product of substrate oxidation, and, so, as predicted by the law of mass action, increases in Δp cause the rate of substrate oxidation to decline whereas decreases in Δp have the opposite effect. By contrast, Δp in the substrate of ADP phosphorylation and proton leak, and, therefore, increases in Δp cause the rate of these two processes to increase, whereas decreases in Δp cause the rate of these two processes to decline. Given the tremendous effect of Δp on the activity of all components of OxPhos, a change in Δp between two states (brought about by a change in the kinetics of one component of OxPhos) will lead to a change in the activity of all other components of OxPhos even if the kinetics of these other components themselves remain unchanged (Figure A-1). Therefore, in order to determine whether the kinetics of any component of OxPhos changes between two states, we need to determine whether or not the change in activity of the OxPhos component between the two states

can be explained by observed changes in $\Delta\Psi_m$. Any change in activity that cannot be explained by observed changes in $\Delta\Psi_m$ is presumed to reflect a change in the kinetics of the OxPhos component between the two states.

The integrated elasticity coefficient provides a convenient way to measure whether, and by how much, the kinetics of any component of OxPhos has changed between two states. Simply, the integrated elasticity coefficient represents the difference between the predicted change in activity of a particular OxPhos component and the actual (observed) changed in activity (Figure A-2). The predicted change in activity is calculated according to Ainscow and Brand (1999) and involves parameters: i) the elasticity coefficient for the control state, which describes how the OxPhos component responds to changes in $\Delta\Psi_m$ in the absence of any experimental treatment (see A.1.1), and ii) the observed change in $\Delta\Psi_m$ between the two states. The equation is:

$$\Delta J_i^{predicted} = (\varepsilon^i_{\Delta\Psi m}) \times (\Delta_{\Delta\Psi m}), \qquad \text{(Equation A-5)}$$

where $\Delta J_i^{predicted}$ is the predicted change in activity of OxPhos component *i*, $\varepsilon^i_{\Delta\Psi m}$ is the elasticity coefficient of OxPhos component *i* to $\Delta\Psi_m$, and $\Delta_{\Delta\Psi m}$ is the observed change in $\Delta\Psi_m$ between the two states. The integrated elasticity coefficient can than be calculated according the equation in Ainscow and Brand (1999):

$$IE^i_{\Delta q} = \Delta J_i^{observed} - \Delta J_i^{predicted}, \qquad \text{(Equation A-6)}$$

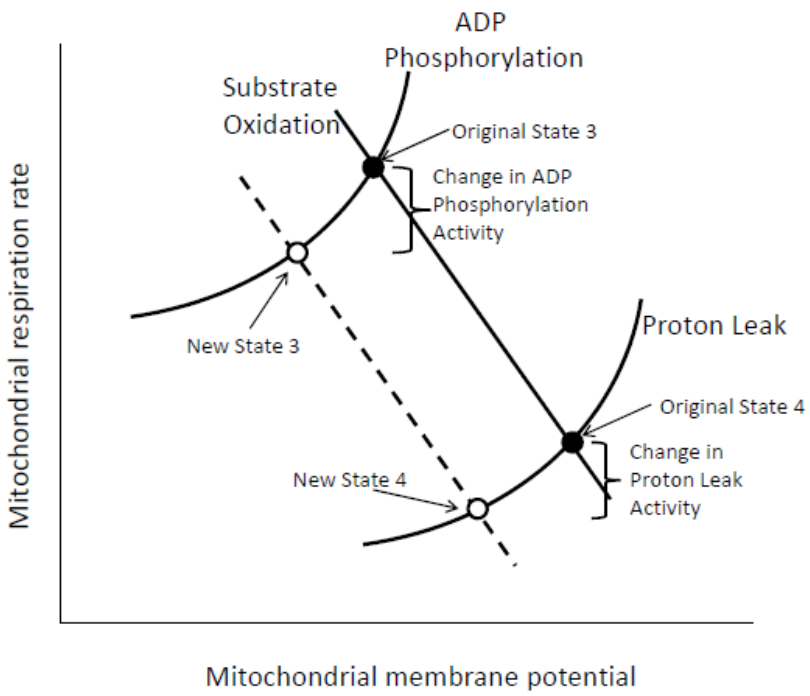

Figure A-1. The effect of changes in mitochondrial membrane potential on the activity of oxidative phosphorylation components. Representative kinetic curves (solid black lines) for all three components of oxidative phosphorylation are shown, and state 3 and 4 values of respiration rate and membrane potential, which represent the points of intersection of the kinetic curves, are indicated (closed circles). A change in the kinetics of substrate oxidation (dashed line) leads to reduced activity of both ADP phosphorylation and proton leak, reflected by lower rates of state 3 and 4 respiration (open circles), respectively, despite that the kinetics of these two components remain unchanged.

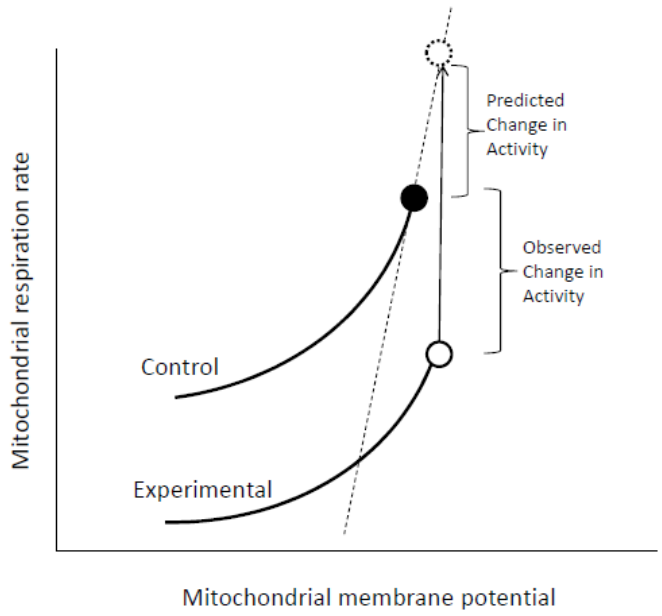

Figure A-2. Integrated elasticity coefficients. Integrated elasticity coefficients compare the predicted activity change of a component of oxidative phosphoryaltion between two states (under state 3 or 4 conditions) to the observed activity change. The kinetics of a component of oxidative phosphorylation in both a control and experimental state are shown, and the filled and open circles on these curves, respectively, represent observed activities and membrane potentials under state 3 or 4 conditions. The observed activity change between the two states is the difference in activity (measured as respiration rate) between these two points. The predicted activity in the experimental state is calculated using the elastsicity of the control state at the point of state 3 or 4 respiration (i.e., the first-derivative of the kinetic curve; indicated by the dashed line; see Equation A-1) and the observed value of membrane potential in the experimental state (indicated by the vertical line). The predicted activity change between the two states is the difference in respiration rate between the control state and this predicted experimental state value.

where $IE^{i}_{\Delta q}$ is the integrated elasticity coefficient of OxPhos component *i* in response to a change in state (Δq, which could be a change in metabolic state or temperature), and $\Delta J_i^{observed}$ is the observed change in activity of OxPhos component *i*.

A.2. Statistical analysis of oxidative phosphorylation kinetics curves

A.2.1. How do oxidative phosphorylation kinetics differ from traditional kinetics? Kinetics curves for typical enzyme-catalyzed reactions are determined by measuring the rate of activity of an enzyme over a range of substrate concentrations. OxPhos kinetics are measured in much the same way, by measuring the activity (via mitochondrial respiration rate) of each component of OxPhos over a range of substrate (or product) concentrations, where $\Delta\Psi_m$ is the substrate (or product; see Figure 1-6). However, unlike when we measure kinetics for typical enzyme reactions, for OxPhos kinetics, we cannot control the level of substrate concentration at which activity is measured; that is, we cannot control the exact values of $\Delta\Psi_m$ at which we are measuring mitochondrial respiration rate. Instead, for each mitochondrial preparation, $\Delta\Psi_m$ is determined by the relative activities of all the components of OxPhos and how they respond to inhibition during the experiment (see Figure 1-7). This means that we generate a range of mitochondrial respiration rates over a range of $\Delta\Psi_m$ values. Most authors have dealt with these data by grouping respiration and $\Delta\Psi_m$ values together according to the level of inhibitor used to acquire the values, as I did in this thesis; however, this creates a data set with variability in terms of both respiration rate and $\Delta\Psi_m$, which makes quantitative data analysis difficult.

As a result, the most common way that this kind of data has been analyzed is to assess whether the standard error bars of the data overlap between the kinetics curve for the control state and that for the experimental state. If standard error bars do overlap, then it is presumed that there is no difference in that particular OxPhos component between the control and experimental states. Because there is variability in terms of both respiration rate and $\Delta\Psi_m$, it is far more difficult to reliably assess whether error bars overlap, and this permits authors too much control over whether differences in OxPhos kinetics curves are considered different or not between states. Moreover, using overlapping standard error bars a method for determining significant differences is only appropriate where no suitable quantitative procedure is available (Payton et al. 2003). Therefore, one of my objectives of was to derive a quantitative approach for analysis of OxPhos kinetics curves.

A.2.2 Repeated-measures analysis of covariance. One possible approach to the quantitative analysis of OxPhos kinetics data is to use a repeated measures analysis of covariance (RM ANCOVA). There is no compelling reason why the data for respiration rate and $\Delta\Psi_m$ must be grouped according to their level of inhibition—except for simplicity of presentation in figures—and, in fact, this arrangement of the data seems to be the most significant hurdle to analyzing kinetic curve data. An ANCOVA would account for the variability in $\Delta\Psi_m$ by considering $\Delta\Psi_m$ as a covariate that significantly affects respiration rate, and a repeated measures design allows us to account for the multiple measurements of respiration rate and $\Delta\Psi_m$ made using various levels of inhibitors in the same mitochondrial preparation. The statistical question that we would be asking with the RM ANCOVA, therefore, is whether mitochondrial respiration rate

differ significantly among metabolic states even after accounting for the significant effect of $\Delta\Psi_m$ on respiration rate and simultaneously considering that sets of data points within the overall data set are from the same animal. This approach will yield a P-value. In addition, this approach would distinguish any interactions between states, that is, at what values of $\Delta\Psi_m$ the kinetics curves are different. One disadvantage of this approach is that it requires that the respiration rate data for proton leakiness and ADP phosphorylation kinetics be log-transformed prior to analysis in order to linearize the exponential relationship between respiration rate and $\Delta\Psi_m$.

A.2.3 A Monte Carlo-based approach using top-down elasticity analysis. A second approach, adopted in the present thesis, is to incorporate Monte Carlo analysis into traditional top-down regulatory analysis. The major advantage of this approach is that it does not examine differences in kinetics between states over the entire range of $\Delta\Psi_m$ values, but only at state 3 and 4 $\Delta\Psi_m$. This is important because, in my opinion, the reason that we measure OxPhos kinetics is not simply to determine whether any component of OxPhos changes between two states, but, more importantly, to explain the mechanisms by which state 3 and 4 mitochondrial respiration rates differ between two states. This Monte Carlo-based approach allows us to determine whether there are significant differences in kinetics curves between a control state and experimental state at state 3 and 4 values of $\Delta\Psi_m$ while simultaneously providing information about the extent to which these changes in OxPhos kinetics contribute to changes in state 3 or 4 mitochondrial respiration rate.

The Monte Carlo-based approach generates 500 sets of random state 3 and state 4 respiration rates with sample sizes equal to those from the empirical data set. Random

data sets for the control condition are generated using the mean and standard deviation from the empirical data set, whereas random data sets for the experimental condition are generated using the standard deviation of the experimental condition from the empirical data set but the mean of the control condition from the empirical data set, modified by the extent of the mean integrated elasticity (IE) value for the particular OxPhos component under consideration. For each randomly generated data set, a mean value is calculated for both the control and experimental condition. A P-value is then generated by determining what proportion of the 500 randomly generated data sets show a difference in mean value of respiration rate that is in the same direction as the difference in the empirical data set. For example, let us assume that the respiration rate in state A is lower than in state B in our empirical data set. If 490 out of the 500 random data sets also show that respiration rate is lower in state A than state B, then the P value is 0.02 (reflecting that only 2% of the random data sets showed the opposite direction of difference than the real data set). If, on the other hand, only 10 out of the 500 random data sets show that respiration rate is lower in state A than state B, then the P values is 0.98. What the Monte-Carlo-based approach is really doing, then, is comparing the variability in the respiration rate data against the extent of the difference of a particular OxPhos component between the control and experimental states, and asking which is greater; that is, is the extent of the difference of a particular OxPhos component between the control and experimental state great enough to produce a consistent difference in respiration rate between these states given the amount of empirically-measured variability in respiration rate. The major disadvantage of this approach—

which was the strength of the RM ANCOVA approach—is that the variability in $\Delta\Psi_m$ is not well accounted for.

A.2.4 Improving the Monte-Carlo-based approach. The most ideal method for a Monte-Carlo-based quantitative analysis of OxPhos kinetics data would be to randomly generate 500 sets of kinetics curves for all three OxPhos components in each of the control and experimental states using the empirically-derived mean and standard deviation for both respiration rate and $\Delta\Psi_m$, accounting for the interconnectedness between the data points within a given kinetics curve. Subsequently, pairwise comparisons could be made between randomly generated kinetics curves for the control and experimental condition. For each pairwise comparison, we could derive values for flux control coefficients and IE, and we could calculate P-values for both of these parameters in the same ways as described in section A.2.2. Therefore, using this approach, we would have some estimate of the variability in important parameters such as flux control coefficients and IE, and we would have statistical data about whether they significantly differ from zero.

What makes this approach difficult to employ—and the reason that it was not used in the present thesis—is the nature of the relationship between respiration rate and $\Delta\Psi_m$ for proton leakiness and ADP phosphorylation. The relationship is best approximated by a three-parameter exponential equation of the form $y = y_0 + ae^{bx}$. Parameter estimation for this kind of equation requires initial parameter estimates and an iterative approach, and I have not yet found software that can do this reliably in an automated manner (which is necessary given that we are dealing with hundreds of randomly generated data sets). Once these parameters are estimated, we can quite easily

derive values for flux control coefficients and IE values using the same approach used in the Excel-based algorithm already constructed. Therefore, I hope to revisit this approach in the future.

A.3 References

Ainscow EK, Brand MD (1999) Quantifying elasticity analysis: how external effectors cause changes to metabolic systems. Biosystems 49: 151-159.

Fell DA (1992) Metabolic control analysis: a survey of its theoretical and experimental development. Biochem J 286: 313-330.

Hafner RP, Brown GC, Brand MD (1990) Analysis of the control of respiration rate, phosphorylation rate, proton leak rate and protonmotive force in isolated mitochondria using the 'top-down' approach of metabolic control theory. Eur J Biochem 188: 313-319.

Payton ME, Greenstone MH, Schenker N (2003) Overlapping confidence intervals or standard error intervals: what do they mean in terms of statistical significance? J Ins Sci 3: 34-44.

APPENDIX B

Animal Use Ethics Approval

Western

June 5, 2008

This is the Original Approval for this protocol
A Full Protocol submission will be required in 2012

Dear Dr. Staples:

Your Animal Use Protocol form entitled:
Metabolism in Mammalian Hibernation and Daily Torpor
Funding Agency NATIONAL SCIENCE & ENGINEERING RESEARCH COUNCIL DISCOVERY - Grant #TGPIN 227230

has been approved by the University Council on Animal Care. This approval is valid from **June 5, 2008** to **June 30, 2009**. The protocol number for this project is **#2008-055-06 and replaces #2004-055-06.**

1. This number must be indicated when ordering animals for this project.
2. Animals for other projects may not be ordered under this number.
3. If no number appears please contact this office when grant approval is received.
   If the application for funding is not successful and you wish to proceed with the project, request that an internal scientific peer review be performed by the Animal Use Subcommittee office.
4. Purchases of animals other than through this system must be cleared through the ACVS office. Health certificates will be required.

ANIMALS APPROVED FOR 4 Years

Species	Strain	Other Detail	Pain Level	Animal # Total for 4 Years
Hamster	Dwarf Siberian	30 gm M/F	C	240
Mouse	Balb/C	25gm M/F	C	140
Mouse	CD1	25 gm M/F	C	152
Mouse	C57	25 gm M/F	C	64
Other, add to detail	Ground Squirrel	200 gm M/F - Breeders	C	48
Other, add to detail	Ground Squirrel	200 gm M/F	C	160

STANDARD OPERATING PROCEDURES
Procedures in this protocol should be carried out according to the following SOPs. Please contact the Animal Use Subcommittee office (661-2111 ext. 86770) in case of difficulties or if you require copies.
SOP's are also available at http://www.uwo.ca/animal/acvs
310 Holding Period Post-Admission
320 Euthanasia
321 Criteria for Early Euthanasia/Rodents
330 Post-Operative Care/Rodent
343 Surgical Prep/Rodent/Recovery Surgery

REQUIREMENTS/COMMENTS
Please ensure that individual(s) performing procedures on live animals, as described in this protocol, are familiar with the contents of this document.

c.c. Approved Protocol - J. Staples, J. Weber, D. Cheshuk
Approval Letter - J. Weber, D. Cheshuk

The University *of* Western Ontario
Animal Use Subcommittee / University Council on Animal Care
Health Sciences Centre, • London, Ontario • CANADA – N6A 5C1

CIRRICULUM VITAE

Name: Jason C. L. Brown

Education:
PhD Biology – 2011
University of Western Ontairo

MSc Biology – 2007
University of Western Ontario

BSc Biology – 2005
Wilfrid Laurier University

Scholarships/
Fellowships:
Helen Battle Postdoctoral Fellowship (UWO) – 2011
Queen Elizabeth II Scholarship in Science and Technology – 2010
NSERC Postgraduate Doctoral – 2007
NSERC Postgraduate Masters – 2005
NSERC Undergraduate Student Research Award – 2003, 2004, 2005
President's Centennial Scholarship (WLU) – 2001

Awards:
UWO Faculty of Science Teaching Award – 2011
EPCOR Water Ltd Student Travel Award – 2010
Malcolm Ferguson Award in Life Sciences (UWO) – 2010
WLU Biology Silver Medal – 2005

Publications:
Brown JCL, Chung DJ, Belgrave KR, Staples JF. Changes in mitochondrial reactive oxygen species (ROS) production in the liver and skeletal muscle of thirteen-lined ground squirrels (*Ictidomys tridecemlineatus*) during hibernation. (In Revision).

Brown JCL, Marshall KE, Fieldes MA, Staples JF. Differences in tissue concentrations of hydrogen peroxide in roots and cotyledons of annual and perennial species of flax (*Linum*). (In Preparation).

Brown JCL, Staples JF. Mitochondrial metabolic suppression in fasting and daily torpor: consequences for reactive oxygen species production. Physiological and Biochemical Zoology (In Press).

Birceanu O, McClelland GB, Wang YS, **Brown JCL**, Wilkie MP (2011) The lampricide 3-trifluoromethyl-4-nitrophenol (TFM) uncouples mitochondrial oxidative phosphorylation in both sea lamprey (*Petromyzon marinus*) and TFM-tolerant rainbow trout (*Oncorhynchus mykiss*). Comparative Biochemistry and Physiology C 153: 342-349.

Brown JCL, Staples JF (2010) Mitochondrial metabolism during fasting-induced daily torpor in mice. Biochimica et Biophysica Acta 1797: 476-486.

Brown JCL, McClelland GB, Faure PA, Klaiman JM, Staples JF (2009) Examining the mechanisms responsible for lower ROS release rates in liver mitochondria from the long-lived house sparrow (*Passer domesticus*) and big brown bat *(Eptescus fuscus*) compared to the short-lived mouse *(Mus musculus*). Mechanisms of Ageing and Development 130: 467-476.

Brown JCL, De Decker MM, Fieldes MA (2008) A comparative analysis of developmental profiles for DNA methylation in 5-azacytidine-induced early-flowering flax lines and their controls. Plant Science 175: 217-225.

Staples JF, **Brown JCL** (2008) Mitochondrial metabolism in hibernation and daily torpor: a review. Journal of Comparative Physiology B 178: 811-827.

Gerson AR, **Brown JCL**, Thomas R, Bernards MA, Staples JF (2008) Effects of dietary polyunsaturated fatty acids on mitochondrial metabolism in mammalian hibernation. Journal of Experimental Biology 211: 2689-2699.

Brown JCL, Gerson AR, Staples JF (2007) Mitochondrial metabolism during daily torpor in the dwarf Siberian hamster: the role of active regulated changes and passive thermal effects. American Journal of Physiology: Regulatory, Integrative, and Comparative Physiology 293: R1833-R1845.

Fieldes MA, Schaeffer S, Krech MJ, **Brown JCL** (2005) DNA hypomethylation in 5-azacytidine-induced early-flowering lines of flax. Theoretical and Applied Genetics 111: 136-149.